

2022

Development and evaluation of computational methods for measuring free-living gait and uncovering neuropathology in Parkinson's disease

<https://hdl.handle.net/2144/44021>

Downloaded from DSpace Repository, DSpace Institution's institutional repository

BOSTON UNIVERSITY
SCHOOL OF MEDICINE

Dissertation

**DEVELOPMENT AND EVALUATION OF COMPUTATIONAL METHODS
FOR MEASURING FREE-LIVING GAIT AND UNCOVERING
NEUROPATHOLOGY IN PARKINSON'S DISEASE**

by

MATTHEW CZECH

B.S., University of Pittsburgh, 2014

Submitted in partial fulfillment of the
requirements for the degree of
Doctor of Philosophy

2022

© 2022 by
MATTHEW CZECH
All rights reserved

Approved by

First Reader

Kevin Thomas, Ph.D., M.B.A
Associate Professor of Anatomy and Neurobiology
Boston University School of Medicine

Second Reader

Paolo Bonato, Ph.D.
Associate Professor of Physical Medicine and Rehabilitation
Harvard Medical School

Third Reader

Nancy Kopell, Ph.D.
Professor of Mathematics and Statistics
Boston University

ACKNOWLEDGMENTS

I feel incredibly lucky to have had such incredible support over my graduate career. First, I would like to thank my graduate advisor, Kevin Thomas, for his guidance and mentorship. Kip has taught me to love what you do, always do your best, and enjoy the little things (like compelling my industry colleagues to come onsite to complete jump rope challenges). Importantly, Kip taught me everything I needed to know and more regarding neurobiology, digital technologies, publishing papers, presenting, and everything else that goes into a graduate education. Despite his busy schedule he always made himself available to me whenever I needed him (or with whatever trouble I got myself into), and I have no doubt he will be there for me in the future, which I wholeheartedly do not take for granted.

Next, I would like to express my deepest thanks to all of my Pfizer mentors over the years. The opportunity for me to complete a graduate education while gaining experience in industry was a dream come true and would not have been a possibility if not for Peter Bergethon's and M. Kelley Erb's support and advocacy. Both are unbelievable mentors to me and friends. Following their departure from Pfizer, many other colleagues helped me along the way as well, and I would like to express my sincere thanks to Charmaine Demanuele, Shyamal Patel, Xuemei Cai, Mar Santamaria, and Hao Zhang for their continued scientific mentorship and friendship over the years. By extension, I would like to thank all of my other Pfizer colleagues and friends who supported my development, offered flexibility when I needed it, and were always ready for a drink after a long week.

I am also extremely grateful to Nancy Kopell and Michelle McCarthy for their mentorship over the past few years. Interested in learning about computational modeling of neuropathology, but without much time on my schedule, I approached Nancy and Michelle inquiring whether I could observe the work they do, or perhaps offer any programming support. Not only did Nancy and Michelle allow me to participate in lab meetings and encourage me to meet with lab members, they created a project for me and met with me weekly to check in. Despite my inconsistent schedule and unpredictable progress, they greeted me with wide smiles every week and were extremely flexible. I am so happy and grateful to them and their lab members that I was able to learn so much and make neuro-modeling part of my graduate experience.

I would also like to express my gratitude to my classmates and all of the faculty and staff within the Anatomy and Neurobiology Department. The department is truly unique, supportive, and fun. I truly enjoyed learning from and getting to know such fantastic people and I look forward to keeping in touch going forward. Thank you to my friends in Kip's lab for always being supportive, kind, and just so much fun to work with. Additionally, I would like to pay my special regards to my thesis committee, consisting of Drs. Kevin Thomas, Paolo Bonato, Nancy Kopell, Tara Moore, and M. Kelley Erb. Thank you for your approachability and continued advice on my thesis and future. My graduate training would not have been as comprehensive if not for your expertise and support.

Lastly, I would like to thank my family and lifelong friends for providing an incredible foundation of support in my life. To my mom and dad, I am so lucky to have

such unconditional love and support to be whomever I wanted to be. Thank you for always being there to celebrate my accomplishments and lift me up during hard times. To my siblings, thank you for always being there, your wisdom and support, and for knowing how to make me laugh. Lastly, to my wife, Victoria, and my young son, Theodore, thank you for inspiring me to work hard every day. You bring endless joy and happiness to my life and I am truly grateful.

I have been in love with the idea of being a neuroscientist since I was a young, naïve high school student. It is quite surreal to me that I have been able to learn and accomplish so much. I am very grateful to be where I am today and owe my accomplishments to all of the wonderful people around me.

**DEVELOPMENT AND EVALUATION OF COMPUTATIONAL METHODS
FOR MEASURING FREE-LIVING GAIT AND UNCOVERING
NEUROPATHOLOGY IN PARKINSON'S DISEASE**

MATTHEW CZECH

Boston University School of Medicine, 2022

Major Professor: Kevin Thomas, Ph.D., M.B.A., Associate Professor of Anatomy
and Neurobiology

ABSTRACT

Novel advances in engineering and data analytics are revolutionizing both our ability to monitor Parkinson's disease (PD) patient symptoms and our understanding of neuropathology. Despite promise, key challenges exist before patient monitoring technologies become standard in clinical settings, including 1) industry standardization of sensor-based analytical approaches; 2) validation of endpoint sensitivity to degree of impairment and medication state; and 3) consensus regarding appropriate devices, algorithms, data requirements, and statistical analysis requirements for symptom measurement outside of the clinic. In addition to the need for better patient monitoring, no disease-modifying therapeutics currently exist and thorough understanding of the neuropathology of PD remains elusive. To this end, large network brain simulations that leverage efficient computational frameworks are beginning to provide insight into mechanisms that facilitate pathological oscillations and may serve to identify new therapeutic targets.

To address current limitations in patient monitoring and our understanding of neuropathology, in this dissertation I 1) develop and evaluate validity and reliability of an

open-source, wearable sensor-based algorithm for measuring gait in PD patients, 2) evaluate and compare sensitivity of at-home measurements relative to in-clinic measurements, 3) evaluate sensitivity of wearable-derived features for measuring degree of gait impairment and treatment response in PD patients, and 4) investigate the effect of synaptic parameters on beta synchrony and entrainment in a large-scale spiking model of the subthalamic nucleus-globus pallidus externa (STN-GPe) network of the basal ganglia. Importantly, I find that sensor-derived features derived from the at-home environment differ from and are more sensitive to small changes compared to in-clinic, traditional assessments. Furthermore, I demonstrate the capacity for a single, lower back sensor-based algorithm to estimate gait features with sufficient sensitivity to detect degree of gait impairment and treatment effect in a mild-to-moderate PD population. Lastly, I demonstrate that weak synaptic connections between STN and GPe allows the STN-GPe network to entrain to a wide range of frequencies outside of the beta range, thus elucidating constraints on conditions required for beta production. Together, my work provides new insights into the feasibility and benefits of sensor-based symptom monitoring and PD-related neuropathology.

TABLE OF CONTENTS

ACKNOWLEDGMENTS	iv
ABSTRACT	vii
TABLE OF CONTENTS.....	ix
LIST OF TABLES	xv
LIST OF FIGURES	xvi
LIST OF ABBREVIATIONS.....	xx
CHAPTER ONE: INTRODUCTION.....	1
Introductory Overview.....	1
Parkinson’s Disease Treatment and Evaluation.....	3
Background and Treatment.....	3
Clinical Evaluation and Limitations	5
Digital Health Technologies Toward Better Symptom Monitoring.....	8
Challenges for Sensor-Based Measurement	10
Neuroanatomy and Significance of Gait.....	11
Sensor-Based Gait Measurement.....	14
CHAPTER TWO: GAITPY: AN OPEN-SOURCE PYTHON PACKAGE FOR GAIT ANALYSIS USING AN ACCELEROMETER ON THE LOWER BACK	18
Authors.....	18
Affiliations	18
Introduction.....	18
Processing Pipeline	20

Algorithms	24
Gait Classification.....	24
Gait Features	25
Acknowledgements.....	25
License	25
CHAPTER THREE: AGE AND ENVIRONMENT-RELATED DIFFERENCES IN	
GAIT IN HEALTHY ADULTS USING WEARABLES	
Authors.....	26
Affiliations	26
Abstract.....	27
Introduction.....	28
Results.....	32
Gait Speed Can Be Derived Accurately From Single Lumbar-Worn Accelerometer.	
.....	32
In-Lab Gait Speed Did Not Distinguish Between Age Groups.	34
At-Home Gait Speed Differed Significantly Between Age Groups.	36
Weak Association Between At-Home and In-Lab Gait Speed.....	37
Data From Three Days At Home Are Sufficient For Estimating Gait Speed.....	38
Discussion.....	40
Validity of Sensor-Based Estimates of Gait Speed.....	41
Impact of Environment on the Assessment of Gait Speed.	42
Impact of Data Quantity on Gait Speed Estimation.....	46

Impact of Gait Characterization on Future Studies.....	47
Limitations.....	47
Conclusion	48
Methods	49
Subjects and Procedure	49
Gait Feature Extraction.....	51
Statistical Analysis.....	52
 CHAPTER FOUR: THE IMPACT OF REDUCING THE NUMBER OF WEARABLE DEVICES ON MEASURING GAIT IN PARKINSONS DISEASE: NONINTERVENTIONAL EXPLORATORY STUDY	
Authors.....	55
Affiliations	55
Abstract.....	55
Introduction.....	56
Methods	59
Study Participants	59
Device Setup	60
Experimental Protocol	61
Gait Feature Extraction.....	62
Results.....	64
Accuracy of Gait Features Derived Using a Single Device.....	64
Reliability of Gait Features Derived Using a Single Device	65

Criterion Validity of Sensor-Derived Gait Features	66
Discriminative Validity of Sensor-Derived Gait Features.....	68
Discussion.....	69
Principle Findings	69
Accuracy and Reliability of Gait Features Derived Using a Single Device	70
Tradeoffs Between Gait Features Derived Using Different Device Setups	71
Limitations	72
Conclusion	73
Acknowledgement	74
CHAPTER FIVE: CONDITIONS ENABLING ENTRAINMENT OUTSIDE OF BETA RANGE IN THE SUBTHALAMIC NUCLEUS-GLOBUS PALLIDUS NETWORK... 75	
Contributions	75
Introduction.....	75
Methods	77
Network Model and Simulation.....	77
Statistical Analysis.....	78
Results.....	78
Weak Synaptic Connection Strength Between STN and GPe and Strong Reciprocal GPe Connection Strength Allows Network Entrainment to a Wide Range of Frequencies	78
STN Firing Rate Correlates With Beta Synchrony When Connections Between STN and GPe Are Strong	81

Discussion.....	82
Principle Findings.....	82
Origin and Mechanisms of Pathological Oscillations.....	83
Role of STN in Beta Oscillations.....	85
Future Work.....	86
CHAPTER SIX: DISCUSSION.....	87
Principal Findings and Significance.....	87
Evidence for Benefits of At-Home Measurement.....	89
Considerations for At-Home Measurement.....	91
Barriers to Digitization of Clinical Trials.....	94
Concluding Remarks.....	96
APPENDIX.....	99
Chapter 3 Supplementary Information.....	99
Chapter 4 Supplementary Information.....	106
Chapter 5 Supplementary Information.....	113
BIBLIOGRAPHY.....	114
CURRICULUM VITAE.....	145
Education.....	145
Research Experience and Employment.....	145
Teaching and Mentorship.....	146
Publications.....	146
Journal Publications.....	146

Journal Manuscripts in Preparation	147
Presentations	147
Technical Skills.....	147
Volunteering and Other Activities	147

LIST OF TABLES

Table 3.1. Participant Demographics	33
Table 3.2. The Minimum Number of At-Home Monitoring Days Required to Differentiate the At-Home Gait Speed Between Younger and Older Groups Similar to Full Data.	40
Table 4.1. Clinical and Demographic Characteristics.....	60
Table 4.2. Agreement Between Gait Features Derived Using the APDM Mobility Lab and GaitPy, and Test-Retest Reliability of Gait Features Derived With GaitPy in Healthy Volunteers. ICC coefficient values showing excellent agreement (between 0.75 and 1) are highlighted.....	66
Supplementary Table A.1: In-Clinic Gait Metrics Derived From Instrumented Mat (GAITRite), APDM 6-Sensor Set, and GaitPy Algorithm Using One Lumbar Mounted Sensor. The common gait metrics were summarized for each visit and age group. The repeated mixed model regression showed that there is a significant effect of device on all gait metrics (Device: $p < 10^{-16}$). Posthoc analyses showed no age group differences in any of the gait metrics for any device (the p-values were not corrected for multiple comparisons for this analysis). a Mean \pm sd.....	104
Supplementary Table A.2: The Regression Analysis of All Gait Metrics Derived From the At-Home Monitoring Data. There were age group differences for almost all gait metrics except single support time. There was also a difference between the gait observed in the weekdays compared to the weekend. There was no effect of sex or muscle mass or height (except step length). There were no interaction effects between any of the variables. All the p-values were corrected for multiple comparisons using FDR. a Mean \pm sd WD: Weekdays, WE: Weekend, M.Mass: Muscle Mass.....	105
Supplementary Table A.3. Gait Features Derived Using GaitPy With a Single Lumbar-Mounted Device, APDM Mobility Lab With 3 Devices, and APDM Mobility Lab With 6 Devices. *Step length is not calculated by APDM Mobility Lab.....	108
Supplementary Table A.4. Kruskal-Wallis Rank Sum Statistics and P Values for Sensor-Derived Features of Gait in Participants With Parkinson disease That Varied Significantly ($P \leq .01$) With MDS-UPDRS Gait Score in Order of Significance.....	111

LIST OF FIGURES

- Figure 2.1. Location of the wearable device on the lower back and orientation of the vertical acceleration axis of the accelerometer relative to the body. 19
- Figure 2.2. A high-level overview of GaitPy API and functions associated with various modules. 20
- Figure 2.3. Time-series plot generated by plot_contacts module of the raw vertical acceleration data labeled with detected gait events (initial contact/heel strike and final contact/toe off) and bout classifications. The start and end times of classified bouts are labeled by green and red vertical lines respectively. During the period shown, the participant walked for about 30 seconds, paused, performed 5 sit-to-stand repetitions, paused again, and continued walking for about 30 seconds..... 24
- Figure 3.1. Gait speed validation based on in-lab 4-m gait task. a Comparison of gait speed estimated using a six-sensor system (APDM) and an instrumented gait mat (GAITRite). The gait speeds derived from two systems were highly correlated (Pearson's $r = 0.98$, left). Bland-Altman plots (right) showed minimal mean difference (mean difference = 0.07, blue solid line; LoA = [-0.03, 0.13], red solid lines; corresponding confidence intervals are in dashed lines). b Comparison of gait speed estimated using a single lumbar-worn sensor (GaitPy) and an instrumented gait mat (GAITRite). The gait speeds derived from two systems were also highly correlated (Pearson's $r=0.72$, left). Bland-Altman plots (right) showed mean difference (mean difference = 0.17, blue solid line; LoA = [-0.09, 0.43] red solid lines; corresponding confidence intervals are represented by dashed lines). Both APDM and GaitPy had consistent bias compared to GAITRite and underestimated gait speed. LoA limits of agreement. 34
- Figure 3.2. In-lab gait speed did not show any age group differences. a Gait speed estimated using different methods differed ($\chi^2 = 199$, $p < 10^{-16}$). Both APDM and GaitPy underestimated gait speed during in-lab gait task compared to GAITRite ($p < 10^{-6}$), which is used as the gold standard. b Gait speed estimated using any of the three methods did not differ between the two age groups (younger group, $n = 33$, age = 29.2 ± 4.6 , 17F; older group, $n = 32$, age = 72.3 ± 5.8 , 16F; main age group effect: $\chi^2 = 0.28$, $p = 0.6$). Box and whiskers plots show the median and interquartile range, the lines extend to the smallest/largest value within 1.5 times interquartile range below/above the 25th/75th percentile, and the dots represent each individual data value..... 35

Figure 3.3. At-home gait speed estimated using a single lumbar-worn sensor (GaitPy) differed between age groups. a The median gait speed estimated by GaitPy showed significant group differences between younger and older groups ($p = 0.006$). There was also significant main effect of day type ($\chi^2 = 42.08, p < 10^{-5}$), and group by day type interaction ($\chi^2 = 13.38, p = 0.002$); i.e., the group difference was larger during weekdays than weekends. b The 95th percentile gait speed was also different between younger and older groups ($p = 10^{-5}$). Box and whiskers plots show the median and interquartile range, the lines extend to the smallest/largest value within 1.5 times interquartile range below/above the 25th/75th percentile, and the dots represent each individual data value... 37

Figure 3.4. Weak association between in-lab and at-home gait speed. a The median gait speed at home showed a significant slope and an intercept ($\beta = 0.57, p < 10^{-3}, I = 0.65; p < 10^{-5}$). The two gait speed measures were moderately correlated (Spearman's $\rho = 0.35, p = 0.004$), and at-home median gait speed explained only 18% of the variance of in-lab gait speed. b When a regression analysis was performed to explain the in-lab gait speed with the 95th percentile gait speed, at-home gait speed showed a significant slope and an intercept ($\beta = 0.47, p < 10^{-4}; I=0.54, p=10^{-4}$). The two gait speed measures showed moderate correlation (Spearman's $\rho=0.42, p=0.0005$). At-home 95th percentile gait speed explained only 25% of the variance of in-lab gait speed. Shaded area shows the 95% confidence interval..... 38

Figure 3.5. Amount of data needed to reliably estimate gait speed at home. Subset of data in terms of successive steps or randomly selected days was compared to the full data set (ICC > 0.75 represents excellent agreement between two measurements). Minimum required data to estimate both (a) median gait speed and (b) 95th percentile gait speed was 2–3 days of monitoring data. (c, d) At least 15,000 and 10,000 concurrent steps were required to reliably estimate median and 95th percentile gait speed, respectively. Box and whiskers plots show the median and interquartile range, the lines extend to the smallest/largest value within 1.5 times interquartile range below/above the 25th/75th percentile, and the dots represent each individual data value..... 39

Figure 4.1. MDS-UPDRS gait score model performance fit using gait features from (a) single device at the lumbar (L5) location (GaitPy), (b) 3 devices (APDM Mobility Lab), and (c) 6 devices (APDM Mobility Lab)..... 68

Figure 4.2. Distribution of the (a) clinician-rated gait score, (b) single-device predicted gait score, (c) three-device predicted gait score, and (d) six-device predicted gait score, grouped by patient reported ON and OFF motor states... 69

Figure 5.1. Network model schematic..... 78

Figure 5.2. An STN-GPe network model with (A) weak connection strength between STN and GPe and strong reciprocal GPe connection strength is entrainable to frequencies outside of beta range. In contrast, (B) strong connection strengths prevent entrainment to frequencies outside of beta range. Legend colors represent power spectral density values from the beta range calculated from normalized STN population rate..... 79

Figure 5.3. Network connection strengths control degree of theta entrainment. (A-C) GPe to STN connection strength is evaluated in relation with (A) STN firing rate, (B) GPe firing rate, and (C) beta synchrony. (D-F) Reciprocal GPe connection strength is evaluated in relation with (D) STN firing rate, (E) GPe firing rate, and (F) beta synchrony. Lastly, (G-I) STN to GPe connection strength is evaluated in relation with (G) STN firing rate, (H) GPe firing rate, and (I) beta synchrony. Legend colors represent power spectral density values from the theta range calculated from normalized STN population rate..... 80

Figure 5.4. Network connection strengths control degree of gamma entrainment. (A-C) GPe to STN connection strength is evaluated in relation with (A) STN firing rate, (B) GPe firing rate, and (C) beta synchrony. (D-F) Reciprocal GPe connection strength is evaluated in relation with (D) STN firing rate, (E) GPe firing rate, and (F) beta synchrony. Lastly, (G-I) STN to GPe connection strength is evaluated in relation with (G) STN firing rate, (H) GPe firing rate, and (I) beta synchrony. Legend colors represent power spectral density values from the gamma range calculated from normalized STN population rate..... 81

Figure 5.5. The relationship between STN firing rate and beta synchrony is less pronounced in an entrainable model. (A-C) The relationships between STN and GPe firing rates and beta synchrony in entrainable and (D-F) non-entrainable STN-GPe network models. Legend colors represent power spectral density values from the beta range calculated from normalized STN population rate.. 82

Supplementary Figure A.1: Effect of sex and age group interaction in in-lab measurements. (a) GAITRite and APDM showed a significant age group by sex interaction in in-lab measurements, in which younger males were slower than younger females whereas older males walked faster than older females. (b) Similar trend was observed with uninstrumented measurements as well. The uninstrumented gait speed was computed by dividing the walking distance; i.e., 4 meters, by the average time to walk 4 meters measured by stop watch as part of standard clinic assessment; i.e., SPPB. 99

Supplementary Figure A.2: Effect of day type and bout length on median gait speed. (a) Both age groups walked slower during weekends compared to weekdays,

however, the age group differences were driven by weekdays, not weekends.
(b) Gait speed significantly differed and increased with increasing bout lengths (effect of bout length: $\chi^2 = 557$, $p < 10^{-16}$). Moreover, we observed significant or trending age group differences in all bout lengths (effect of age group: $\chi^2 = 6.62$, $p = .02$) with decreasing effect size; i.e., normalized χ^2 , with increasing bout length..... 100

Supplementary Figure A.3: Quantity of data needed to estimate at-home gait speed reliably is different between younger and older cohorts. (a) Younger participants require at least two days of data to reliably estimate at-home gait speed, whereas (b) older participants require at least 1 day of data. 101

Supplementary Figure A.4: Number of monitoring days required for various criteria. Varying the minimum threshold for steps per day to be considered for analysis between (a) 10, (b) 250, and (c) 1,000 does not impact the quantity of data needed to estimate at-home gait speed reliably but does reduce the participants available for analysis. 102

Supplementary Figure A.5: Reliability of gait speed for weekends vs weekdays. Including one weekend day, but not two, out of three total days only slightly enhances reliability of estimated at-home (a) median and (b) 95th percentile gait speed. Random subsets of data that included three, two, and one weekdays out of three total days were compared to the full data set. 103

Supplementary Figure A.6. Participants instrumented with six wearable devices (Opal, APDM, Inc) located bilaterally on the wrist and foot, and at the lumbar (approximately at the L5 vertebra) and sternum. *(A) Adapted with permission from APDM Wearable Technologies..... 106

Supplementary Figure A.7. Bland-Altman analysis comparing (A) stance time, (B) stride length. and (C) gait speed agreement between GaitPy and APDM Mobility Lab in healthy volunteers (HV) and patients with Parkinson disease (PD)..... 109

Supplementary Figure A.8. A comparison between MDS-UPDRS gait scores and predicted score changes between (Off - ON) visits in patients with Parkinson disease..... 112

Supplementary Figure A.9. STN-GPe network model validation. (A) As expected, based on previous work, population rate in the beta frequency range increases with increasing striatal input. (B) By extension, as previously shown, beta synchrony is quenched by reducing excitability of STN neurons, even in the presence of strong striatal input. 113

LIST OF ABBREVIATIONS

AIC	Akaike information criterion
BG	basal ganglia
BMI	body mass index
EMA	European Medicines Agency
FC	final contact
FDA	Food and Drug Administration
g	unit of gravity
GP	globus pallidus
GPe	globus pallidus externus
H5	hierarchical data format 5
HTML	HyperText Markup Language
Hz	unit of frequency in hertz
IC	initial contact
ICC	intraclass correlation coefficient
IMU	inertial measurement unit
IRB	Institutional Review Board
L5	fifth lumbar spine vertebrae
L-DOPA	levodopa
MDS-UPDRS	Movement Disorder Society-Sponsored Revision of the Unified Parkinson's disease Rating Scale
MEMS	micro-electro-mechanical system

m/s^2	unit of meters per second squared
MSN	medium spiny neuron
PD	Parkinson's disease
R^2	coefficient of determination
R	Pearson correlation coefficient
RMSE	root mean squared error
SPPB	Short Physical Performance Battery
STDP	spike timing-dependent plasticity
STN	subthalamic nucleus
UPDRS	Unified Parkinson's Disease Rating Scale
X^2	chi-squared statistic

CHAPTER ONE: INTRODUCTION

Introductory Overview

Parkinson's disease (PD) is the second-most common neurodegenerative disorder that manifests as a variety of stereotypical motor and non-motor abnormalities (Poewe et al., 2017). PD affects approximately 1 million individuals in the US aged greater than 45 years and global incidence estimates range from 5 to 35 new cases per 100,000 individuals yearly (Marras et al., 2018; Poewe et al., 2017). Despite high prevalence, no disease-modifying treatments currently exist to prevent or slow the progression of PD. Rather, the current standard of care is to manage primary motor and non-motor symptoms.

Novel computational approaches aim to improve symptom monitoring and prognoses for individuals with PD. For over 50 years, the use of the dopamine precursor amino acid, levodopa, to replace lost dopaminergic signal in the nigrostriatal pathway has been the standard of care for managing the symptoms of PD. However, long term adverse effects such as levodopa-induced dyskinesia and end-of-dose wearing off are major drawbacks of current therapeutic options (Rascol et al., 2003). By extension, although dopaminergic treatments can be effective at managing motor symptoms of PD, most do not improve, and can often exacerbate, non-motor symptoms (Wishart & Macphee, 2011). To this end, ongoing clinical trials for treatments covering a broad range of targets aim to improve prognosis (Soderbom, 2020). However, evaluation of therapeutic efficacy suffers from infrequent monitoring and lack of quantitative assessments (Erb et al., 2020). For example, a well-accepted standard for measuring motor fluctuations and

dyskinesias, the Patient Hauser Diary, has significant caveats including reduced compliance, recall bias, and diary fatigue (Papapetropoulos, 2011). Therefore, there is a need for obtaining quantitative, longitudinal endpoints related to everyday functioning and quality of life from individuals with PD (Espay et al., 2019).

Furthermore, in addition to patient monitoring, novel computational algorithms have the potential to improve understanding of underlying disease pathology and create new treatment options (Humphries et al., 2018). For example, abnormally amplified and sustained beta-frequency oscillations (~20 Hz), found throughout the cortico-basal ganglia-thalamic loop, are implicated in motor impairments in PD patients, most significantly with bradykinesia and rigidity at rest (Little & Brown, 2014). Deep brain stimulation treatment has demonstrated that modulation of pathological oscillations can reduce troubling motor symptoms and is currently part of the standard of care for managing symptoms in refractory PD (Hartmann et al., 2019). However, current standard of care deep brain stimulation is ineffective, and can oftentimes exacerbate, gait impairment, speech, and affective and cognitive symptoms, and is thus insufficient for treating dysfunction of multiple circuits (Lozano et al., 2019). Therefore, there is a need for better understanding of systems level network dynamics and development of novel oscillation-modulating therapeutic approaches (Holt & Netoff, 2016). To this end, computational modeling offers the ability to manipulate and record from large simulated networks of neurons, thus providing insight into pathological network dynamics. Current research in computational modeling aims to improve oscillation-modulating treatment

options by generating new insights into the origin and network conditions that facilitate pathological oscillations.

In summary, novel computational analytical approaches are revolutionizing our ability to investigate disease pathology and monitor patient symptoms, thus facilitating development and evaluation of novel therapies that change patient lives. In this dissertation, I aim to leverage new computational techniques toward improving patient monitoring and elucidate a better understanding of the underlying brain pathology of PD. Specifically, I 1) develop and open-source a sensor-based, analytical approach to measure gait in PD patients; 2) evaluate the degree to which sensor-based approaches can measure gait impairment and medication state; 3) evaluate key differences between at-home patient monitoring relative to in-clinic monitoring; and 4) investigate STN-GPe network conditions that facilitate pathological oscillations throughout the cortico-basal ganglia-thalamic loop. It is my hope that the results of this work will help move the needle toward better patient monitoring and a clearer understanding of neuropathology in PD.

Parkinson's Disease Treatment and Evaluation

Background and Treatment

Parkinson's disease affects over 6 million people worldwide, making it the second most common neurodegenerative disorder after Alzheimer's disease (GBD 2016 Parkinson's Disease Collaborators, 2018). Historically, Parkinson's disease has been described by its motor manifestations, most notably tremor, which was the focus of the original clinical description of the disease by James Parkinson in 1817 (Parkinson, 2002). Since then, clinical diagnosis of the disease has expanded to include other cardinal,

movement-related symptoms, including rest tremor, bradykinesia, rigidity, and loss of postural reflexes (Jankovic, 2008). Flexed posture and motor freezing are also among classical signs of Parkinson's disease. In addition to motor symptoms, non-motor symptoms are an increasingly appreciated feature of Parkinson's disease and include autonomic dysfunction; cognitive and neurobehavioral disorders; and sensory and sleep abnormalities (Wishart & Macphee, 2011).

The neuropathology of PD is not fully understood, however the pathological hallmark is α -synuclein protein build up in various regions of the brain as well as accompanied neurodegeneration of dopaminergic neurons in the substantia nigra pars compacta (McGregor & Nelson, 2019). Loss of substantia nigra pars compacta dopaminergic neurons, and consequential striatal dopamine loss, is thought to be the core mechanism underlying cardinal motor symptoms in PD. Currently, there are no disease modifying treatment options for PD, only management of symptoms, and for over 50 years, L-DOPA has been the standard of care. L-DOPA is an amino acid precursor to dopamine and functions by supplementing loss of striatal dopamine. Despite initial effectiveness at treating motor symptoms of PD, chronic L-DOPA exposure leads to motor complications in ~30% of patients after 2-3 years of exposure and greater than 50% after 5 years. Therefore, there is unmet patient need for novel dopaminergic and non-dopaminergic treatments to address L-DOPA-induced motor fluctuations, dyskinesia, and L-DOPA-resistant motor features such as treatment-resistant tremor, freezing of gait, postural instability, falls, and swallowing and speech disturbances (Poewe et al., 2017).

To this end, new treatment options are on the horizon for both managing symptoms and neuroprotection in PD. For example, dopaminergic treatments and invasive, later-line therapies such as deep brain stimulation are in ongoing clinical development for primary motor symptoms of PD. Additionally, various non-dopaminergic therapies are being investigated for management of non-motor symptoms, including psychosis, dementia, and gastrointestinal symptoms. Despite numerous clinical trials to date, no disease modifying treatments have shown therapeutic efficacy. However, compounds targeting α -synuclein aggregates or protecting neurons via alleviation of mitochondrial dysfunction and neuroinflammation are in ongoing development (Soderbom, 2020).

Clinical Evaluation and Limitations

Despite the promising landscape of therapeutic opportunities in PD, the ability to diagnose, evaluate treatment efficacy, and measure progression is limited. PD is clinically defined by the presence of bradykinesia combined with either resting tremor, rigidity, or both (Postuma et al., 2015). However, onset of motor symptoms may only occur years or decades after the earliest, prodromal stages of PD (Gaenslen et al., 2011). Indeed, early manifestations, including constipation, rapid eye movement sleep disorder behavior, hyposmia, asymmetric vague shoulder pain, and depression, are not on their own sufficient to diagnose PD, which therefore leads to a long delay in diagnosis (Bloem et al., 2021). Furthermore, the presence of comorbidity may complicate the diagnostic process, commonly leading to misclassification of early stage PD (Beach & Adler, 2018).

Progression of PD and the effect of treatment to both motor and non-motor symptoms are commonly measured using the Movement Disorder Society-Sponsored Revision of the Unified Parkinson's Disease Rating Scale (MDS-UPDRS) in clinical trials (Goetz et al., 2008). The MDS-UPDRS consists of four parts in which a patient answers a series of questions, completes self-administered questionnaires, and conducts several movement related tasks under the supervision of a trained neurologist. Although the MDS-UPDRS addresses several drawbacks of the previously administered UPDRS developed in the 1980's, including ambiguities in scoring and administration, there are still limitations related to precision of motor symptom measurement, especially in early PD (Holden et al., 2018; Regnault et al., 2019).

Despite widespread use and utility, several challenges exist generally when using patient-reported measures (Kingsley & Patel, 2017). Depending on disease severity, patients may not be in a physical or psychological state to give reliable opinions related to their health. Furthermore, patients may have a preconceived notion concerning how their answers will be interpreted and impact their care leading to adjusting their answers accordingly. To this end, the Hawthorne effect is a concept widely reported that may cause bias, idiosyncratically changing patient behavior when being observed and leading to over or underestimation of health experiences (McCambridge et al., 2014; Pickering et al., 2002). Additionally, difficulty reaching the clinic is a major drawback of in-clinic patient-reported measures. Factors such as remote geographic location, time constraints, and disease outbreaks largely impact recruitment and data collection in clinical research studies.

Another limitation of the MDS-UDPRS is related to mobility assessment and evaluation. Part III of the MDS-UPDRS consists of a motor examination that evaluates various aspects of mobility, including, but not limited to, speech, facial expression, rigidity, tremor, bradykinesia, and gait. For example, in order to evaluate the degree of gait impairment in a PD patient, the patient will be asked to walk at their normal pace approximately 10 meters, before turning around and returning to the examiner. A trained clinician, based on their observations related to stride amplitude, stride speed, height of foot lift, heel striking, turning, and arm swing will assign a rating between 0 and 4 based on the degree of gait impairment (Goetz et al., 2019). The ability for a neurologist to reliably evaluate gait impairment by eye is challenging and may be biased based on the experience of the doctor and how well they are able to see and quantify symptoms. In addition to subjectivity, the UPDRS is burdensome, as it relies on patients, commonly with reduced mobility, to travel and spend several hours at a local clinic. Furthermore, the MDS-UPDRS only provides a description of symptoms during a single snapshot in time. In contrast, symptoms of PD are dynamic and may change over the course of the day depending on various factors, including time of day, day of week, sleep the day before, and timing of medication, especially during later stages of the disease when motor fluctuations are more common.

Alternative methods of symptom measurements exist in addition to the UDPRS. For example, questionnaires and motor diaries are commonly used to monitor symptoms and evaluate treatment efficacy in clinical trials (Hauser et al., 2000; Stacy et al., 2005). The Hauser diary is a written home diary that requires patients to complete an assessment

of functional status every 30 minutes during normal living. The change in time reported in the “OFF” period and “ON” period with troublesome dyskinesia may be used as a clinical marker for treatment efficacy. Despite being a gold standard in clinical trials, the Hauser diary has significant limitations, including reduced accuracy and reliability largely due to poor adherence and recall bias, limited time resolution, added burden to patients, and insufficient measurement of impairment severity (Erb et al., 2020). In summary, gold standard methods for monitoring PD patient disease progression and response to therapy have significant drawbacks. Therefore, new biomarkers and methods for symptom evaluation are needed.

Digital Health Technologies Toward Better Symptom Monitoring

New advances in engineering and computational algorithms have the potential to significantly improve patient monitoring. Specialized camera systems and sensors have been researched and used extensively for decades to quantitatively measure aspects of health such as sleep and gait. However, specialized laboratories and trained technicians are generally needed to conduct these studies and therefore prohibit widespread use for clinicians and clinical studies. In contrast, the past few decades have seen the emergence of many technologies that facilitate remote monitoring, including sensor-embedded smart phones, wearable devices, smart home equipment and appliances, and interconnectivity of embedded computing devices in everyday objects via the internet (Majumder & Deen, 2019; Morgan et al., 2020).

Remote patient monitoring has the capacity to address many limitations of traditional clinical assessments including observer bias, difficulty reaching a clinic, and

subjective measurements. Additionally, researchers, clinicians, and patients are hopeful that digital health technologies will provide a more complete picture of disease burden. At-home patient monitoring has the potential to provide a nuanced perspective not currently provided by in-clinic assessments of micro level detail, including continuous symptom measurement and medication response, and macro level detail, including habitual behavioral patterns, activity levels, and sleep quality (Del Din, Godfrey, Mazzà, et al., 2016). For clinicians and patients, improved measurement may contribute to enhanced symptom management and care, thus improving patient outcomes. From the industry perspective, the potential for early disease identification and progression monitoring, better diagnostics, enhanced recruitment and assessment of treatment efficacy are attractive aspects of digital health technologies.

Over the past decade, positive regulatory engagement and feedback is bolstering the development of digital health technologies. The concept of digital health has evolved significantly since its first introduction in 2000 as encompassing internet-focused applications and media to improve medical content, commerce, and connectivity (S. R. Frank, 2000; Mathews et al., 2019). Since then, regulatory authorities, such as the Food and Drug Administration (FDA), have expanded the scope of digital health to include categories such as mobile health, health information technology, wearable devices, telehealth and telemedicine, and personalized medicine. Key guidance were issues in 2016 by the FDA and World Health Organization regarding evaluation and validation frameworks for all digital health solutions (Guo et al., 2020). Additionally, targeted guidance on solution classification and evidence requirements, including the FDA Pre-

certification Program, are enabling streamlined approval of digital health solutions (*Digital Health Software Precertification (Pre-Cert) Program, 2021*). Regulatory initiatives will continue to facilitate development and productionization of digital health technologies toward revolutionizing healthcare.

Challenges for Sensor-Based Measurement

Improvements in form factor and battery life have enabled small wearable inertial measurement unit (IMU) devices to continuously record inertial data for periods of days and weeks in free-living settings. The small form factor and extended battery life reduces burden to patients as the device is not overly intrusive or uncomfortable and removal for charging is unnecessary. Despite advancements, several challenges exist before clinical adoption of wearable sensors.

First, data acquired from wearable devices in raw form is challenging to interpret. This is especially true considering traditional signal processing-based time series features lack clinical relevance and interpretability. Therefore, computational algorithms are needed to translate raw inertial data into clinically interpretable symptom features that are relevant to patient function and quality of life. Indeed, the past several decades have produced a large array of tools and algorithms that aim to measure a variety of symptoms. Despite progress, lack of open-source algorithms are available for research and clinical studies, thus limiting accessibility and standardization of measurement approaches.

Another challenge facing widespread clinical adoption of wearable sensor technologies is lack of standardization and sufficient validation. Generally speaking, studies demonstrating analytic approaches, outcome measures, protocol design, devices,

and device placement are small and inconsistent (Del Din, Godfrey, Mazzà, et al., 2016). The lack of large scale studies and study variability lead to difficulty comparing results and increases uncertainty in the interpretation of results (Walton et al., 2020). For example, gait speed may seem like a straightforward clinical feature that can be measured in at-home environments. However, differences between how algorithms define walking bouts (whether length cutoffs exist for bouts or whether minimum step requirements exist for shorter bouts) may critically impact post-hoc statistical analysis (Del Din, Godfrey, Mazzà, et al., 2016). Therefore, standardized devices, algorithms, protocols, and evidence frameworks are needed in order to support regulatory acceptance and clinical adoption.

Neuroanatomy and Significance of Gait

Research to develop and validate standardized algorithmic solutions to translate raw inertial data to meaningful patient symptom measurements is needed. One active area of research, largely applicable to PD, is the use of wearable sensors to measure gait. Specifically, gait speed has been regarded as the sixth vital sign and is a significant component of patient quality of life (Middleton et al., 2015). Previous literature has shown gait to be influenced by various factors including age, personality, and mood and there is strong association between gait speed and general health and mortality (Pirker & Katzenschlager, 2017).

Studies in feline animal models have been largely used to study the nervous system regulation of gait. Higher order brain regions, including the cerebral cortex and basal ganglia, have been shown in decerebrate cats to play a role in skilled locomotor performance and goal-oriented gait behavior. Specifically, bilateral pyramidal tract

lesions in cats leads to severe impairment of skilled locomotor performance on tasks requiring the cat to walk along a narrow beam or ladder (Liddell & Phillips, 1944). In addition to skilled locomotion, higher order brain regions have a role controlling goal-oriented gait behavior. For example, bilateral removal of the caudate nucleus in cats results in a persistent approach-attachment behavior in which the cat will approach and attempt to contact any moving person, cat, or object, seemingly unable to terminate the locomotor behavior (J. R. Villablanca, 2010). Furthermore, removal of both cerebral cortex and striatum results in incessant gait, without the necessity of any external stimulus (J. Villablanca & Marcus, 1972).

In addition to the effect of higher order brain regions on gait, lower level brain regions such as the brainstem and spinal cord also play a large role in healthy gait behavior. For example, when a decerebration is made at the precollicular-premamillary level, cats retain the ability to spontaneously initiate locomotion and maintain postural control, albeit gait is machine-like and control of distal forelimb is often defective (Armstrong, 1986; Hinsey et al., 1930). However, a slightly lower transection at the precollicular-postmamillary level disrupts the cat's ability to spontaneously elicit gait and introduces the need for electrical or chemical stimulation to the midbrain locomotor region (which roughly corresponds to the cuneiform nucleus and pedunculopontine tegmental nucleus in humans) in order to initiate locomotion (Takakusaki, 2017). The critical brainstem region between these transactions is recognized as the subthalamic locomotor region, and mostly corresponds to the lateral hypothalamic area. In addition to multiple areas of the brain controlling gait, spinal neural circuitry, termed central pattern

generators, are also crucial for basic locomotor motor pattern. All of these processing steps have their own impact on the ability to walk normally. To this end, gait may be impacted in specific ways based on the particular pathogenesis of neurodegenerative disease.

The complex, multimodal nature of gait regulation facilitates the ability to measure nervous and muscular system disruptions by measuring specific characteristics of gait, thus provide insight into the state and progression of neurodegenerative and muscular disorders. In the case of PD, gait impairment and freezing of gait progressively worsen from early to later stages of the disease and can offer insight into disease severity and subtype (Mirelman et al., 2019). For example, in the early stages of PD, patient gait speed slows, step length shortens, arm swing amplitude shortens, and interlimb asymmetry is common. In contrast, gait in mild-to-moderate and advanced stage PD is altered, so that asymmetry decreases, double limb support increases, and cadence increases, reflecting a stereotypical shuffling of gait. Additionally, trouble initiating gait, freezing of gait, and higher fall risk become more pronounced as disease severity progresses. Thus, gait features serve as a method to observe severity and progression of disease. Additionally, gait may be used to monitor the effect of treatment. To this end, dopaminergic treatments generally improve certain aspects of impaired gait including speed and step length. However, many temporal gait characteristics may not respond to dopaminergic medication, and in fact, dopaminergic treatment can even further impair gait via L-DOPA-induced motor fluctuations, freezing of gait, postural instability, and

falls (Mirelman et al., 2019; Poewe et al., 2017). Therefore, gait may act as a useful marker for therapeutic effect.

Furthermore, measuring gait provides utility not only for PD patients, but for various muscular and neurodegenerative disease patients. Gait can be affected at multiple locations in the nervous and musculoskeletal systems. In PD, gait and postural disturbance is thought to be impacted via several mechanisms, including disturbances in dopaminergic and cholinergic systems, cognitive impairment leading to failure of integrative sensory processing, impaired motor cortical areas, and disturbances in posture-gait areas of the brainstem (Takakusaki, 2017). However, there are many neurodegenerative diseases and muscular dystrophies that produce their own unique symptoms of gait impairment based on affected locations. For example, Friedreich's ataxia is the most common inherited ataxia that consists of peripheral sensory neuropathy, spinocerebellar tract degeneration, and cerebellar pathology that manifests as characteristically unsteady gait with loss of balance and incoordination of the lower extremities (Ashizawa & Xia, 2016; Cook & Giunti, 2017). In contrast, knee osteoarthritis is a particularly common arthritis that consists of joint disease creating meaningful differences in knee adduction, flexion moment, and flexion angle during gait (Favre & Jolles, 2016). In each case, unique gait signatures can be measured to provide insight into disease state and treatment effect.

Sensor-Based Gait Measurement

In order to measure clinical aspects of gait, gait can be broken down into component parts. To this end, temporal features describe the amount of time it takes for a

patient to accomplish certain phases of a stride. For example, the stance phase of gait, refers to the period between when the heel first touches the floor and the toe, of that same foot, comes off the floor. In contrast, spatial features, such as stride length, measure distances of particular phases of gait. Healthcare specialists evaluate patient health using a variety of spatiotemporal gait parameters (Muro-de-la-Herran et al., 2014).

Recently, novel algorithms have been proposed to derive spatiotemporal components of gait using inertial measurement unit (IMU) devices. IMU devices consist of a micro-electro-mechanical system (MEMS) transducer that transforms mechanical movement signal into an electrical signal (Brognara et al., 2019). A MEMS device of significant interest to the digital health community is the accelerometer. Due to minimal size, battery efficiency, and reduced cost, accelerometers have been the subject of significant research efforts with the goal of developing a patient compliant method of translating electrical, time-series signals into clinically relevant information (Del Din, Godfrey, Mazzà, et al., 2016).

Various numbers and placements of IMU devices have been proposed for measuring biomechanical behaviors, such as gait. Generally speaking, the closer a device lies to the movement of interest, the better the data quality and ability to measure that movement is. However, other logistics come into play when attempting to measure patient movement in free-living conditions. For example, device wearability and comfort is a major requirement when designing digital health solutions. The detriment of non-compliance for a particular device or a particular location supersedes any benefit of an exceptionally accurate algorithm. Furthermore, battery life and number of sensors are

also considerations when choosing a device. For example, a device that does not require a patient to remove, charge, and place the device back on at a later time is largely beneficial compared to a device requiring frequent charging. To this end, the requirement of multiple sensors adds additional burden to patients. Therefore, various logistics, such as device, number of devices, and placement, must be considered when developing a digital health solution.

One sensor set-up, that has been largely investigated by several research labs, consists of a single device on the lower back (Del Din, Godfrey, & Rochester, 2016a; Esser et al., 2011, 2012; Trojaniello et al., 2014, 2015). In fact, a recent review of relevant articles from 2008-2018 reports the most common set-up is a single sensor (13/36) and the most common placement of a single sensor is the lower back (8/13) (Brognara et al., 2019). The benefits of a sensor on the lower back for measuring gait include the ability to measure gait features from both sides of the body using a single sensor, measurement of asymmetries, measurement of other relevant clinical behaviors such as sit-to-stand transitions, and overall patient willingness to wear the device on the lower back location.

A recently proposed algorithm for estimating temporal features of gait from the lower back has shown strong validity compared to other approaches (McCamley et al., 2012), reliability in patient populations (Trojaniello et al., 2015), and robustness to small variabilities in positioning at the lower back (Trojaniello et al., 2014). The approach leverages a gaussian continuous wavelet and peak detection to estimate initial (heel strike) and final (toe off) contacts toward estimation of temporal gait features (McCamley

et al., 2012). The approach becomes quite powerful in combination with another robust inverted pendulum model algorithm to measure spatial features of gait (Del Din, Godfrey, & Rochester, 2016a; Zijlstra & Hof, 2003). Despite these novel approaches, a standardized, open-source implementation of these algorithms does not exist, thus limiting accessibility, replication of results, and improvements from the community. By extension, questions remain regarding sensor-based algorithm effectiveness at measuring patient relevant changes in gait, including degree of impairment and effect of treatment.

CHAPTER TWO: GAITPY: AN OPEN-SOURCE PYTHON PACKAGE FOR GAIT ANALYSIS USING AN ACCELEROMETER ON THE LOWER BACK

Published in: Journal of Open Source Software

Authors

Matthew D. Czech^{1,2}

Shyamal Patel¹

Affiliations

¹ Department of Anatomy and Neurobiology, Boston University School of Medicine, Boston, MA, USA

² Early Clinical Development, Pfizer Inc., Cambridge, MA, USA

Introduction

Gait impairments are present across a broad range of conditions and often have a significant impact on the functional mobility and quality of life of an individual.

Clinicians and researchers commonly assess gait using either observational scales (e.g. Unified Parkinson's Disease Rating Scale) or performance-based tests (e.g. timed-up-and-go). However, these assessments can only be performed intermittently because of the need for a trained clinician. In contrast, wearable devices can be used for continuously capturing data from sensors (e.g. accelerometer, electrocardiogram) outside the clinic. Recently, several groups (Del Din, Godfrey, & Rochester, 2016a; McCamley et al., 2012; Trojaniello et al., 2014; Zijlstra & Hof, 2003) have published algorithms for deriving features of gait from data collected using inertial sensors like accelerometers. However,

an implementation of these algorithms is not readily available to researchers, thus hindering progress.

GaitPy is an open-source Python package that implements several published algorithms in a modular framework for extracting clinical features of gait from a single accelerometer device mounted on the lower back (L5 vertebra, illustrated in figure 2.1). The package has been developed to make it easy for researchers to derive measures of gait from raw accelerometer data. As shown in figure 2.2, the package includes modules with three main functions: 1) classify bouts of gait; 2) extract clinical features of gait from each bout; and 3) visualize detected gait events.

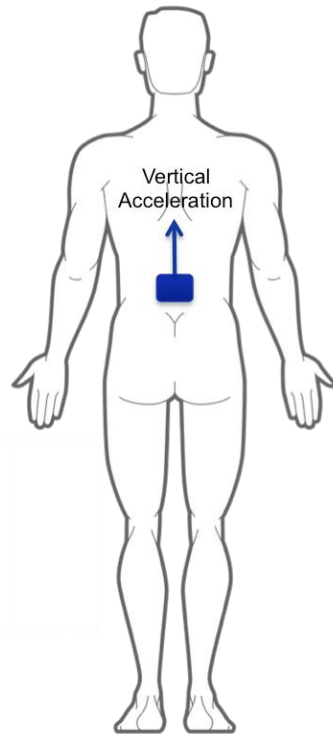


Figure 2.1. Location of the wearable device on the lower back and orientation of the vertical acceleration axis of the accelerometer relative to the body.

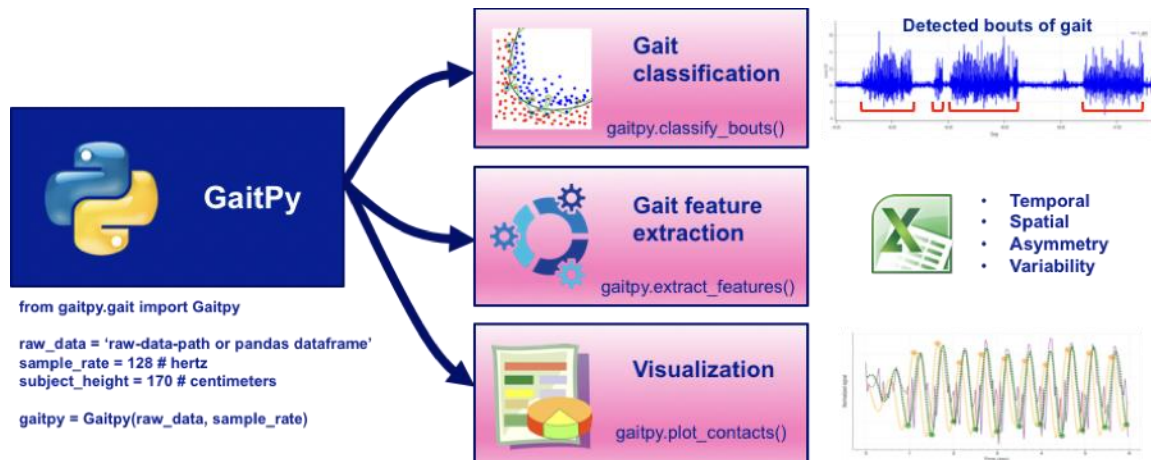


Figure 2.2. A high-level overview of GaitPy API and functions associated with various modules.

Processing Pipeline

GaitPy can be used to derive gait features from data collected in the clinic as well as under free- living conditions (e.g. at home). The package accepts input data in a customizable format, thereby not restricting the user to a standard file type. GaitPy utilizes vertical acceleration data from a wearable device located on the lower back (lumbar region) and consists of three main processing modules.

classify_bouts is an optional module intended to be used for processing data collected under free-living or unsupervised conditions. The module uses a pre-trained gait classification model to detect bouts of gait from a continuous stream of raw accelerometer data. It first converts data to units of gravity (g) and down-samples it to 50Hz. Data is then segmented into non- overlapping 3-second epochs and signals features are derived for each epoch. The pre-trained gait classification model then classifies each 3-second epoch as gait or not-gait.

extract_features module utilizes a Gaussian continuous wavelet transform based approach (McCamley et al., 2012) and inverted pendulum model (Zijlstra & Hof, 2003) to calculate spatial and temporal gait features. Vertical acceleration data is first converted from units of gravity (g) to meters per second squared (m/s^2) and down-sampled to 50 Hz. Using the approach described in Del Din et al. 2016 (Del Din, Godfrey, & Rochester, 2016a), we then derive spatial and temporal features of gait. Additionally, an optimization procedure is performed to remove extraneous event detections and is described in more detail below. The `extract_features` module expects data segments that only contain gait. So, if input data consists of both gait and non-gait data, it is recommended to first apply the `classify_bouts` function in order to identify periods of gait at the resolution of 3-second epochs. `extract_features` will then concatenate concurrent 3-second epochs of gait into bouts and extract features for each bout.

plot_contacts module generates an interactive plot of raw data along with the initial and final contact events detected by the gait event detection algorithm (McCamley et al., 2012). The plot facilitates debugging and presentation of results.

Outputs

As shown in figure 2.2, the outputs of GaitPy modules include classification of gait bouts, a set of gait feature values extracted for each bout, and a plot of raw sensor data marked with detected gait events (initial contact/heel strike and final contact/toe off).

We describe outputs of each of the processing modules below:

classify_bouts generates a pandas dataframe or a H5 file containing the following columns:

- a) `window_start_time`: Unix timestamp associated with the beginning of each 3-second epoch in the data.
- b) `window_end_time`: Unix timestamp associated with the end of each 3-second epoch in the data.
- c) `prediction`: Output of the gait classification model (1=gait or 0=not gait) for each 3-second epoch in the data.

extract_features generates a pandas dataframe or a csv file containing:

- a) Bout number for each bout detected by `classify_bouts` (column name: `bout_number`).
- b) Length of bout in seconds (column name: `bout_length_sec`).
- c) Start time of bout (column name: `bout_start_time`).
- d) Total number of steps detected within each bout (column name: `steps`).
- e) Initial and final contact event timestamps in Unix time (column names: `IC` and `FC` respectively).
- f) Values of the following gait features are derived per stride: stride duration, step duration, cadence, initial double support, terminal double support, double support, single limb support, stance, swing, step length, stride length, gait speed. In addition, we calculate variability and asymmetry associated with a set of features.

plot_contacts generates a HTML file containing an interactive time-series plot of raw vertical acceleration data labeled with detected gait events and bouts (shown in figure 2.3).

- a) Initial contact: The moment in the gait cycle when foot touches the ground (i.e. heel strike)
- b) Final contact: The moment in the gait cycle when foot lifts off the ground (i.e. toe off)
- c) Gait bouts: A green vertical line marks the beginning of each detected gait bout and a red vertical line marks the end of the bout (Figure 2.3).

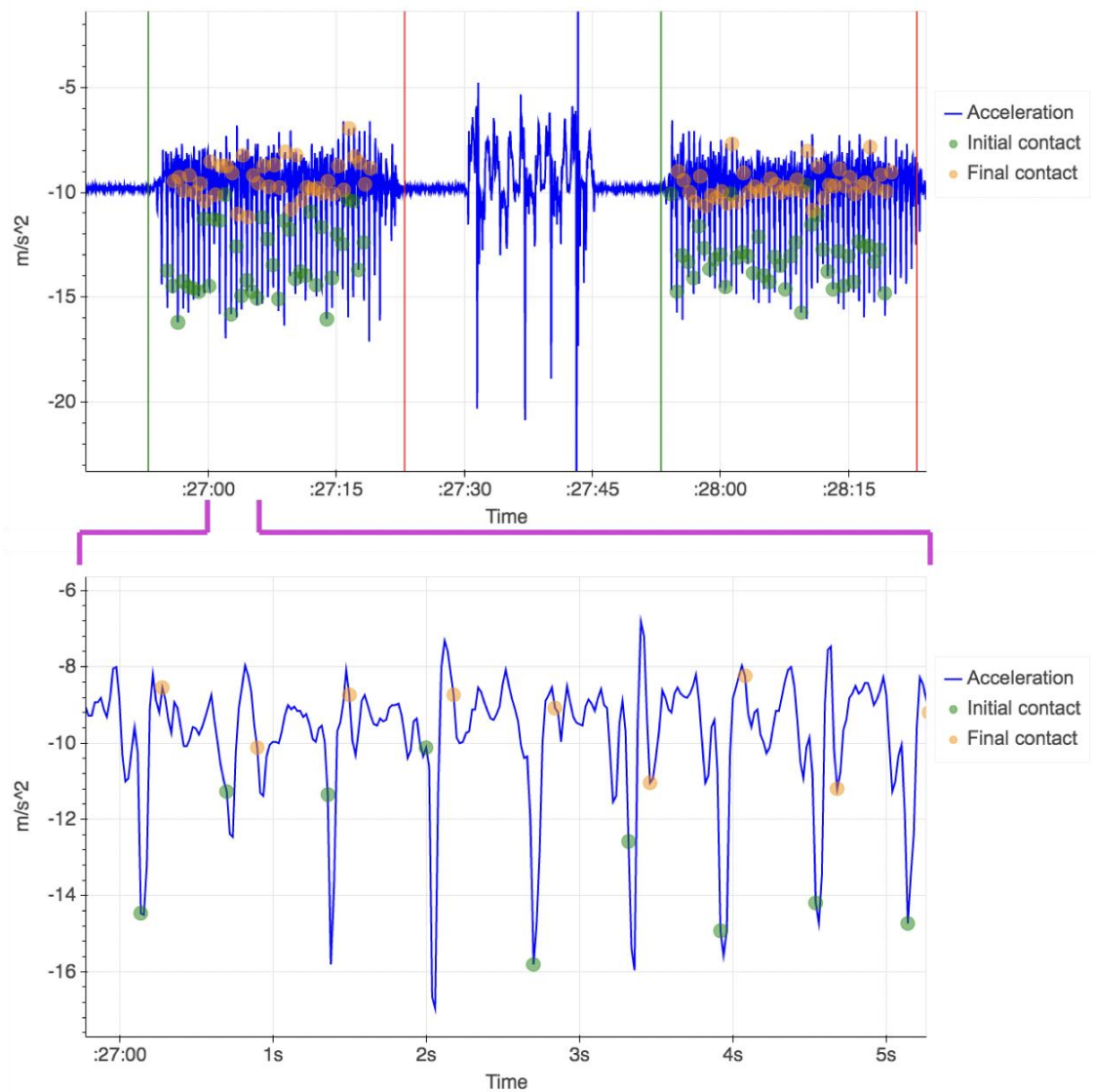


Figure 2.3. Time-series plot generated by plot_contacts module of the raw vertical acceleration data labeled with detected gait events (initial contact/heel strike and final contact/toe off) and bout classifications. The start and end times of classified bouts are labeled by green and red vertical lines respectively. During the period shown, the participant walked for about 30 seconds, paused, performed 5 sit-to-stand repetitions, paused again, and continued walking for about 30 seconds.

Algorithms

GaitPy includes two key algorithms for processing raw accelerometer data to derive gait features. The first algorithm is used for detecting bouts of gait from continuous accelerometer data collected under free-living conditions and the second algorithm derives temporal and spatial features of gait from pre-identified bouts of gait. Below is a brief description of the algorithms.

Gait Classification

In order to derive gait features from data collected under free-living conditions, it is essential to identify periods of walking activity. GaitPy includes a pre-trained random forest (Breiman, 2001) binary classifier that operates on time and frequency domain features extracted from 3-second epochs of vertical acceleration data. Prior to feature extraction, raw vertical acceleration data is down-sampled to 50Hz and band-pass filtered using a 0.5-3Hz 1st order Butterworth filter. Extracted signal features include dominant frequency, the ratio of the energy associated with the dominant frequency component to the total energy, the range of amplitude, the root mean square value of the signal, and the signal entropy. Gaitpy's classify_bouts module applies this binary classifier to input data to classify each non-overlapping 3-second epoch as either gait or not-gait.

Gait Features

GaitPy implements a slightly modified version of a Gaussian continuous wavelet-based method (McCamley et al., 2012) and an inverted pendulum model (Zijlstra & Hof, 2003) to extract features from data collected during bouts of gait.

Three post-processing steps are applied to remove extraneous stride detections beyond physiological limits. Step 1: Strides longer than 2.25 seconds or shorter than 0.25 seconds are removed (Najafi et al., 2003). Step 2: Strides with stance times exceeding 70% of the maximal stride time of 2.25 seconds are removed (Hollman et al., 2011). Step 3: Strides with an initial double support that exceed 20% of the maximal stride time of 2.25 seconds are removed (Hollman et al., 2011).

Acknowledgements

The Digital Medicine & Translational Imaging group at Pfizer, Inc supported the development of this package.

License

This project is licensed under the MIT License - see the LICENSE.md file for details

**CHAPTER THREE: AGE AND ENVIRONMENT-RELATED DIFFERENCES IN
GAIT IN HEALTHY ADULTS USING WEARABLES**

Published in Nature Partner Journals: Digital Medicine

Authors

Matthew D. Czech ¹

Dimitrios Psaltos ¹

Hao Zhang ¹

Tomasz Adamusiak ¹

Monica Calicchio ¹

Amey Kelekar ¹

Andrew Messere ¹

Koene R. A. Van Dijk ¹

Vesper Ramos ¹

Charmaine Demanuele ¹

Xuemei Cai ¹

Mar Santamaria ¹

Shyamal Patel ¹

F. Isik Karahanoglu ¹

Affiliations

¹ Early Clinical Development, Pfizer, Inc., Cambridge 02139 MA, USA.

Abstract

Technological advances in multimodal wearable and connected devices have enabled the measurement of human movement and physiology in naturalistic settings. The ability to collect continuous activity monitoring data with digital devices in real-world environments has opened unprecedented opportunity to establish clinical digital phenotypes across diseases. Many traditional assessments of physical function utilized in clinical trials are limited because they are episodic, therefore, cannot capture the day-to-day temporal fluctuations and longitudinal changes in activity that individuals experience. In order to understand the sensitivity of gait speed as a potential endpoint for clinical trials, we investigated the use of digital devices during traditional clinical assessments and in real-world environments in a group of healthy younger ($n = 33$, 18–40 years) and older ($n = 32$, 65–85 years) adults. We observed good agreement between gait speed estimated using a lumbar-mounted accelerometer and gold standard system during the performance of traditional gait assessment task in-lab, and saw discrepancies between in-lab and at-home gait speed. We found that gait speed estimated in-lab, with or without digital devices, failed to differentiate between the age groups, whereas gait speed derived during at-home monitoring was able to distinguish the age groups. Furthermore, we found that only three days of at-home monitoring was sufficient to reliably estimate gait speed in our population, and still capture age-related group differences. Our results suggest that gait speed derived from activities during daily life using data from wearable devices may have the potential to transform clinical trials by non-invasively and unobtrusively providing a more objective and naturalistic measure of functional ability.

Introduction

Gait is the primary means of mobility for most individuals and many conditions directly or indirectly have an impact on gait. Gait speed is considered an informative and reliable clinical measure in a wide range of disease populations; it is often referred to as the sixth vital sign (Fritz & Lusardi, 2009; Middleton et al., 2015). Previous studies have shown that lower gait speed is associated with cognitive decline, falls, and mortality (Hornyak et al., 2012; Pirker & Katzenschlager, 2017) and is an important indicator of health and function in ageing and disease (Peel et al., 2012). Conventional gait assessment is performed in the laboratory or clinic using a combination of observational scales (e.g. functional gait assessment) and performance tests (e.g. 6-minute walk test) where individuals perform prescribed walking tests under observation. These types of assessments may not be able to provide a reliable estimate of real world gait because 1) they are administered episodically, 2) can be subjective in nature, and 3) gait can be altered under observation (Hawthorne effect) (Mayo, 1934; McCambridge et al., 2014).

Advances in wearable technology have enabled the measurement of gait using inertial sensors in free-living conditions (Tao & Feng, 2012). Using ground truth references such as instrumented mats and motion capture systems, researchers have validated novel gait measurement approaches that rely on a small number of battery-efficient inertial sensors (Godfrey et al., 2015; Trojaniello et al., 2014). Comparative analysis has revealed that while these methods generally perform well, there are considerations such as study population and device location that can influence the reliability of measurements (Storm et al., 2016; Trojaniello et al., 2015). Therefore, the

validity of such methods needs to be rigorously assessed in different populations to establish their performance characteristics. In addition to assessing the accuracy with which they can measure spatial and temporal aspects of gait, it is also necessary to evaluate the sensitivity of measures derived during daily life for detecting clinically meaningful changes. Shah et al. showed that measures of quantity were able to better discriminate between patients with multiple sclerosis and controls whereas measures of quality were more discriminative for patients with Parkinson's disease (PD) and controls (Shah et al., 2020).

There is a growing body of research showing that gait assessments performed under controlled conditions (e.g. in the laboratory or clinic) are unable to capture the variability observed during daily life (e.g. in the home and community) (Brodie et al., 2016; Hillel et al., 2019; Mueller et al., 2019; Takayanagi et al., 2019). Specifically, gait speed derived from data captured under continuous free-living conditions is slower than gait speed measured in the clinic in frail elderly or community-dwelling older adults (Takayanagi et al., 2019). It has been hypothesized that continuous, at-home monitoring provides a richer and more comprehensive view of an individual's experience with the disease (Del Din, Godfrey, Mazzà, et al., 2016; Maetzler & Rochester, 2015). In fact, Del Din et al. showed that distinguishing PD patients and healthy volunteers using gait characteristics was improved in free-living conditions (Del Din, Godfrey, Galna, et al., 2016). In addition to the prospect of enhanced sensitivity of measurements, at-home monitoring has the potential to improve patient engagement in clinical research studies by reducing the need for frequent visits to the clinic, enabling more patients to participate,

and reducing the burden on patients and caregivers. For these reasons, at-home measurements are gaining traction as valid clinical endpoints from regulatory agencies. For example, the European Medicines Agency (EMA) recently approved 95th percentile stride velocity measured using a valid and suitable wearable device, as an acceptable secondary endpoint in pivotal or exploratory clinical studies for Duchenne muscular dystrophy (Committee for Medicinal Products for Human Use (CHMP), 2019).

Despite growing evidence that at-home monitoring provides a more comprehensive assessment of gait, several hurdles need to be addressed to enable broader clinical adoption. Further clinical research that adopts and validates standardized sensor-based methods in various populations under free-living conditions is needed to translate research findings and novel methods into practice (Steins et al., 2014). Additionally, questions remain regarding the processing and interpretation of at-home data (Hubble et al., 2015). An open question is the optimal monitoring duration necessary for reliable characterization of gait under free-living conditions. Obtaining data from multiple days and investigating day-to-day variability of at-home measures is necessary in order to assess the minimum required acquisition period and obtain reliable real-world estimates. However, additional days of monitoring results in increased patient burden and might reduce compliance in clinical trials, especially for patients suffering from particularly debilitating diseases. The required number of at-home monitoring days still remains arbitrary and can be affected by multiple factors such as the type of disease, treatment, age, geographical location, and socioeconomic status. In fact, previous studies have used data captured during monitoring durations that ranged from one day to several weeks for

their analysis (de Bruin et al., 2007; Del Din, Godfrey, Galna, et al., 2016; Godfrey et al., 2014; Orendurff et al., 2008; Weiss et al., 2011). Several studies have also investigated day-to-day variability of at-home measures (de Bruin et al., 2007; Gretebeck & Montoye, 1992; Hart et al., 2011; Kang et al., 2014; Levin et al., 1999; Matthews et al., 2002; Van Schooten et al., 2015). These studies have reported a minimum of three to six days of measurements required to obtain reliable estimates of physical activity, energy expenditure, and heart rate. However, the monitoring duration necessary for deriving a reliable estimate of gait speed under free-living conditions is not well understood. We are aware of only one recent study that reported a minimum monitoring duration of three days for reliable estimation of gait speed in slow-walking older adults with sarcopenia (Mueller et al., 2019).

Herein, we present our work on assessment of gait in healthy younger (18-40 years) and older (65-85 years) adults in both the laboratory and home setting using a single lumbar-worn wearable accelerometer. We aim to 1) assess the validity of measurements derived using the lumbar-worn wearable device by comparing them with those provided by a system that use multiple wearable devices (APDM) and an instrumented mat (GAITRite), 2) test the sensitivity of the median and 95th percentile gait speed derived from in-lab walk test and continuous at-home monitoring data to detect age-related group differences, and 3) propose a minimal at-home monitoring period for estimating gait speed reliably.

Results

Gait Speed Can Be Derived Accurately From Single Lumbar-Worn Accelerometer.

During in-lab assessments, participants walked three 4-meter laps on an instrumented mat (GAITRite) at their typical walking speed. While performing the task participants wore 6 devices (Opal, APDM), which were located at the sternum, lumbar, and bilaterally on the wrists and feet. We assessed the accuracy and reliability of gait features derived using 1) the APDM (6 sensor set) method (Mancini & Horak, 2016) and 2) the GaitPy (single lumbar-mounted sensor) method (M. D. Czech & Patel, 2019) by comparing them with gait features provided by GAITRite (considered here as the gold standard). Figure 3.1 depicts the agreement of gait speed derived from APDM and GaitPy with respect to the GAITRite through correlation and the Bland-Altman plots. The intraclass correlation coefficient (ICC) between gait speed derived using the three methods showed moderate agreement (ICC = .66, lower and upper bounds = [.27 - .83]). While GaitPy had higher variability than APDM measurements (GAITRite vs GaitPy ICC = .49, lower and upper bounds = [-.07 - .77], after mean bias correction ICC = .72, lower and upper bounds = [.63 - .79]), both APDM and GaitPy had good agreement with GAITRite. The distributions of both APDM and GaitPy derived gait speeds were

	Younger	Older	<i>p</i> Value
Number of participants	33	32	
Sex (F/M)	17/18	16/18	1
Age (years)	29.2 ± 4.6 [23–39]	72.3 ± 8.8 [65–85]	
BMI (kg/m ²)	23.4 ± 2.6 [19–29]	24.5 ± 2.6 [19–29]	0.9
Education	13 College 20 Postgrad	3 High school 7 College 22 Postgrad	0.14
Ethnicity	25 White 6 Asian 2 Other	30 White 1 Asian 1 Other	0.07

In total, 65 participants were included in the study, which was conducted at the Pfizer Innovation Research Laboratory (PfIR Lab), MA. The younger and older age groups were equibalanced in terms of sex and BMI. The younger group included one American Indian or Alaska Native, and one Native Hawaiian or Pacific Islander; the older group included one Black or African American participant, which were included in the "other" category. *BMI* body mass index.

Table 3.1. Participant Demographics

homoscedastic with consistent

mean biases with respect to

GAITRite (GAITRite - APDM =

.07m/s (5%), GAITRite - GaitPy =

.17m/s (13%).

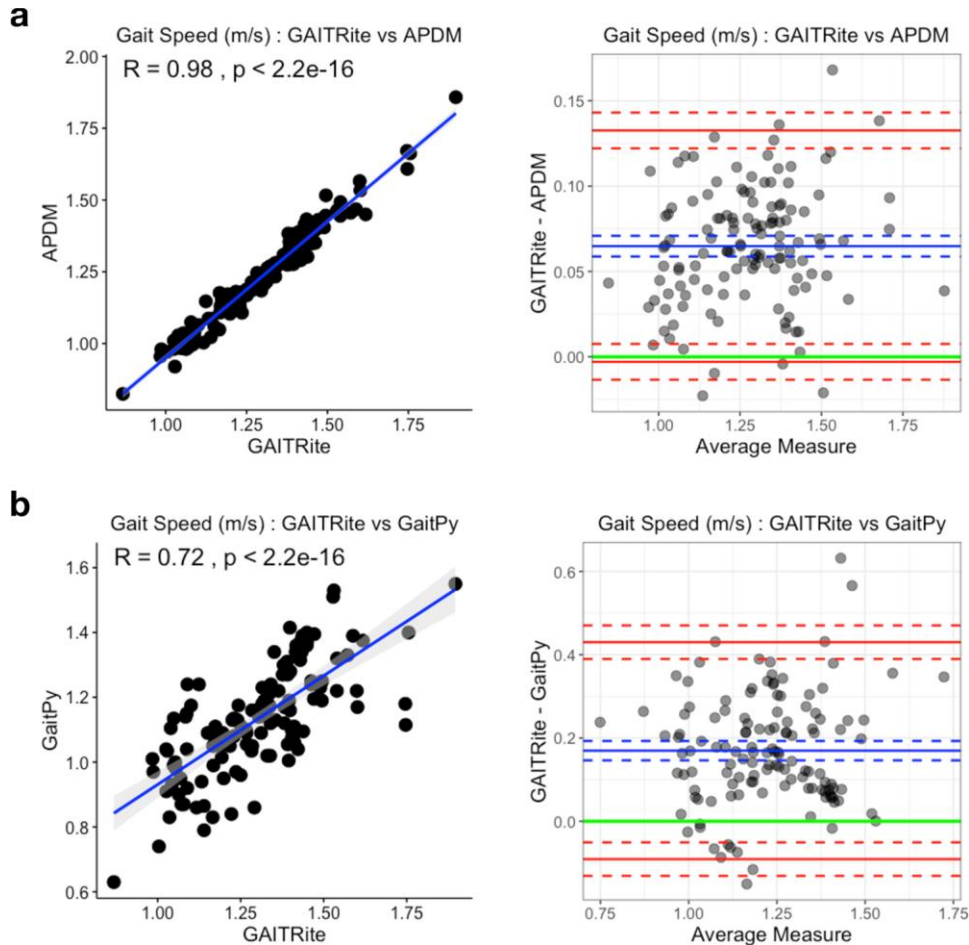


Figure 3.1. Gait speed validation based on in-lab 4-m gait task. **a** Comparison of gait speed estimated using a six-sensor system (APDM) and an instrumented gait mat (GAITRite). The gait speeds derived from two systems were highly correlated (Pearson's $r = 0.98$, left). Bland–Altman plots (right) showed minimal mean difference (mean difference = 0.07, blue solid line; LoA = $[-0.03, 0.13]$, red solid lines; corresponding confidence intervals are in dashed lines). **b** Comparison of gait speed estimated using a single lumbar-worn sensor (GaitPy) and an instrumented gait mat (GAITRite). The gait speeds derived from two systems were also highly correlated (Pearson's $r=0.72$, left). Bland–Altman plots (right) showed mean difference (mean difference = 0.17, blue solid line; LoA = $[-0.09, 0.43]$ red solid lines; corresponding confidence intervals are represented by dashed lines). Both APDM and GaitPy had consistent bias compared to GAITRite and underestimated gait speed. LoA limits of agreement.

In-Lab Gait Speed Did Not Distinguish Between Age Groups.

In order to test if gait speed differs between the younger and older age groups (younger group, $n = 33$, age= 29.2 ± 4.6 years; older group, $n=32$, age= 72.3 ± 5.8 years,

full demographics in Table 3.1), we first performed group analysis on the in-lab gait speed. The overall repeated measures regression model included methods (GAITRite/APDM/GaitPy), age group (younger/older), visit (visit1/visit2), sex (F/M), height, and muscle mass as independent variables (fixed effects) and subject (random effect). The average gait speed estimated by different methods was significantly different (main effect of method: $X^2 = 199$, $p < 10^{-16}$; Fig. 3.2a). Pairwise comparisons further showed that both APDM (6-sensor) and GaitPy (single lumbar sensor) underestimated in-lab gait speed compared to GAITRite (p values of all pairwise comparisons $< 10^{-6}$). There was no main effect of age group ($X^2 = .28$, $p = .6$). When pairwise comparisons of the age group differences were tested, none of the methods were able to differentiate between younger and older groups (Fig. 3.2b). There were a trending main effect of visit ($X^2 = 3.79$, $p = .051$), significant age group by sex interaction ($X^2 = 5.43$, $p = .02$), and age group by sex by method interaction ($X^2 = 14.67$, $p < 10^{-3}$). No other variables or covariates had significant effects on gait speed.

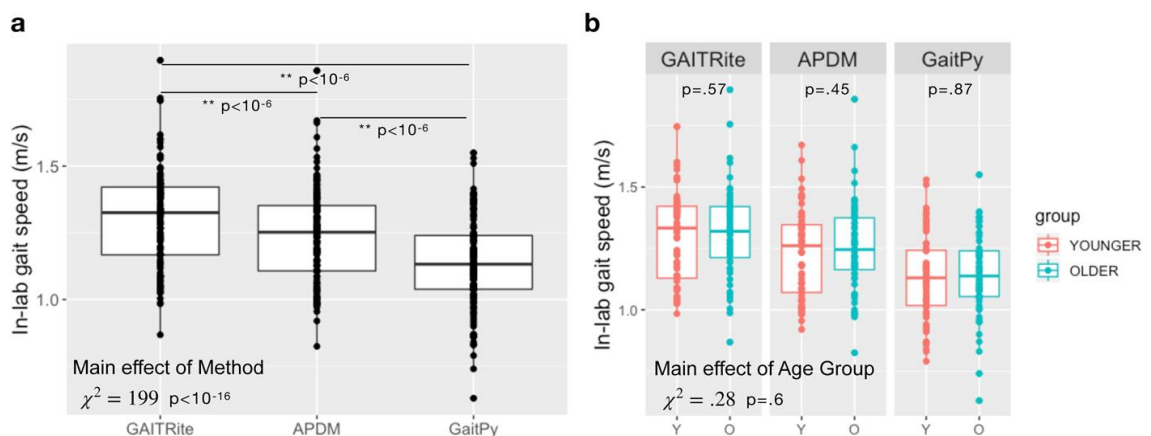


Figure 3.2. In-lab gait speed did not show any age group differences. a Gait speed estimated using different methods differed ($\chi^2 = 199$, $p < 10^{-16}$). Both APDM and GaitPy underestimated gait speed during in-lab gait task compared to GAITRite ($p < 10^{-6}$), which is used as the gold standard. **b** Gait speed estimated using any of the three methods did not differ between the two age groups (younger group, $n = 33$, age = 29.2 ± 4.6 , 17F; older

group, n = 32, age = 72.3 ± 5.8, 16F; main age group effect: $\chi^2 = 0.28$, p = 0.6). Box and whiskers plots show the median and interquartile range, the lines extend to the smallest/largest value within 1.5 times interquartile range below/above the 25th/75th percentile, and the dots represent each individual data value.

At-Home Gait Speed Differed Significantly Between Age Groups.

Participants were asked to continuously wear an accelerometer (GeneActiv) attached to the lumbar region with an elastic belt for a period of approximately one week (range=[6-15] days, mean ± SD = 8.72 ± 1.88 days; younger group = 8.61 ± 1.73 days; older group = 8.84 ± 2.05 days}. There were no group differences between the number of walking bouts of younger and older groups during the at-home monitoring period (p = .8). We then performed group analysis on at-home gait speed of the two age groups. The linear mixed effects model showed significant age group differences for both median gait speed ($X^2 = 12.54$, p = .006) and the 95th percentile gait speed (F = 22.59, p = 10⁻⁵) between the younger and older groups (Fig. 3.3a, b, respectively). The older group walked significantly slower than the younger group. There was a significant effect of day type (weekday/weekend, $X^2 = 42.08$, p < 10⁻⁵) as well as a group by day type interaction for median gait speed ($X^2 = 13.38$, p = .002), indicating that the age group difference was larger during weekdays than weekends. The pairwise comparisons showed significant age group differences for weekdays ($X^2 = 21.81$, p < 10⁻⁴), but not for weekends ($X^2 = 3.23$, p = .33). There were no other effects of covariates or interactions.

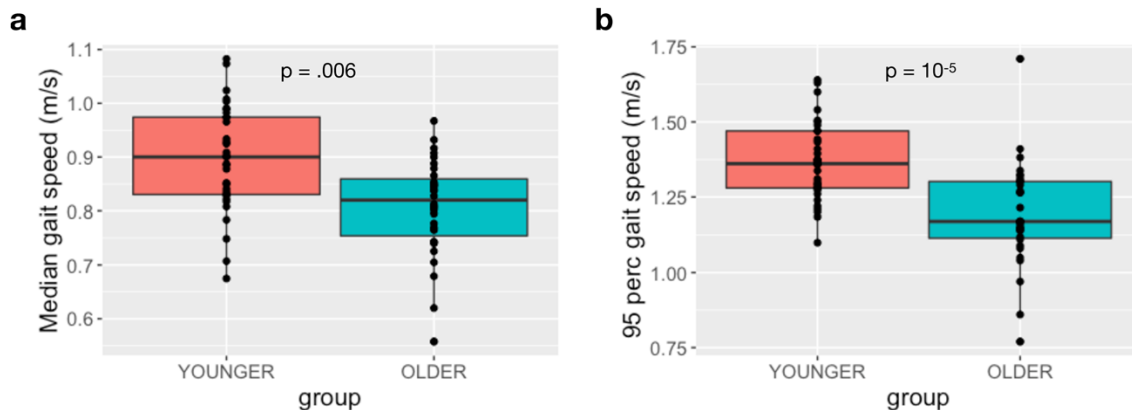


Figure 3.3. At-home gait speed estimated using a single lumbar-worn sensor (GaitPy) differed between age groups. **a** The median gait speed estimated by GaitPy showed significant group differences between younger and older groups ($p = 0.006$). There was also significant main effect of day type ($\chi^2 = 42.08$, $p < 10^{-5}$), and group by day type interaction ($\chi^2 = 13.38$, $p = 0.002$); i.e., the group difference was larger during weekdays than weekends. **b** The 95th percentile gait speed was also different between younger and older groups ($p = 10^{-5}$). Box and whiskers plots show the median and interquartile range, the lines extend to the smallest/largest value within 1.5 times interquartile range below/above the 25th/75th percentile, and the dots represent each individual data value.

Weak Association Between At-Home and In-Lab Gait Speed.

We evaluated the agreement between in-lab and at-home gait speed, both estimated from the lumbar sensor using the GaitPy method (M. D. Czech & Patel, 2019). Separate regression analyses were used to test if the median and the 95th percentile gait speed at-home predicted the in-lab gait speed. Although both the median and 95th percentile gait speed at-home significantly predicted the in-lab gait speed, they only explained around 20% of the variance with significant intercept (median: Adjusted $R^2 = .18$, $F(1,62) = 14.77$, $\beta = .57$, $p < 10^{-3}$, 95th percentile: Adjusted $R^2 = .25$, $F(1,62) = 21.45$, $\beta = .47$, $p < 10^{-5}$). Correlation analysis showed only a moderate relationship between at-home and in-clinic gait speed metrics (Spearman's $Rho = .35$ and $.42$, Fig. 3.4).

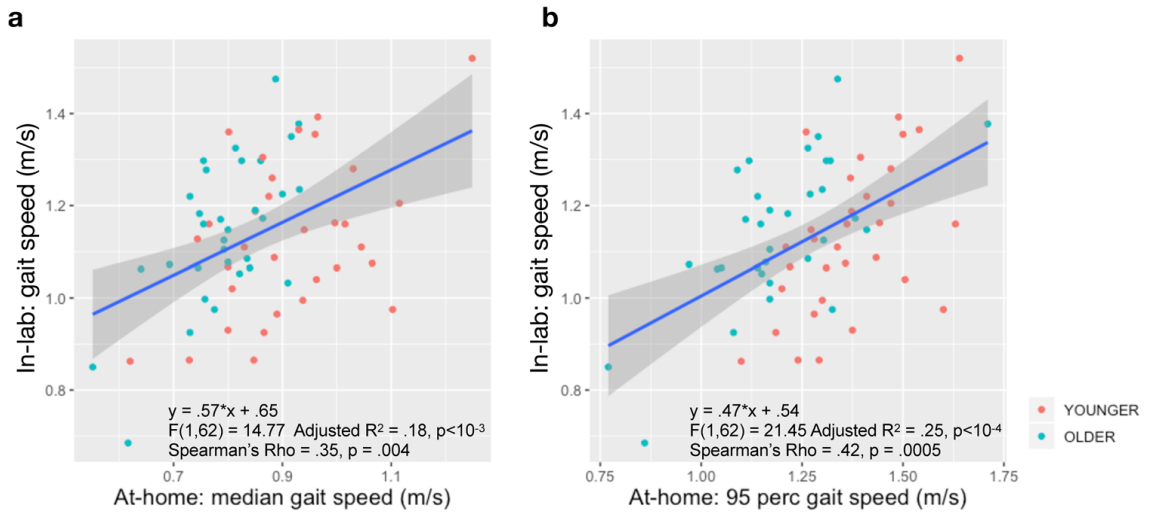


Figure 3.4. Weak association between in-lab and at-home gait speed. a The median gait speed at home showed a significant slope and an intercept ($\beta = 0.57$, $p < 10^{-3}$, $I = 0.65$; $p < 10^{-5}$). The two gait speed measures were moderately correlated (Spearman's rho = 0.35, $p = 0.004$), and at-home median gait speed explained only 18% of the variance of in-lab gait speed. **b** When a regression analysis was performed to explain the in-lab gait speed with the 95th percentile gait speed, at-home gait speed showed a significant slope and an intercept ($\beta = 0.47$, $p < 10^{-4}$; $I = 0.54$, $p = 10^{-4}$). The two gait speed measures showed moderate correlation (Spearman's rho = 0.42, $p = 0.0005$). At-home 95th percentile gait speed explained only 25% of the variance of in-lab gait speed. Shaded area shows the 95% confidence interval

Data From Three Days At Home Are Sufficient For Estimating Gait Speed.

We investigated the minimum amount of data (in terms of steps or days) required from at-home monitoring in order to reliably estimate gait speed. Median ICC was used to assess agreement between gait speed estimated using subsets of data (bootstrap with replacement across various days of monitoring) and gait speed estimated using full data set (i.e. all available days). Compared to the full data, the agreement between {two days or more and full data was excellent (ICC > .75) for both median (ICC = .85, [.65-.93]) and 95th percentile gait speed (ICC = .89, [.66-.95], Fig. 3.5a, b). The improvement on ICC values becomes minimal starting from three days with ICC > .75 for all bootstraps. Moreover, good agreement was observed for both median and 95th percentile gait speed for 5,000 steps, and excellent agreement was observed for both median and 95th

percentile gait speed when participants walked 15,000 or more successive steps, though there was substantial variance, especially for median gait speed (Fig. 3.5c, d). The improvement in 95th percentile gait speed becomes minimal starting from 20,000 steps.

Based on these findings, we investigated the impact of monitoring duration on detecting differences between the two age groups based on at-home measures of gait speed. We applied a t-statistic bootstrapping method (Efron, 1979) to create various subsets of days and compared them to the entire data set collected outside the lab. Similar to the results above, differences between median gait speed for the two age groups were significant with data from only two at-home days (all at-home data vs two days: $p \geq .05$, Table 3.2). Moreover, for 95th percentile gait speed, distinguishability between younger and older groups for one day of data was comparable to full data set obtained outside the lab (all at-home data vs one day: $p > .05$, Table 3.2).

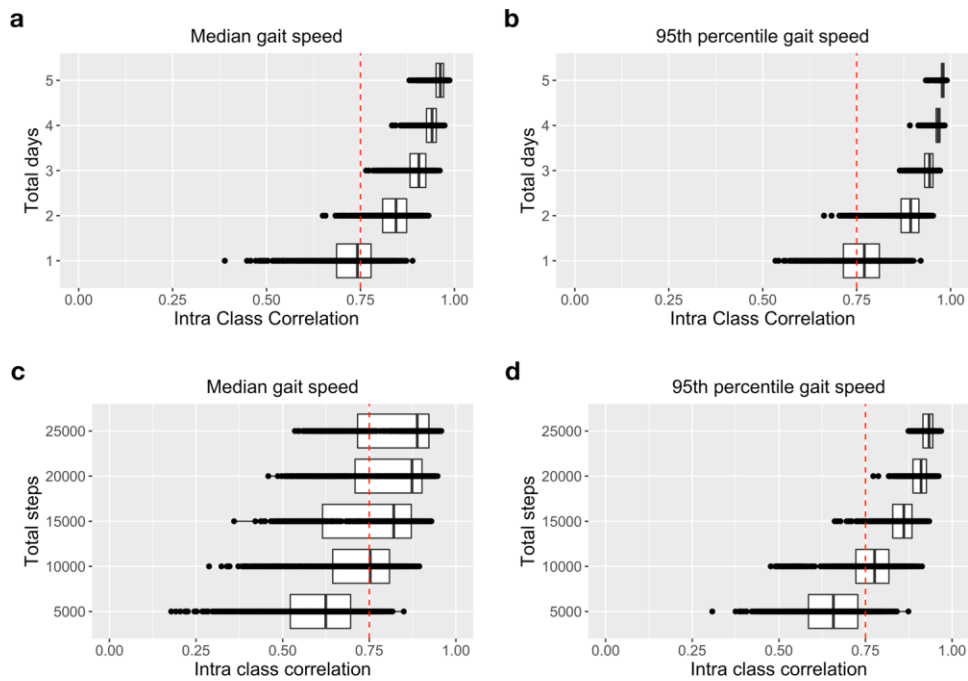


Figure 3.5. Amount of data needed to reliably estimate gait speed at home. Subset of data in terms of successive steps or randomly selected days was compared to the full data set (ICC

> 0.75 represents excellent agreement between two measurements). Minimum required data to estimate both (a) median gait speed and (b) 95th percentile gait speed was 2–3 days of monitoring data. (c, d) At least 15,000 and 10,000 concurrent steps were required to reliably estimate median and 95th percentile gait speed, respectively. Box and whiskers plots show the median and interquartile range, the lines extend to the smallest/largest value within 1.5 times interquartile range below/above the 25th/75th percentile, and the dots represent each individual data value.

Days	Median gait speed			95 th Percentile gait speed		
	t-Original	t-Bootstrap ^b	p Value	t-Original	t-Bootstrap ^b	p Value
1		3.01 ± 0.67	0.048		3.35 ± 0.68	0.08 ^a
2		3.57 ± 0.51	0.146 ^a		3.73 ± 0.53	0.147 ^a
3		3.79 ± 0.42	0.225 ^a		3.96 ± 0.41	0.214 ^a
4		3.91 ± 0.33	0.259 ^a		4.06 ± 0.33	0.243 ^a
5		3.99 ± 0.26	0.292 ^a		4.15 ± 0.26	0.288 ^a
all	4.13			4.29		

For both 95th and median gait speed 1000 bootstraps were drawn for various number of days [1–5] and the t-values were compared to the original t-values. In order to obtain similar group distinguishability compared to full data set, at least 2 and 1 days of at-home monitoring data with 1000 steps were required for median and 95th gait speed, respectively ($p > 0.05$). t-Original shows the t-statistic for the group difference using the full data, t-bootstrap indicates the mean t-statistic over the bootstrap samples.
^a $p < 0.05$.
^bMean ± sd.

Table 3.2. The Minimum Number of At-Home Monitoring Days Required to Differentiate the At-Home Gait Speed Between Younger and Older Groups Similar to Full Data.

Discussion

In this cross-sectional study involving healthy adults divided into two age groups (younger [18-40 years], older [65-85 years]), we derived gait speed from participants during in-lab gait tasks as well as from approximately nine days of continuous at-home monitoring. We aimed to 1) validate and evaluate the performance of a method for measuring gait relying on a single lumbar-worn accelerometer (GaitPy) with respect to a reference method relying on 6 devices (APDM), and an instrumented mat (GAITRite) as the gold standard device in-lab; 2) test the ability of gait speed estimated in-lab and at-home to distinguish between the two age groups; 3) determine the amount of at-home data required to reliably estimate the median and 95th percentile gait speed, and 4) evaluate the sensitivity of gait speed measured at-home for detecting age-related differences in a healthy population.

Validity of Sensor-Based Estimates of Gait Speed.

Assessing the validity of sensor-based methods for estimating gait speed in a controlled setting (e.g. laboratory or clinic) is essential for understanding its performance characteristics. The algorithm we implemented in GaitPy for estimating gait speed using a single lumbar-worn sensor has been shown to be comparable to gait measures derived using bilaterally worn ankle-mounted devices and has previously been successfully applied in a variety of disease populations, including Parkinson's disease, Huntington's disease, and stroke patients, both in-lab and at-home (Del Din, Godfrey, & Rochester, 2016a; Esser et al., 2011; Storm et al., 2016; Trojaniello et al., 2015). Compared to shin or foot sensors, a single lumbar-worn sensor enables relatively easy removal and reapplication during certain periods of the day, including bathing and sleeping. Additionally, the lumbar position is a convenient location for measuring bilateral asymmetries of gait which may be important in certain disease populations, including Parkinson's disease. In this study, we confirmed the validity of a lumbar-worn sensor and observed that in-lab gait speed estimated using data from a single lumbar-worn sensor (GaitPy) showed good agreement with an instrumented mat (GAITRite). We further observed a consistent bias for both GaitPy (13%) and APDM (5%, reference 6-device system) compared to the instrumented mat. However, GaitPy derived gait speed had higher variability than APDM, likely the result of reliance on a single device. This suggests that there might be a sensitivity trade off when utilizing fewer devices for measuring gait speed. Although, based on our previous findings, this trade off may be minimal (M. Czech et al., 2020). Using gyroscope in combination with the accelerometer

could potentially lead to better gait characterization, especially important to capture rotational information for turns and falls, with a cost of higher battery usage. Despite limitations in sensitivity, gait speed estimated using a single lumbar-worn device has been shown to distinguish between disease states as well as detect the effects of treatment (Del Din, Godfrey, Galna, et al., 2016). Additional work investigating the validity of gait feature estimation using a single lumbar-mounted device in various disease populations is still needed. Our results suggest that a single lumbar-worn device can provide sufficient accuracy for monitoring gait under free-living conditions and at the same time minimize participant's burden.

Impact of Environment on the Assessment of Gait Speed.

There is mounting evidence that gait measurements differ between in-lab and at-home environments (Brodie et al., 2016; Hillel et al., 2019; Mueller et al., 2019; Takayanagi et al., 2019). In our study, in-lab gait speed derived using either wearable sensors or GAITRite was unable to distinguish between the two age groups, whereas at-home gait speed showed the older group walked significantly slower than younger participants. We further confirmed our findings using uninstrumented measurements, which were collected as part of the traditional Short Physical Performance Battery (SPPB) assessment on the same participants (i.e. the time for participants to perform the walk test timed using a stop watch), and found no differences between age groups based on stop watch time (average time to walk 4-meters, younger group: $3.8 \pm 0.5s$, older group: $3.7 \pm 0.5s$, $X^2 = 1.08$, $p = 0.3$). Furthermore, other gait metrics such as step time and stride length derived from in-lab assessments failed to differentiate the age groups

(Supplementary Table A.1). In-lab measures are acquired during single visits whereas at-home measurements enable continuous evaluation over prolonged periods, providing the ability to capture nuanced therapeutic effects (Del Din, Godfrey, Mazzà, et al., 2016). Our findings are consistent with evidence that while a participant might change his/her behavior for a short period of time under observation (e.g. no age group difference for gait speed during in-lab assessments), it is unlikely that they will be able to do so during long periods of passive monitoring under free-living conditions (Takayanagi et al., 2019).

We have not observed a sex effect, but there was an age group by sex interaction during the short in-lab walk test captured by both instrumented and uninstrumented measurements (see Supplementary Fig. A.1). This effect did not exist in the at-home monitoring data, and we suggest that the interaction effect is due to the participants' change of behavior during short, observed assessments in the lab environment (i.e., observer effect). Therefore, healthy volunteer studies interested in at-home gait speed as an endpoint may not need independent grouping based on sex. However, controlling for age may be needed in studies with wide age ranges.

Several studies have proposed that gait should be considered as the sixth vital sign (Fritz & Lusardi, 2009). For example, higher gait speed predicted better survival (Hardy et al., 2007) and lower gait speed was associated with serious falls that resulted in a visit to the emergency room in older adults with mild cognitive impairment (Pieruccini-Faria et al., 2020). In healthy adults, real world gait speed is expected to decrease approximately 0.03 m/s every decade over the life span of an adult, resulting in a difference of around 0.12 m/s after 40 years (Schimpl et al., 2011). In our study, we

observed that at-home gait speed differed by ~0.9 m/s on average between the younger and older groups (approximately four decades apart), and that group difference in median gait speed was driven by weekday rather than weekend periods (Supplementary Fig. A.2a). We also observed that age-based differences existed for various bout length, especially for short (ranging between 10s to 30s) and medium bouts (ranging between 30s to 60s), although gait speed increased with bout length (effect of age group: $X^2 = 6.62$, $p = .02$, effect of bout length: $X^2 = 557$, $p < 10^{-16}$ Supplementary Fig. A.2b). Furthermore, not only gait speed but other gait features differed by age group (Supplementary Table A.2). Similar trend was observed in patient populations such as Parkinson's disease, where significant group differences in at-home gait features were observed compared to healthy volunteers (Del Din, Godfrey, Galna, et al., 2016). Although these are cross sectional studies, accurate estimation of real-world gait and evaluating its sensitivity to clinically meaningful change; e.g., the disease state or its progression, are extremely important. We have shown that gait metrics derived from at-home monitoring with a single lumbar-worn sensor provided more sensitive information to differentiate two age groups compared to in-clinic assessments, and that there is only a weak association between at-home and in-lab gait speed. This result was recently reported in older adults (Hillel et al., 2019; Mueller et al., 2019; Takayanagi et al., 2019), and it was also shown that gait speed derived during longer walking bouts in the laboratory appears to be better correlated with at-home measurements (Mueller et al., 2019). These findings provide further evidence for implementing wearable devices in clinical trials for monitoring physical function at-home instead of in-clinic assessments.

The use of wearable devices out-of-lab settings not only provides a better assessment of real-world activity but also brings additional benefits of remote monitoring. For example, it enables to enroll patients who live in remote regions with difficult access to clinic or reduces the exposure of participants who may be vulnerable to healthcare settings during a pandemic. In summary, remote data capturing offers the ability to design decentralized trials, which may become crucial for a wide variety of clinical trials in the near future.

Overall, the median gait speed measured at-home was lower than in-lab gait speed for both age groups. This result suggests that at-home gait speed may be affected by one or more factors that are present during daily life. One possible factor may be the cognitive challenges that are typically present during performance of activities of daily living. Several studies suggest that mobility relies on cognitive resources (Beauchet et al., 2016; Mielke et al., 2013; Verghese et al., 2007). In fact, it has been recently shown that mobility assessments performed at home better reflect cognitive functioning compared to those performed in the laboratory (Giannouli et al., 2018). Additionally, Hillel et al. showed that gait speed measured during in-lab dual-task walking is comparable to the gait speed measured during at-home monitoring (Hillel et al., 2019). The presence of a relationship between cognition and mobility performance may explain the reduced at-home gait speed compared to in-lab gait speed we observe in our data. Additional factors such as mood and fatigue may also contribute to the at-home gait, more so than in-lab, where participants may put forth their best effort.

Impact of Data Quantity on Gait Speed Estimation.

Our results suggest that at least two to three days of monitoring is required to estimate both median and 95th percentile gait speed in healthy volunteers. When the age groups were analyzed separately, we found only one to two days of data was needed to reliably estimate gait speed in the older cohort whereas two to three days were needed for the younger cohort. This result suggests more day-to-day variance in gait speed in the younger cohort (Supplementary Fig. A.3), as also reflected by the significant effect of day type as well as age group by day type interaction (Supplementary Fig. A.2a). Additionally, our results (Table 3.2) suggest that two days of data was necessary to estimate differences between young and old using median gait speed, whereas one day was needed for 95th percentile gait speed. Indeed, the upper and lower ICC bounds were tighter for 95th percentile gait speed compared to median gait speed, suggesting less day-to-day variability of 95th percentile gait speed. The lower variability of 95th percentile gait speed could have contributed to the improved distinguishability of young and older groups with less data compared to median gait speed. It may also be the case that median gait speed is a more sensitive indicator of age. A previous study employed a similar approach to quantify the minimum days required for reliable estimation of physical activity in older adults, and found that two days were sufficient for seven of the nine activities (Van Schooten et al., 2015). In accordance with our results, another study in older adults found that three days of accelerometer data were needed to accurately predict physical activity levels (Hart et al., 2011), and another recent study found that a

monitoring period of three days is necessary for gait speed estimation in frail older adults (Mueller et al., 2019).

Impact of Gait Characterization on Future Studies.

We believe our results on healthy participants with two age groups will be helpful for future studies with multiple disease populations; e.g., for selecting important variables, deciding the test environment, and minimal monitoring period. Moreover, we suggest this study provides an evidence on the ability of gait speed to detect minimal change between two close populations, especially important during the early stages of gait impairment, where only subtle differences may be detected relative to healthy participants, and during disease progression. However, validation of GaitPy performance in advanced disease populations may be needed to verify accuracy of the algorithm. Additionally, disease specific effects, such as motor fluctuations seen in some PD patients due to wearing off medication, could produce changes in variability of at-home gait speed. Therefore, future work would be needed to consider the potential impact of disease-specific changes on algorithm reliability and gait speed variability.

Limitations.

In the present study, we measured gait speed in healthy adults for just over one week, (mean \pm SD = 8.72 \pm 1.88 days). The group analyses were conducted based on the full data, however, we limited gait speed reliability analysis to participants with at least five days of data (number of participants who had five days of data with at least 1,000 steps per day = 64, number of participants who had five days of data with at least 100

steps per day = 65). Although we instructed our participants to wear the device continuously, we did not have a robust way to determine participant compliance for a lumbar-worn accelerometer. Therefore, we set a minimum threshold of 100 steps for including a day in our analyses. We investigated different step threshold values (10, 250 and 1,000 per day) but they did not have any significant impact on the results (Supplementary Fig. A.4). Accurate determination of participant compliance remains a challenge in the field and a limitation of this study.

Another limitation of this analysis is that the randomly selected days, varying from one to five days, were compared to the full data set which captured on average nine days of at-home monitoring. Moreover, we have observed that the type of day (weekend/weekdays) has a significant effect on gait metrics (Supplementary Table A.2 and Supplementary Fig. A.2a). In our analysis, we only tested for steps or days without labeling the type of day, since that would introduce another limit for bootstrapping. Further analysis accounting for the day type showed that including weekend day out of a total of three days only slightly improved reliability of both median and 95th percentile gait speed estimation (Supplementary Fig. A.5). Future studies may benefit from longer monitoring periods in order to obtain more substantial baseline data to replicate these findings.

Conclusion

Our results suggest that a single lumbar-worn sensor can be used for monitoring gait under free-living conditions and capture meaningful information about real-world function that might not be possible in controlled settings (e.g. laboratory or clinic). We

have shown that, despite higher variability, at-home gait speed was able to capture age-related group differences in healthy volunteers. In contrast, in-lab gait speed measured using either of the three methods did not differentiate between the two age groups. Moreover, we found that there was a weak correlation between at-home and in-lab gait speed, and gait speed measured at-home was lower than in-lab for both age groups. Finally, two to three days of at-home monitoring is sufficient for reliably estimating median and 95th percentile gait speed in both older and young healthy adults.

Methods

Subjects and Procedure

We recruited 65 participants in total, 33 healthy young participants (age = 29.2 ± 4.6 years, 17F, BMI = 23.4 ± 2.6) and 32 healthy older participants (age = 72.3 ± 5.8 years, 16F, BMI = 24.5 ± 2.6 , Table 3.2) to take part in two instrumented in-lab assessments each lasting approximately two hours in duration about 7-14 days apart, and an at-home portion in between the two visits (range = [6-15] days, mean \pm SD = 8.72 ± 1.88 days; younger group = 8.61 ± 1.73 days; older group = 8.84 ± 2.05 days). Throughout this manuscript at-home activity monitoring refers to monitoring all activity outside the laboratory; i.e., real-world environment or daily life. The in-lab portion was completed at the Pfizer Innovation Research Lab (PfIRe Lab) in Cambridge, Massachusetts. The study was reviewed and approved by Advarra IRB (protocol number: Pro00029419). All participants signed the written informed consent. The eligibility criteria included no significant health problems, as reviewed by the study physician

during medical history intake; body mass index (BMI) ≥ 18.5 kg/m² and < 30 kg/m² or absolute weight < 125 kg; and the predetermined score for VES-13 (Vulnerable Elders Survey).

During the in-lab portion, participants were instrumented with six wearable inertial devices (Opal, APDM Inc., Portland, Oregon) consisting of 3-axis accelerometer, gyroscope, and magnetometer worn on the sternum, lumbar (L4 position), and bilaterally on the wrists and feet. The devices recorded data from 3-axis accelerometer, gyroscope and magnetometer at a sampling rate of 128 Hz. Subjects were asked to complete a battery of activities, including sit-to-stand tasks, postural/balance tasks, and a gait task, as part of the SPPB (Short Physical Performance Battery) assessment. The analysis presented herein was limited to data from the gait task during which participants walked three laps on an instrumented mat (GAITRite, CIR Systems Inc., Franklin, New Jersey) while wearing the APDM 6-sensor set. Uninstrumented measurements were also acquired using stop watch to register the time to complete the tasks as part of the standard SPPB assessment.

For the at-home portion, participants were instructed to wear a device (GENEActiv, Activinsights Ltd., UK) on their lower back and wrist continuously for a period of about 7 to 14 days. Both devices recorded 3-axis accelerometer data at sampling rate of 50Hz. Only accelerometer data from the lumbar-worn device was used for the analysis presented herein.

Gait Feature Extraction.

Three separate methods were used for estimating gait speed during the performance of a gait task in the laboratory. Ground truth gait speed was estimated from data collected using an instrumented mat (GAITRite) using a vendor supplied proprietary algorithm (GAITRite Software version 4.8.5). Additionally, 6 inertial sensors (Opal, APDM) located on the sternum, lower back, and bilaterally on the wrists and feet, were used to estimate gait speed using a vendor supplied proprietary algorithm (APDM Mobility Lab v2.0.0.2018). Lastly, we estimated gait speed from accelerometer data recorded using a lumbar-mounted device (Opal, APDM), using an open-source algorithm (GaitPy v1.6.0) we implemented in Python v3.6 (M. D. Czech & Patel, 2019). GaitPy uses a wavelet-based method to enhance patterns that occur in the vertical acceleration signal for first detecting heel strike and toe off events during a gait cycle (McCamley et al., 2012). Gait speed is then estimated by integrating the vertical acceleration signal to derive vertical displacement and applying an inverted pendulum model as described by Zijlstra et al. (Zijlstra & Hof, 2003).

GaitPy was also used to estimate gait speed from data collected at home. For at-home data, GaitPy first uses a binary classifier to detect bouts of gait. Bouts of gait less than three seconds apart are concatenated into a single bout before estimating gait speed on a stride by stride basis.

Statistical Analysis.

Statistical analysis was performed in R version 3.5.2 with following main packages: 'lme4' for linear mixed effect regression (lmer), 'car' for type-III Anova, 'BlandAltmanLeh' for Bland-Altman plots, and 'psych' for ICC.

For in-lab walk test, for each digital device and algorithm aforementioned, the median of gait metrics across all steps for each lap was computed. Then, the median values across all laps per visit were used for statistical analysis. Bland-Altman plots were used to test the homoscedasticity of the gait speed derived from APDM and GaitPy compared to the instrumented mat (GAITRite). Agreement of gait speed across multiple devices were characterized with ICC_{2,1} (two-way random effects, absolute agreement, with respect to single measurement). Pearson's correlation coefficients were also computed to test for the consistency between gait speed estimated using different methods.

The group analysis of in-lab walk tests was performed using a linear mixed effects regression model with repeated measures followed by ANOVA. Each participant had data from two in-lab visits. The statistical model included method (GAITRite/APDM/GaitPy), age group (younger/older), sex (F/M) as main factors, and height and muscle mass as covariates. Random effects (participant/visit and participant/device) were also included to account for within participant variability.

The statistical testing of the at-home data was conducted using linear mixed effects model with repeated measures followed by ANOVA. In order to account for outliers, which are upper and lower extremes in bout length, bouts that lasted less than 10

seconds or more than 3,000 seconds were excluded from the analysis. Moreover, only bouts with at least four detected gait cycles were included in the analyses to ensure robust gait parameter estimation. For each participant, median gait speed was estimated per walking bout and then fed into the statistical model. Age group (younger/older), sex (F/M), and type of day (weekday/weekend) were added as main fixed factors, and height and muscle mass were added as covariates. Random effects (participant/type of day/each day) were also added to account for within participant variability. 95th percentile gait speed was summarized over all walking bouts and fed into the same linear model excluding type of day and random effects.

In addition, the same analyses including ICC, Bland-Altman, and group analysis were repeated for each gait metric. The group analysis p-values were corrected for multiple comparisons using false discovery rate (FDR) correction.

The association between in-lab and at-home gait speed was evaluated using a linear regression model (lm in `lme4` package), using in-lab gait speed as the dependent variable and at-home gait speed as the independent variable. The agreement between in-lab and at-home gait speed was assessed using Spearman's rho to account for outliers.

The amount of data required for reliable estimation of gait speed under free-living conditions was determined by drawing bootstrap samples (with replacement) from the at-home data by increasing 1) the number of consecutive steps to estimate the gait speed from 5,000 steps to 25,000 steps, and 2) the number of days to estimate the gait speed from 1 days to 5 days. 1,000 bootstraps were performed in each subgroup, and the analysis included participants with at least total 25,000 steps (62 participants) and 5 days

of data (65 participants) during the continuous at-home monitoring period for steps and days analyses, respectively. For each bootstrap, we computed the median gait speed and the 95th percentile gait speed per participant, and then computed the ICC with respect to the gait speed estimated from the full data for that participant. Full data for a participant ranged from 6 to 15 days based on the detected gait cycles. Reliability of estimated gait speed was assessed according to the following benchmarks: $ICC \leq 0.4$ indicates ‘poor’, 0.4 to 0.59 ‘moderate’, 0.6 to 0.74 ‘good’, and 0.75 to 1 ‘excellent’ reliability (Domenic V, 1994).

The number of at-home monitoring days required for detecting differences in gait speed of the younger and older groups’ was determined using bootstrapping followed by group analysis (Efron, 1979). Specifically, participants with at least 100 steps per day and 5 days of data were included and 1,000 bootstraps were drawn for each number of days varying from 1 to 5 days. For each bootstrap, the t-statistic with the contrast of age group difference was compared (t-bootstrap, Fig. 3.5) with respect to the t-statistic of the full data (t-original, Fig. 3.5), and the proportion of t-bootstrap that were greater than the original t-statistic were used to compute the p-value.

**CHAPTER FOUR: THE IMPACT OF REDUCING THE NUMBER OF
WEARABLE DEVICES ON MEASURING GAIT IN PARKINSONS DISEASE:
NONINTERVENTIONAL EXPLORATORY STUDY**

**Published in Journal of Medical Internet Research: Rehabilitation and Assistive
Technologies**

Authors

Matthew D. Czech ¹

Charmaine Demanuele ¹

Michael Kelley Erb ¹

Vesper Ramos ¹

Hao Zhang ¹

Bryan Ho ²

Shyamal Patel ¹

Affiliations

¹ Digital Medicine & Translational Imaging, Early Clinical Development, Pfizer, Inc.,
Cambridge, MA, USA.

² Tufts Medical Center, Boston, MA, United States

Abstract

Background: Measuring free-living gait using wearable devices may offer higher granularity and temporal resolution than the current clinical assessments for patients with Parkinson disease (PD). However, increasing the number of devices worn on the body adds to the patient burden and impacts the compliance.

Objective: This study aimed to investigate the impact of reducing the number of wearable devices on the ability to assess gait impairments in patients with PD.

Methods: A total of 35 volunteers with PD and 60 healthy volunteers performed a gait task during 2 clinic visits. Participants with PD were assessed in the On and Off medication state using the Movement Disorder Society version of the Unified Parkinson Disease Rating Scale (MDS-UPDRS). Gait features derived from a single lumbar-mounted accelerometer were compared with those derived using 3 and 6 wearable devices for both participants with PD and healthy participants.

Results: A comparable performance was observed for predicting the MDS-UPDRS gait score using longitudinal mixed-effects model fit with gait features derived from a single (root mean square error [RMSE]=0.64; R²=0.53), 3 (RMSE=0.64; R²=0.54), and 6 devices (RMSE=0.54; R²=0.65). In addition, MDS-UPDRS gait scores predicted using all 3 models differed significantly between On and Off motor states (single device, $P=.004$; 3 devices, $P=.004$; 6 devices, $P=.045$).

Conclusions: We observed a marginal benefit in using multiple devices for assessing gait impairments in patients with PD when compared with gait features derived using a single lumbar-mounted accelerometer. The wearability burden associated with the use of multiple devices may offset gains in accuracy for monitoring gait under free-living conditions.

Introduction

Gait is a complex sensorimotor activity involving dynamic spatial-temporal coordination of the legs, trunk and arms. Gait impairments negatively impact the

functional mobility of patients with Parkinson's disease (PD) (Bouca-Machado et al., 2018; Mirelman et al., 2019). In the early stages of PD, gait impairments manifest as reduced gait speed, shorter stride lengths, gait asymmetry with higher variability of gait measures and reduced amplitude of arm swing. As the disease progresses, gait measures become less asymmetric, but impairments continue to increase in severity. Worsening gait impairments coupled with balance and postural control issues lead to a significant reduction in mobility and an increased risk for falls in advanced PD (Ebersbach et al., 2013; Hausdorff, 2009; Mirelman et al., 2019).

Clinical assessment of gait in PD is limited to observational scales such as the Movement Disorder Society-Sponsored Unified Parkinson's Disease Rating Scale (MDS-UPDRS) (Goetz et al., 2008) and performance-based tests such as the Timed Up and Go (Podsiadlo & Richardson, 1991). While these tools have been clinically validated, assessments are influenced by the observer effect (Hawthorne effect) and quality of instructions (McCambridge et al., 2014). Assessments are susceptible to rater bias and, because symptoms are rated on an ordinal scale, they lack the resolution to detect changes that occur on a continuum. In addition, because trained raters can only perform these assessments infrequently, they provide intermittent snapshots, which are inadequate for fully characterizing day-to-day variability of symptoms (Galperin et al., 2019).

Advances in wearable technology allow for the development of systems for objective measurement of gait (Maetzler et al., 2013; Salvi et al., 2020; Tao & Feng, 2012; Zhong & Rau, 2020). While many of these systems (e.g. APDM Mobility Lab) (Mancini & Horak, 2016) provide a broad range of measures quantifying various spatial

and temporal aspects of gait, they require the use of multiple sensing devices making continuous, long-term monitoring outside the lab or clinic difficult. Recent research efforts to develop methods employing a single waist-mounted inertial sensing (accelerometer and gyroscope) device demonstrate feasibility of monitoring gait in patients with mobility deficits, including PD, Huntington's disease, post-stroke, and sarcopenia (Del Din, Godfrey, & Rochester, 2016a; Godfrey et al., 2015; Mueller et al., 2019; Trojaniello et al., 2014, 2015). Studies show moderate to good agreement between frequency domain features (e.g. dominant frequency amplitude, dominant frequency width) extracted from the accelerometer time series and subscales of the MDS-UPDRS associated with gait and balance (Rodriguez-Molinero et al., 2017; Weiss et al., 2011). However, unlike gait features like stride length and gait speed, such signal features do not have direct clinical meaning and are therefore difficult to use for the purpose of clinical decision-making. Temporal (e.g. swing time) and spatial (e.g. stride length) gait features derived from a single accelerometer on the lower back (L5 vertebrae) have demonstrated moderate to excellent agreement with an instrumented walkway for 8 out of 14 gait parameters in healthy older adults and patients with PD (Del Din, Godfrey, & Rochester, 2016a). Furthermore, gait features derived under free-living conditions had greater discriminative power compared to laboratory-based gait assessments for differentiating between healthy older adults and patients with PD (Del Din, Godfrey, Galna, et al., 2016). Compared to bilaterally worn ankle-mounted devices, lumbar-mounted accelerometers were satisfactory for measuring temporal gait features in young healthy adults despite being less accurate (Storm et al., 2016).

While it is feasible to monitor gait using a single lumbar-mounted wearable device, the relationship between number of devices used for deriving temporal and spatial gait features, and their ability to detect clinically meaningful changes is not well understood. Herein, we employ a method that relies on a single lumbar-mounted accelerometer that presents a significantly lower usability burden and affords better wearability compared to methods that rely on 3 or 6 devices (M. D. Czech & Patel, 2019; Del Din, Godfrey, & Rochester, 2016a; McCamley et al., 2012; Zijlstra & Hof, 2003). However, the tradeoffs of reducing the number of devices may include lower accuracy in the estimation of gait features, measuring fewer aspects of gait, and reduced sensitivity for detection of clinically meaningful differences. Therefore, in order to objectively evaluate this tradeoff, we 1) assessed the accuracy and reliability of gait features derived using a single lumbar-mounted accelerometer relative to a reference system (APDM Mobility Lab) (Mancini & Horak, 2016); and 2) assessed the impact of reducing the number of sensing devices on the criterion and discriminative validity of gait features in patients with PD.

Methods

Study Participants

We recruited 35 participants with mild to moderate PD (Hoehn & Yahr ≤ 3 ; Age: 68.3 ± 8.0 years; males/females: 23/12) taking regular dopaminergic medication (average Levodopa-equivalent daily dose 165.5 ± 81.3 mg) and 60 healthy volunteers (age: 44.1 ± 10.7 ; males/females: 27/33). PD Participants were recruited and tested at Tufts Medical Center, Boston, Massachusetts. All procedures were approved by The Tufts

Health Sciences Institutional Review Board (IRB), #12371. The protocol for the healthy cohort was approved by the Schulman IRB, #201500837, and run at Pfizer Andover, Massachusetts.

One PD participant self-reported as *ON with dyskinesia* and was therefore excluded from the analysis since the dyskinesia might interfere with gait feature measurements. Additionally, one healthy volunteer was removed from the analysis due to technical errors with data capture. The clinical and demographic characteristics of participants whose data were available for analysis are listed in Table 4.1.

Characteristic	Healthy ($n = 59$) Mean \pm SD	PD ($n = 34$) Mean \pm SD
M/F (n)	27/32	23/11
Age (years)	44.4 \pm 10.5	68.1 \pm 8.1
Height (m)	1.7 \pm 0.1	1.7 \pm 0.1
BMI (Kg/m ²)	25.3 \pm 4.8	28.9 \pm 7.1
Hoehn and Yahr (n)	-	HYI – 2 HYII – 26 HYIII – 6
Levodopa Equivalent Daily Dose (mg/day)	-	164.5 \pm 81.1
MDS-UPDRS III Gait score	-	ON 1.0 \pm 0.9 HYI – 0.0 \pm 0.0 HYII – 0.8 \pm 0.7 HYIII – 2.0 \pm 0.9 OFF 1.4 \pm 0.9 HYI – 0.0 \pm 0.0 HYII – 1.2 \pm 0.7 HYIII – 2.7 \pm 0.5

Table 4.1. Clinical and Demographic Characteristics.

Device Setup

As illustrated in Supplementary figure A.6a, participants were instrumented with six wearable devices (Opal, APDM, Inc.) located bilaterally on the wrist and foot, and at

the lumbar (approximately at the L5 vertebra) and sternum locations. Each device recorded raw data from 9-axis inertial sensors (tri-axial accelerometer, tri-axial gyroscope and tri-axial magnetometer) at a sampling rate of 128 Hz.

Experimental Protocol

Participants performed a battery of physical activities and cognitive tasks over the course of two visits. Both visits were identical for healthy participants but were randomized for PD participants so that they were in the ON state (~ 1 hour after medication intake, confirmed with patient self-report and clinician report) during one visit and in the OFF state (~3 hours after last medication intake, confirmed with patient self-report and clinician report) during the other visit. Physical activities during each visit included scripted activities of daily living (e.g. tying a shoe, opening and closing a door) and motor assessments from the MDS-UPDRS part III (e.g. 2-minute gait task, finger tapping). In this paper, we present analyses based on data collected during the 2-minute gait task. This is to ensure uniform testing conditions for determining the agreement of post-experiment sensor data processing. During this gait task, participants were instructed to walk back and forth along a straight 10-meter track at a comfortable pace for a period of two minutes. PD participants were assigned an MDS-UPDRS gait score on an ordinal scale of 0 to 4 by a neurologist to assess the degree of gait impairment. Sample sizes (n) for MDS-UPDRS gait scores of 0, 1, 2, and 3 across both visits were 17, 27, 18, and 6 respectively.

Gait Feature Extraction

APDM Mobility Lab is a commercially available system widely used for objective assessment of gait and requires data from 3 to 6 wireless, body-worn Opal inertial devices (Mancini & Horak, 2016; Washabaugh et al., 2017). We used APDM Mobility Lab to derive a set of lower limb, lumbar and trunk range of motion, and upper limb gait features from 6 wearable devices placed on the lower back, sternum, and bilaterally on the feet and wrists (Supp. Table A.3). Using 3 sensors located on the lower back and both feet, Mobility Lab can only derive features related to the lower limb and lumbar range of motion. Therefore, we used only features related to lower limb and lumbar range of motion as the 3-sensor feature set (Supp. Table A.3). To derive gait features from a single lumbar-mounted tri-axial accelerometer, we developed and implemented a previously published wavelet-based method (Del Din, Godfrey, & Rochester, 2016a) in a Python v3.6 package called GaitPy (Supp. Figure A.6) (M. D. Czech & Patel, 2019). A complete list of gait features derived from a single lumbar-mounted device, and those requiring additional devices can be seen in Supplementary Table A.3.

Statistical Methods

Statistical analysis were performed in R version 3.4.1 (R Core Team, 2017) using the following packages: ‘psych’ for intraclass correlation coefficient (ICC), ‘BlandAltmanLeh’ for Bland-Altman plots, ‘nlme’ for linear mixed-effects model, ‘car’ for type-III Anova, and ‘MASS’ for stepwise model selection.

The median value of each gait feature extracted from data collected during the 2-

minute walking task was calculated for each visit separately. Test-retest reliability of gait features was assessed by calculating the ICC on data collected from healthy volunteers during visit 1 and visit 2. ICC was also used in addition to Bland-Altman plots and 95% limits of agreement to evaluate agreement between gait features derived using GaitPy and APDM Mobility Lab. Results are presented in Table 4.2 where values are ICC_{2,1} coefficient (two-way random effects, absolute agreement) with lower and upper confidence bounds, reported as ICC coefficient [lower upper]. Test-retest reliability and agreement between features were assessed according to the following benchmarks: ICC \leq 0.4 indicates ‘poor’, 0.4 to 0.59 ‘moderate’, 0.6 to 0.74 ‘good’, and 0.75 to 1 ‘excellent’ reliability (Domenic V, 1994). Variation of gait features with the MDS-UPDRS gait score in patients with PD was assessed using the Kruskal-Wallis test. Post-hoc Conover-Iman tests were used for pairwise comparisons and multiplicity was adjusted using false discovery rate correction.

Gait features derived using a single, 3, and 6 devices were separately used to fit three longitudinal mixed effects regression models to predict the clinician’s MDS-UPDRS gait score (using the *lme* function in ‘nlme’ R package). Prior to model fitting, pairwise correlation between sensor features was computed and highly correlated features were removed. Gait features and covariates including *age*, *gender*, *visit number*, *BMI*, and *years since first symptoms* were modeled as fixed effects and participant as a random effect. An unstructured correlation matrix was used. Numerical features were standardized to have zero mean and unit variance. Stepwise model selection was performed using Akaike Information Criterion (AIC) as a cost function to achieve the

optimal model fit (using the *stepAIC* function in ‘MASS’ R package). ANOVA findings were reported as chi-squared (X^2) values and corresponding p-values using Type III sum of squares (statistics were derived using the ‘car’ R package). Final models were used to predict the clinician’s score using leave-one-subject-out cross validation. We report the root mean square error (RMSE) and marginal R^2 representing the variance explained by the model fixed effects. Paired Wilcoxon signed-rank test were used to compare predicted gait scores between ON and OFF states.

Results

Accuracy of Gait Features Derived Using a Single Device

Gait features derived during the 2-minute walk task using GaitPy (single lumbar-mounted device) were compared with the same features derived using the APDM Mobility Lab (6 devices) for healthy and PD participants separately using data from both visits. Gait features derived using the APDM Mobility Lab are used as the reference since APDM has been validated against data from an instrumented treadmill and has been extensively used in both healthy and PD populations (Godinho et al., 2016; Washabaugh et al., 2017). Excellent agreement was observed between the two methods for stride time and step time in both healthy and PD participants ($ICC \geq 0.86$; Table 4.2). Furthermore, excellent agreement was observed for stance time, stride length, and gait speed in PD participants ($ICC = 0.86, 0.88, \text{ and } 0.89$ respectively), and agreement was good in healthy participants ($ICC = 0.68, 0.60, \text{ and } 0.70$ respectively) (Table 4.2). Bland-Altman analysis revealed a trend that mean difference between GaitPy and APDM Mobility Lab was smaller for longer stance times (Supp. Figure A.7a). Good agreement was also observed

for swing time in both healthy and PD patients ($0.64 \leq \text{ICC} \leq 0.73$; Table 4.2). In contrast, double support showed poor agreement in healthy volunteers ($\text{ICC} = 0.20$) and moderate agreement in PD patients ($\text{ICC} = 0.46$; Table 4.2). Asymmetry and variability features also showed poor agreement ($\text{ICC} \leq 0.31$; Table 4.2) between the two methods for both healthy and PD participants.

Reliability of Gait Features Derived Using a Single Device

Test-retest reliability of gait features derived using GaitPy was assessed using data collected from healthy participants only. Excellent-test retest reliability ($\text{ICC} \geq 0.85$; Table 4.2) was observed for all spatial and temporal gait features. Asymmetry and variability features showed poor to excellent test-retest reliability ($0.14 \leq \text{ICC} \leq 0.77$; Table 4.2).

Gait feature	Agreement between gait features derived with APDM Mobility Lab and GaitPy		Test-Retest reliability of gait features derived from GaitPy
	Healthy	PD	Healthy
Spatial and temporal gait features			
Stride time (s)	0.92 [0.02, 0.98]	0.86 [0.73, 0.92]	0.94 [0.84, 0.97]
Step time (s)	0.92 [0.09, 0.98]	0.90 [0.71, 0.95]	0.91 [0.83, 0.95]
Double support (s)	0.20 [-0.07, 0.52]	0.46 [0.16, 0.66]	0.90 [0.84, 0.94]
Stance time (s)	0.68 [-0.05, 0.91]	0.86 [0.48, 0.95]	0.93 [0.84, 0.96]
Swing time (s)	0.73 [0.03, 0.90]	0.64 [0.48, 0.76]	0.92 [0.86, 0.95]
Step length (m)	-	-	0.86 [0.77, 0.91]
Stride length (m)	0.60 [0.25, 0.78]	0.88 [0.79, 0.93]	0.85 [0.76, 0.91]
Gait speed (m/s)	0.70 [0.11, 0.87]	0.89 [0.71, 0.95]	0.88 [0.80, 0.93]
Variability (var) gait characteristics			
Stride time var (s)	0.01 [-0.02, 0.04]	0.04 [-0.04, 0.15]	0.56 [0.36, 0.71]
Step time var (s)	0.01 [0.00, 0.04]	0.04 [-0.03, 0.14]	0.53 [0.31, 0.69]
Double support var (s)	0.02 [-0.03, 0.08]	0.21 [-0.10, 0.51]	0.14 [-0.11, 0.38]
Stance time var (s)	0.01 [-0.02, 0.05]	0.09 [-0.04, 0.30]	0.61 [0.42, 0.75]

Swing time var (s)	0.00 [-0.03, 0.04]	0.02 [-0.03, 0.09]	0.44 [0.21, 0.63]
Step length var (m)	-	-	0.74 [0.59, 0.83]
Stride length var (m)	0.00 [-0.01, 0.03]	0.00 [-0.06, 0.08]	0.75 [0.61, 0.84]
Gait speed var (m/s)	0.01 [-0.01, 0.04]	0.01 [-0.04, 0.09]	0.77 [0.65, 0.86]
Asymmetry (asy) gait characteristics			
Step time asy (s)	0.11 [-0.06, 0.29]	0.16 [-0.05, 0.36]	0.44 [0.21, 0.62]
Double support asy (s)	0.00 [-0.15, 0.16]	0.10 [-0.14, 0.33]	0.39 [0.16, 0.59]
Stance time asy (s)	0.17 [-0.08, 0.41]	0.31 [0.01, 0.54]	0.57 [0.38, 0.72]
Swing time asy (s)	0.22 [-0.09, 0.52]	0.29 [0.02, 0.51]	0.54 [0.33, 0.70]
Step length asy (m)	-	-	0.72 [0.56, 0.82]

Table 4.2. Agreement Between Gait Features Derived Using the APDM Mobility Lab and GaitPy, and Test-Retest Reliability of Gait Features Derived With GaitPy in Healthy Volunteers. ICC coefficient values showing excellent agreement (between 0.75 and 1) are highlighted.

Criterion Validity of Sensor-Derived Gait Features

We assessed the ability of gait features derived using methods relying on different device setups (single device, 3 devices and 6 devices) to discriminate between UPDRS gait scores. Based on available APDM Mobility Lab documentation (APDM, 2019), we were able to determine which gait features are available using either a 3-device setup or a 6-device setup. Therefore, for the purpose of this comparison, we limited our analysis to the 1-device setup (using GaitPy) and 3 and 6 device setups using APDM Mobility Lab.

The spatial features of gait (i.e. gait speed, stride length, and step length) varied most significantly with UDPRS gait score in PD participants (Supp. Table A.4). Using leave-one-subject-out cross validation, the longitudinal mixed effects regression model based on gait features derived using a single lumbar-mounted device predicted the clinician's gait score with an RMSE=0.64 and an $R^2=0.53$. The predicted score significantly distinguished between scores of 1 and 2 ($P<.001$), and marginally distinguished between scores of 0 and 1 ($P=.071$), and 2 and 3 ($P=.178$) (Figure 4.1a).

Stance time ($X^2=12.78$, $P<.001$), step length ($X^2=49.16$, $P<.001$), and step length asymmetry ($X^2=6.65$, $P=.01$) had significant effect on describing the MDS-UPDRS gait score.

Comparable performance was observed for a model based on gait features derived using data from 3 devices (RMSE=0.64, $R^2=0.54$). The R^2 value for the 3-device model was only slightly higher than the single-device model. The predicted gait score could significantly distinguish between MDS-UPDRS gait scores of 0 and 1 ($P=.017$), 1 and 2 ($P<.001$), and 2 and 3 ($P=.025$) (Figure 1b). Pitch at initial contact ($X^2=7.33$, $P=.007$), maximum pitch ($X^2=10.50$, $P=.001$), cadence ($X^2=14.93$, $P<.001$), initial mid-swing duration ($X^2=4.51$, $P=.034$), and pitch at toe off variability ($X^2=6.43$, $P=.011$) had a significant effect on describing the MDS-UPDRS gait score.

The model based on gait features derived using data from 6 devices achieved better performance than the single and 3-device model at predicting clinician gait score (RMSE=0.54, $R^2=0.65$). The predicted gait score significantly distinguished between MDS-UPDRS gait scores of 0 and 1 ($P=.001$), 1 and 2 ($P<.001$), and 2 and 3 ($P=.022$) (Figure 4.1c). Pitch at initial contact ($X^2=8.87$, $P=.003$), maximum pitch ($X^2=5.37$, $P=.021$), cadence ($X^2=19.80$, $P<.001$), initial mid-swing duration asymmetry ($X^2=5.71$, $P=.017$), trunk sagittal average angle ($X^2=18.88$, $P<.001$), upper limb foot phase difference ($X^2=4.98$, $P=.026$), maximum pitch variability ($X^2=8.60$, $P=.003$), trunk sagittal average angle variability ($X^2=5.02$, $P=.025$), BMI ($X^2=9.97$, $P=.002$), and years since first symptom ($X^2=6.98$, $P=0.008$) had a significant effect on describing the MDS-UPDRS gait score.

78

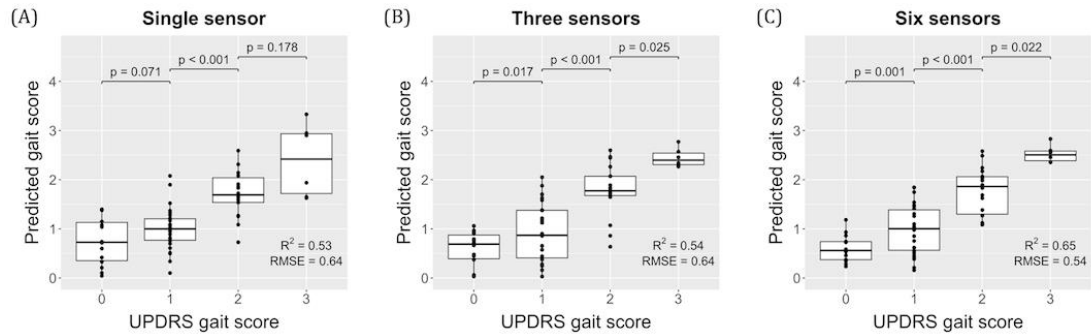


Figure 4.1. MDS-UPDRS gait score model performance fit using gait features from (a) single device at the lumbar (L5) location (GaitPy), (b) 3 devices (APDM Mobility Lab), and (c) 6 devices (APDM Mobility Lab).

Discriminative Validity of Sensor-Derived Gait Features

We assessed the ability of predicted gait scores derived using methods relying on different device setups (single device, 3 devices and 6 devices) to discriminate between ON and OFF motor states. As shown in Figure 4.2a, the clinician-rated MDS-UPDRS gait score was significantly different ($P=.001$) between the patient-reported ON and OFF state. Similarly, predicted gait scores, estimated from 1, 3, and 6 device models (Figure 4.2(b-d)), all significantly differentiated between ON and OFF states ($P=.004$, $.004$, and $.045$ respectively).

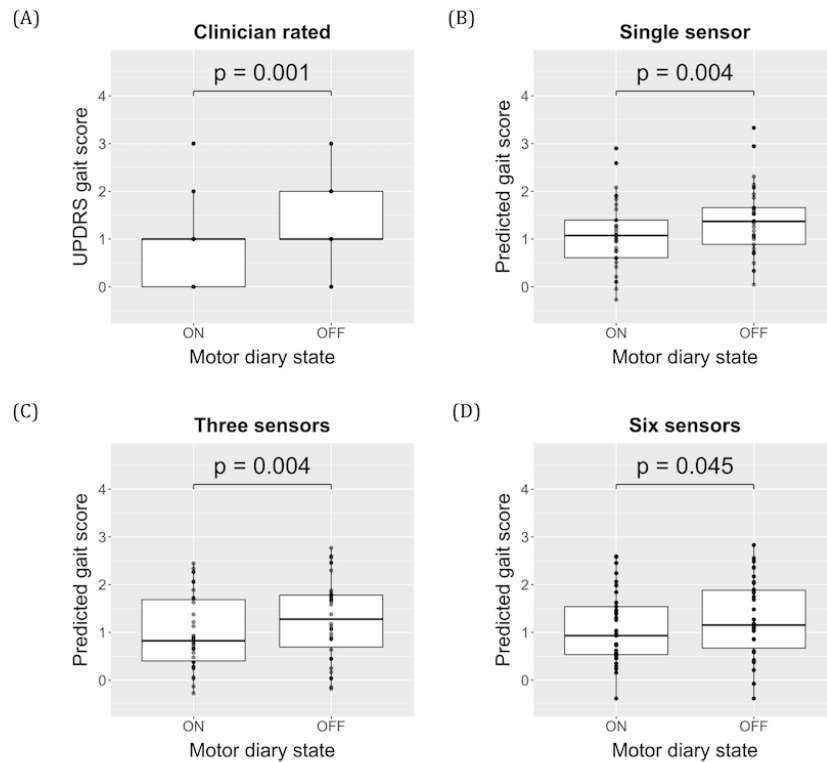


Figure 4.2. Distribution of the (a) clinician-rated gait score, (b) single-device predicted gait score, (c) three-device predicted gait score, and (d) six-device predicted gait score, grouped by patient reported ON and OFF motor states.

Discussion

Principle Findings

In this exploratory, non-interventional study involving healthy and PD participants, we derived gait features from participants during two in-clinic visits using wearable devices. We found that gait features derived from a single lumbar-mounted accelerometer could predict the clinician rated gait impairment score to a similar degree as gait features derived from 3 or 6 sensors. Additionally, analogous to clinician rated scores, predicted gait scores using gait features derived from either 1, 3, or 6 devices all significantly distinguished between ON and OFF medication states. Our results suggest

that a subset of gait features, derivable using a single lumbar-mounted accelerometer, may be sufficient to measure degree of gait impairment and the effects of treatment in PD patients.

Accuracy and Reliability of Gait Features Derived Using a Single Device

Agreement of GaitPy with the reference system (APDM Mobility Lab) was assessed in both healthy and PD participants. While we observed moderate to excellent agreement between most temporal and spatial features of gait derived using GaitPy from a single device and gait features provided by APDM Mobility Lab using 6 devices, agreement was poor for asymmetry and variability features. Notably, agreement was better in PD participants for 4 out of 7 temporal and spatial features. The difference between ICC values for healthy and PD participants was significant for stance time (0.86 vs. 0.68), stride length (0.88 vs. 0.60) and gait speed (0.89 vs. 0.70). This result contrasts prior work (McCambridge et al., 2014) where good agreement with the reference system (gait mat) for both PD participants and age matched healthy controls was observed. However, unlike prior work, the two groups in our study were not age matched. To this end, PD patients showed a wider range of values for gait speed and stride length compared to healthy volunteers, especially in the lower range, which may have contributed to better agreement (Supp. Figure A.7(b,c)).

We evaluated test-retest reliability of gait parameters derived using GaitPy in a sample of 59 healthy volunteers. Test-retest reliability for GaitPy was excellent for all spatial and temporal features, whereas it was poor to excellent for asymmetry and variability features. These results suggest temporal and spatial features of gait can be

reliably measured using a single accelerometer mounted on the lower back. However, as has been reported previously (Del Din, Godfrey, & Rochester, 2016a), agreement and reliability of variability and asymmetry features might be sensitive to the measurement technique employed (e.g. sensing modality, device location). This is partially because asymmetry and variability are small measurements, which are significantly affected by noise or error in the measurement of temporal or spatial features. Potential sources of measurement error for GaitPy include (1) biomechanical approximation of the inverted pendulum model, (2) error in estimation of vertical displacement from vertical acceleration and (3) distal location of the sensing device relative to the feet.

Tradeoffs Between Gait Features Derived Using Different Device Setups

We assessed criterion and discriminative validity of MDS-UPDRS gait scores using linear mixed effects models based on gait features derived using data from a single device, 3 devices and 6 devices. Although a single device provides substantially fewer features of gait compared to either 3 or 6 devices, 17 of the 34 features that varied most significantly ($P<.01$) with MDS-UPDRS gait score can be derived using a lumbar-mounted sensor (Supp. Table A.4). This includes many gait features known to be affected in PD, including stance time, gait speed, step-to-step asymmetries, and gait variability (Ebersbach et al., 2013; Hausdorff, 2009).

While the 6-device model (RMSE=0.54, $R^2=0.65$) performed slightly better at estimating MDS-UPDRS gait score, performance of the 3-device model (RMSE=0.64, $R^2=0.54$) was comparable to the single device model (RMSE=0.64, $R^2=0.53$). However, unlike the 3 and 6 device models, the single device model was unable to significantly

distinguish between adjacent scores of 0 and 1, and of 2 and 3. One potential reason for this could be the small number of observations for class 3 ($n = 6$). Additionally, gait features related to pitch and mid-swing duration that were significant for both the 3 and 6-device model could not be derived using the single device model. This indicates features derived from the lower extremity (e.g. foot) might have a higher predictive power. Indeed, 3 of 10 features in the 6-device model and 3 of 5 features in the 3-device model that were significant were related to pitch of the foot.

When we assessed the ability of gait scores predicted by the linear mixed effects models to differentiate between ON and OFF motor states, we found significant differences ($P < .05$) for gait scores derived using 1, 3, and 6 device models. Additionally, the OFF to ON gait score directionality was largely consistent between those produced by each model and the clinician-rated gait score. In 10 of the 12 subjects, the clinician score and the predicted score differences between ON and OFF state were in the same direction (Supp. Figure A.8a). This was comparable with the 3-device model (10/12) (Supp. Figure A.8b) and 6-device model (10/12) (Supp. Figure A.8c).

Limitations

Data analyzed in this study were collected during performance of motor assessments in the laboratory settings and could be affected by the observer effect and heightened awareness of the patient. Gait features derived using wearable devices were not validated against a gold-standard reference (e.g. an instrumented walkway or a motion capture system). This limitation of our work is mitigated to some extent by prior work, in which the authors evaluated the algorithm implemented in GaitPy against an

instrumented walkway (Psaltos et al., 2019). Another limitation of our work is healthy and PD participants were not age matched. Therefore, the results for accuracy and reliability in our healthy cohort might be different in healthy older adults. Additional work is required to validate the results presented herein on an independent dataset as well as confirm the ability of GaitPy to accurately assess gait impairment in free-living conditions.

Conclusion

Our results suggest that a single tri-axial accelerometer on the lower back may be sufficient to characterize gait impairments in patients with PD. Algorithms that estimate gait features from a lumbar-mounted sensor, such as GaitPy, could provide clinically meaningful measures of changes in severity of gait impairments and changes in motor state associated with effects of treatment in patients with PD. The long battery life of an accelerometer-only device and high degree of utility associated with a single device worn on the lower back, enables further investigations to assess the validity of this approach for monitoring gait under free-living conditions. Comparing sensor-derived gait features with classical patient reported motor diary-based approaches in their ability to detect treatment related effects may enable insight into the utility of a single lumbar-mounted sensor in free-living environments. Our ongoing efforts are focused on performing clinical validation in a semi-supervised setting as an intermediate step between the clinic and at-home.

Acknowledgement

The authors would like to acknowledge Steve Amato, Paul Wacnik, Tairmae Kangarloo and Jonathon Bruno for their contributions to study design, data collection, and manuscript processing. For reviewing and providing feedback on the manuscript, we would like to acknowledge Xuemei Cai, David Caouette, Joe Mather, and Timothy J. McCarthy. The PD study was a collaborative effort between Tufts Medical Center and Pfizer, Inc.; Pfizer, Inc. funded the work and Tufts Medical Center was responsible for study conduct and data validation/storage.

**CHAPTER FIVE: CONDITIONS ENABLING ENTRAINMENT OUTSIDE OF
BETA RANGE IN THE SUBTHALAMIC NUCLEUS-GLOBUS PALLIDUS
NETWORK**

Unsubmitted Work

Contributions

Model development, analysis, visualization, original draft preparation, Matthew D. Czech; Conceptualization, writing review and editing, Michelle M. McCarthy, Nancy Kopell

Introduction

Selective loss of dopaminergic neurons in the substantia nigra that project to the basal ganglia (BG) is a common, though not exclusive, feature in degenerative parkinsonian disorders (PD) (Braak et al., 2004; Dickson, 2018). Progressive neurodegeneration in nigrostriatal pathways is associated with a variety of motor symptoms including bradykinesia, rigidity, and rest tremor (Xia & Mao, 2012). According to the classical model of BG function, loss of midbrain dopamine neurons is hypothesized to have opposing effects on striatal medium spiny neurons (MSN), decreasing direct pathway MSN firing rate and increasing indirect pathway MSN firing rate (McGregor & Nelson, 2019). The net result is an increase in globus pallidus internus-mediated thalamic and cortical inhibition, thereby suppressing movement. However, in addition to firing-rate changes, there is growing evidence that exaggerated synchronization of neuronal activity in the cortico-BG-thalamic loop is mechanistically linked to disease pathology in patients with PD (Halje et al., 2019). The advent of

electrical deep brain stimulation has provided the opportunity to obtain human brain recordings and has confirmed excessive beta oscillatory activity in patients with PD (Brown et al., 2001; Hammond et al., 2007).

Despite considerable attention to beta band (15-30 Hz) frequencies, both lower (1-12 Hz) and higher (>30 Hz) frequencies have been reported in basal ganglia structures of normal and PD patients (Halje et al., 2019; Womelsdorf & Fries, 2007). Although low and high, and even beta (Courtemanche et al., 2003), frequencies have been implicated in healthy physiological function, exaggerated forms have been linked to pathological symptoms in PD (Wiest et al., 2021). Low frequency oscillations in delta, theta, and alpha ranges have been reported throughout the cortico-BG-thalamic loop, including the motor cortex, thalamus, striatum, subthalamic nucleus (STN), and globus pallidus (GP). Additionally, gamma (30-150 Hz) and high frequency oscillations (>150 Hz) have been reported in GP, STN, and cortical structures (see Halje et al., 2019 for extended list of references). Indeed, the ability of cortico-BG-thalamic loop structures to oscillate outside of the beta range is crucial to normal function and is to some degree restored in PD patients following treatment with L-Dopa (Cassidy et al., 2002).

To date, much of the experimental and computational efforts have aimed to elucidate the origin of beta and how treatment such as deep brain stimulation reduces beta synchrony. However, studies investigating the physiological constraints that allow a wide range of frequencies to be transmitted through the cortico-BG-thalamic loop are lacking. In this study we reproduce a large-scale spiking model of the STN-GPe network to elucidate and distinguish network connection strength conditions that control beta

synchrony and those that control entrainment outside of beta range. Understanding network conditions that both reduce beta synchrony and facilitate oscillations outside of beta range may enable better understanding of pathological mechanisms and elucidate novel treatment targets for PD.

Methods

Network Model and Simulation

We implemented a leaky integrate-and-fire model of the STN-GPe network as described in previous work (Mirzaei et al., 2017) in python (v3.8) using the Brian2 (v2.4.2) framework. The model includes 2000 reciprocally connected GPe neurons (2% connection probability), 1000 STN neurons, 500 striatal neurons, and external poisson spike train input driving the GPe and STN at physiologically normal firing rates (~45 Hz and ~15 Hz, respectively) (Figure 5.1). GPe neurons receive excitatory synaptic input from the STN (2% connection probability) and inhibitory synaptic input from the striatum (100% connection probability). STN neurons receive inhibitory synaptic input from the GPe (3.5% connection probability).

Previous results with this model demonstrate increased network beta synchrony and oscillatory power in response to increasing striatal firing rate input to GPe (Kumar et al., 2011). In order to validate expected model performance, we evaluated the effect of striatal firing rate on STN population rate frequency (Supplementary figure A.9). In line with previous results, beta synchrony increases with increasing striatal poisson input (Supplementary figure A.9 A). Furthermore, similar to previous results, beta synchrony is

quenched by reducing STN neuron excitability, even in the presence of strong striatal input (Supplementary figure A.9 B).

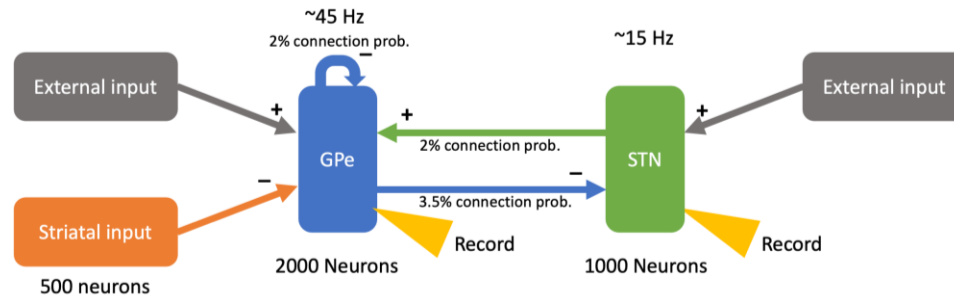


Figure 5.1. Network model schematic.

Statistical Analysis

Spectral analysis of neuron population activity was used to evaluate oscillatory strength of the network. Population rate was calculated using the `smooth_rate` function in Brian2 v2.4.2 with 5 ms width. Power spectral density was then calculated from the normalized population rate using the `mtspec` function of the `mtspec` package (v0.3.2). Pearson correlation coefficient was used to investigate STN firing rate correlation with beta synchrony. Figures were generated and Pearson correlation coefficient was computed in R (v3.6.2) using the `ggplot2` (v3.2.1) package.

Results

Weak Synaptic Connection Strength Between STN and GPe and Strong Reciprocal GPe

Connection Strength Allows Network Entrainment to a Wide Range of Frequencies

We investigated the ability of a network with weak GPe to STN and STN to GPe connection strengths and strong reciprocal GPe connection strength to entrain at frequencies outside of beta. The model entrained to frequencies outside of beta in

response to various rates of striatal periodic input (Figure 5.2A), whereas a model with strong connection weights between STN and GPe and low reciprocal GPe connection weights oscillates at beta regardless of periodic input rate (Fig 5.2B).

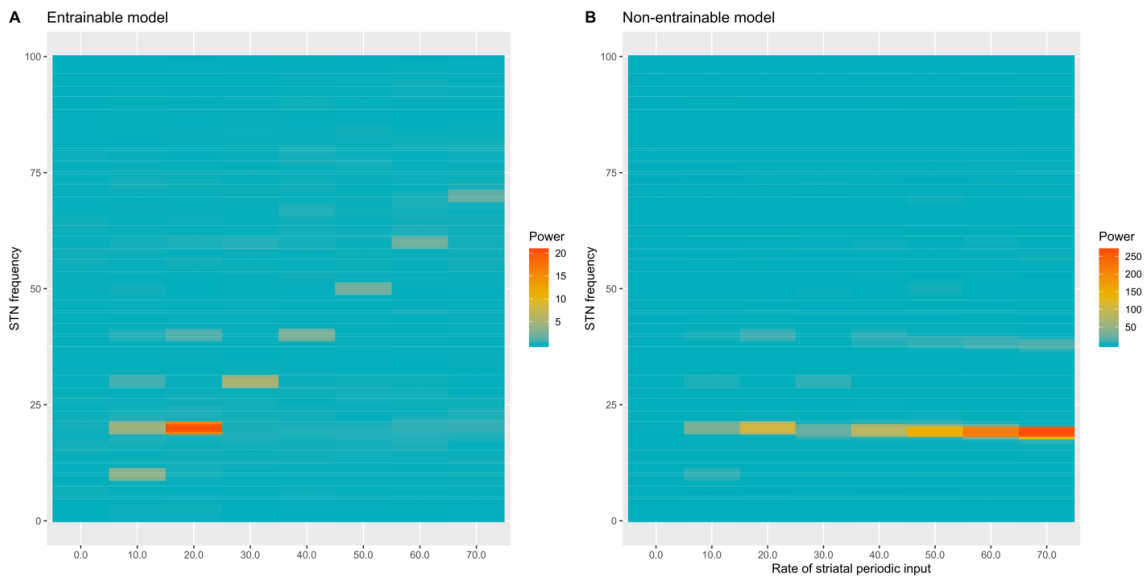


Figure 5.2. An STN-GPe network model with (A) weak connection strength between STN and GPe and strong reciprocal GPe connection strength is entrainable to frequencies outside of beta range. In contrast, (B) strong connection strengths prevent entrainment to frequencies outside of beta range. Legend colors represent power spectral density values from the beta range calculated from normalized STN population rate.

In order to investigate the effect of connection strengths on the ability for the STN-GPe network to entrain outside of the beta range, we simulated various connection weight values for GPe to STN, reciprocal GPe, and STN to GPe connections while inputting either theta (6 Hz) (Figure 5.3) or gamma (70 Hz) (Figure 5.4) periodic striatal inhibition to GPe. Under both theta or gamma striatal periodic input, 1) lower values of GPe to STN connection strength (Figure 5.3A-C, Figure 5.4A-C); 2) higher values of reciprocal GPe connection strength (Figure 5.3D-F, Figure 5.4D-F); and 3) lower values

of STN to GPe connection strength (Figure 5.3G-I, Figure 5.4G-I) showed greater entrainment to the incoming striatal periodic input.

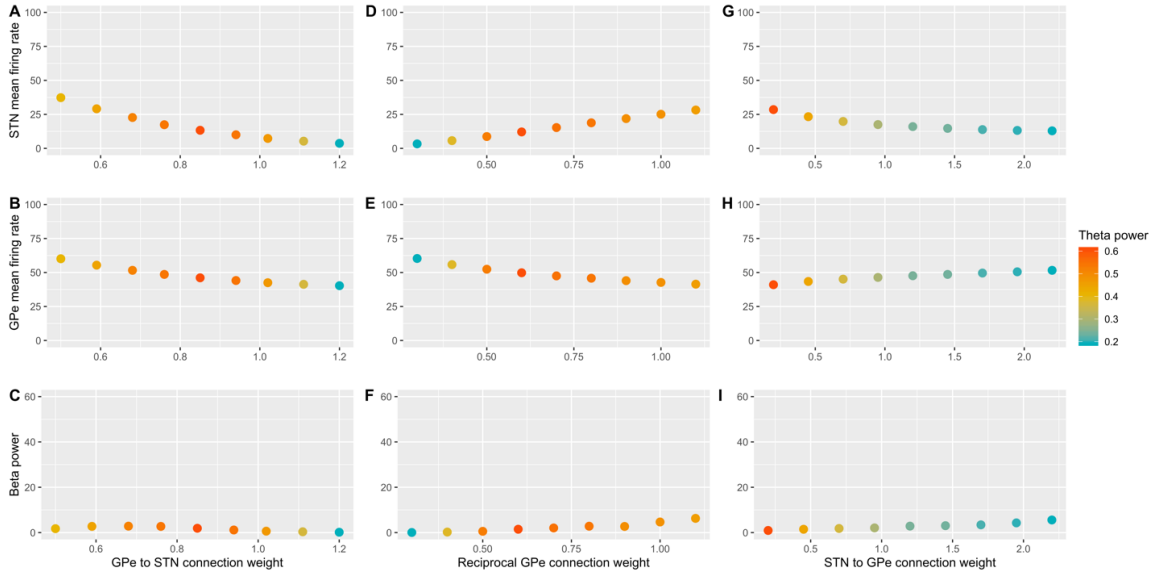


Figure 5.3. Network connection strengths control degree of theta entrainment. (A-C) GPe to STN connection strength is evaluated in relation with (A) STN firing rate, (B) GPe firing rate, and (C) beta synchrony. (D-F) Reciprocal GPe connection strength is evaluated in relation with (D) STN firing rate, (E) GPe firing rate, and (F) beta synchrony. Lastly, (G-I) STN to GPe connection strength is evaluated in relation with (G) STN firing rate, (H) GPe firing rate, and (I) beta synchrony. Legend colors represent power spectral density values from the theta range calculated from normalized STN population rate.

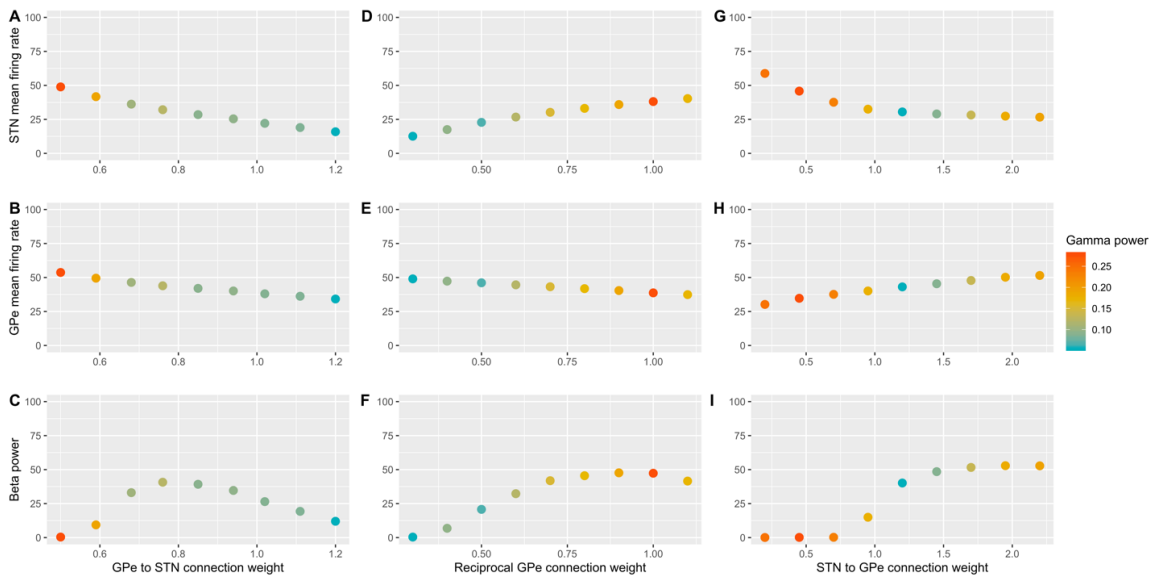


Figure 5.4. Network connection strengths control degree of gamma entrainment. (A-C) GPe to STN connection strength is evaluated in relation with (A) STN firing rate, (B) GPe firing rate, and (C) beta synchrony. (D-F) Reciprocal GPe connection strength is evaluated in relation with (D) STN firing rate, (E) GPe firing rate, and (F) beta synchrony. Lastly, (G-I) STN to GPe connection strength is evaluated in relation with (G) STN firing rate, (H) GPe firing rate, and (I) beta synchrony. Legend colors represent power spectral density values from the gamma range calculated from normalized STN population rate.

STN Firing Rate Correlates With Beta Synchrony When Connections Between STN and GPe Are Strong

In an STN-GPe network model with strong connection strength between STN and GPe and weak reciprocal GPe connection strength, beta power strongly correlates with STN firing rate ($R=0.93$) (Figure 5.5 D,E). In contrast, GPe mean firing rate is weakly predictive of beta synchrony ($R=-0.13$) (Figure 5.5 F). However, the relationship between STN firing rate and beta power is strongly reduced ($R=0.52$) in an entrainable model where STN and GPe connection strengths are weak and reciprocal GPe connection strength is high (Figure 5.5 A,B). In fact, STN firing rate is only slightly more predictive than GPe firing rate ($R=-0.32$) of network beta power in an entrainable network regime (Figure 5.5 C).

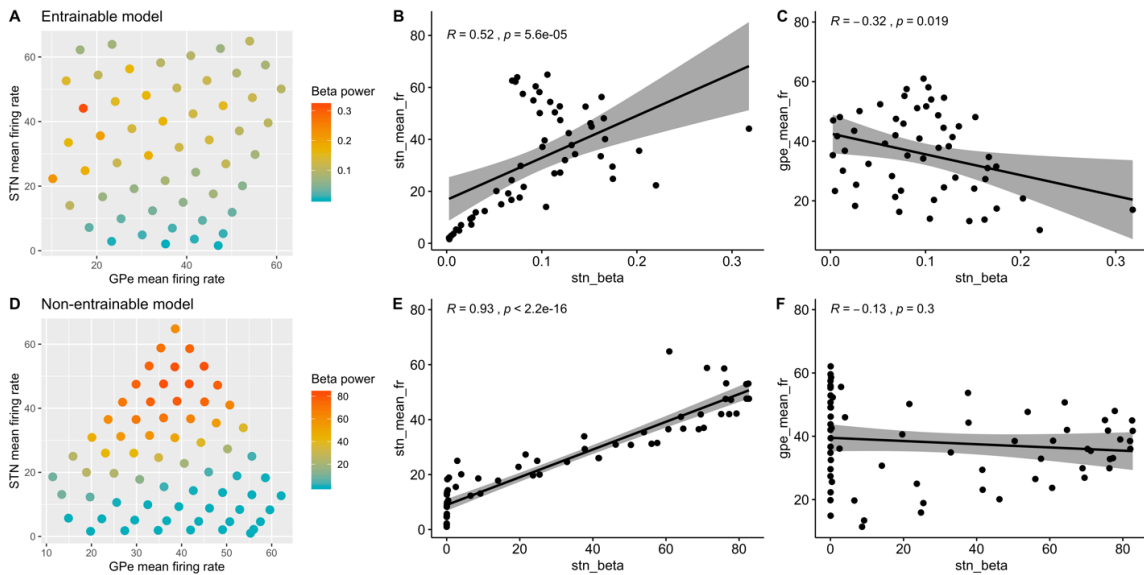


Figure 5.5. The relationship between STN firing rate and beta synchrony is less pronounced in an entrainable model. (A-C) The relationships between STN and GPe firing rates and beta synchrony in entrainable and (D-F) non-entrainable STN-GPe network models. Legend colors represent spectral density values from the beta range calculated from normalized STN population rate.

Discussion

Principle Findings

The advent of novel neural stimulation and recording technologies have facilitated discovery of important symptom-altering aspects of PD neuropathology. Specifically, beta oscillations have emerged as a clear contributor to motor symptoms of PD and exaggerated levels have been found throughout the cortico-basal ganglia-thalamic loop in untreated PD patients. However, with new information, comes additional questions, and understanding the origin and neural dynamics of beta oscillations have remained elusive. In this work, we investigate the neural dynamics of pathological oscillations in a computational model of the STN-GPe network. We demonstrate that synaptic connection strength has a crucial role controlling entrainability of the STN-GPe network.

Specifically, weak synaptic connections between the STN and GPe facilitate entrainment to a wide range of frequencies, whereas strong synaptic connections support intrinsic beta oscillations and prevent entrainment to all other frequencies. We also find that the ability of STN firing rate to drive beta oscillations is reduced as synaptic connection strengths are weakened.

Origin and Mechanisms of Pathological Oscillations

Beta oscillations in the cortico-basal ganglia-thalamic loop have been causally linked to motor impairments in PD patients, though, mechanics and origin have remained elusive. The cerebral cortex (Brittain & Brown, 2014; Hirschmann et al., 2011; Litvak et al., 2011; Marceglia et al., 2006), striatum (Corbit et al., 2016; McCarthy et al., 2011), and STN-GPe network (Bevan et al., 2002; Cruz et al., 2011; Fan et al., 2012; Plenz & Kital, 1999), have all been implicated in the generation of beta oscillations in pathological states. Indeed, it is even possible that beta is generated in multiple, coherently oscillating locations, facilitating the exaggerated beta synchrony seen across nuclei in the cortico-basal ganglia-thalamic loop (Fries, 2005). Better understanding of network conditions in which beta oscillations occur will facilitate a clearer understanding of the origin and mechanisms at play and provide a path to improved treatment options for patients. To this end, we investigate the dynamics of an STN-GPe network model and observe that weak synaptic connections between the STN and GPe prevents intrinsic production of beta oscillations and allows entrainment to a wide range of frequencies. In contrast, strong synaptic connections create a strong beta resonance in the STN-GPe network, regardless of input frequency, and prevent entrainment to all other frequencies.

Importantly, in healthy adults, the STN-GPe network has been shown to produce oscillations outside of the beta range, and indeed various oscillation frequencies are vital to normal function (Halje et al., 2019). Thus, based on our findings, we hypothesize that synaptic connections must be weak enough in healthy adults to produce physiologically appropriate oscillations at a wide range of frequencies.

By extension, if the STN-GPe network is indeed acting as a source of pathological beta oscillations in PD, the network may undergo plastic changes that increase synaptic strength in order to produce exaggerated beta oscillations. Based on the results of our network model, the STN-GPe network does not intrinsically resonate at beta in its weak connection strength, non-pathological state. Indeed, our results suggest that external beta input is required to entrain the network to the beta frequency range. Thus, plastic changes increasing synaptic connection strengths between STN and GPe may occur in the pathological state. Limited studies to date have investigated the extent to which plastic changes occur based on oscillatory activity (King et al., 1999; Wespata et al., 2004; Zanos et al., 2018). However, it has been theorized that spike timing-dependent plasticity (STDP) does indeed occur from oscillations, and, in fact, may be more efficient compared with conventional rate-based codes for STDP-based learning (Masquelier et al., 2009). Furthermore, in-vitro and computational modeling evidence has directly implied a role of plasticity in modulating spiking rates and temporal patterns of GPe activity (Hanson & Jaeger, 2002). By extension, animal models of PD and human studies in both the motor cortex and basal ganglia have cited evidence for defective synaptic plasticity, possibly contributing to the development of pathological synchrony in the

cortico-basal ganglia-thalamic loop (Udupa & Chen, 2013). Therefore, it is conceivable that plastic changes, increasing synaptic connection strengths between STN and GPe, drive exaggerated beta oscillations in the STN-GPe network. Further investigation into the extent of plastic changes occurring in the STN-GPe network in pathological conditions is warranted.

Alternatively, the STN-GPe network may not be acting as the origin of beta in pathological conditions, but rather a conveyer or amplifier of beta from a preceding input. In our STN-GPe network model, weak synaptic connections were necessary to facilitate entrainment to frequencies outside of beta. Indeed, evidence has shown that even in pathological conditions, the basal ganglia should retain the ability to resonate at frequencies outside of beta (Brown, 2003). Thus, with the requirement of retaining entrainability, it may be the STN-GPe network preserves weak synaptic connections in pathological conditions, receives beta from upstream neurons, and conveys beta downstream through the cortico-basal ganglia-thalamic loop. This is in line with studies suggesting cortical or striatal origins of pathological beta production (Brittain & Brown, 2014; McCarthy et al., 2011).

Role of STN in Beta Oscillations

Additionally, our results provide new insight into the role of STN and GPe firing rates in controlling oscillations in the STN-GPe network. Our results suggest that the strength of beta oscillations in a beta-producing STN-GPe model with strong synaptic connections correlates strongly with STN firing rate and not GPe firing rate. The causal relationship between STN firing rate and beta oscillations has been previously observed

in computational models (Bahuguna et al., 2020). The relationship is also in line with conceptual theories that increased STN activity suppresses movement (M. J. Frank, 2006) and experimental observations that indicate STN firing rates are decreased in response to DBS treatment (Meissner et al., 2005). However, based on our observations, the strong relationship between STN firing rate and beta synchrony weakens in an entrainable STN-GPe network with weak synaptic connections. Thus, it may be the case that the amplifying effect of STN firing rate to beta oscillations in the STN-GPe network is exaggerated in a pathological state, compared to healthy, entrainable conditions.

Future Work

Although we do not resolve the debate surrounding the origin of beta oscillations, our results do provide constraints on the conditions for beta production. However, significant questions and additional work remain. Our results to date are observational and we have not yet established a mechanism to explain the relationship between synaptic connection strength and network entrainment. For example, it is unclear whether there exist subsets of neurons that have the capacity to entrain to frequencies outside of beta when STN-GPe synaptic connections are weak. By extension, it is unclear whether these subsets lose the capacity to entrain when synaptic connections are strong. Future work investigating the effects of firing rate, synaptic connectivity, and external input on model entrainment are of interest.

CHAPTER SIX: DISCUSSION

Principal Findings and Significance

From the original description of Parkinson's disease by James Parkinson (Parkinson, 2002), to clinical scales and quantitative measurements (Godinho et al., 2016; Goetz et al., 2008), our understanding of symptoms and the effects of treatment in Parkinson's disease continues to expand as we probe neurological circuits involved and monitor effects. The traditional model of site-centric, controlled clinical trials has enabled development and evaluation of revolutionary medications. Though, as our desire for deeper insight into disease burden and quality of life persists, the pursuit for enriched measurement inevitably leads us to the home environment. Insight provided from measuring symptoms and treatment effect in free-living conditions may aid in elucidating diverse Parkinsonian phenotypes and facilitate novel, personalized medication treatments and plans.

Studies investigating at-home monitoring technologies are in their infancy. Thus, challenges and questions regarding feasibility of continuous free-living data collection, interpretation, and standardization of algorithms, devices, and statistical methods remain. My work presented in this dissertation explores the feasibility and benefits of remotely monitoring symptoms related to Parkinson's disease. In Chapter 2, I describe the development of a publicly available computational package for deriving gait features from a single accelerometer device on the lower back. In Chapter 3, I demonstrate strong accuracy and reliability of this algorithm in a healthy population made up of a younger and older cohort. I investigate the differences in gait speed between an in-clinic walking

task and daily, continuous monitoring of gait speed in free-living conditions and find a weak correlation between the two. Furthermore, I find that at-home gait speed is more sensitive in distinguishing between younger and older cohorts. I hypothesize that one reason for differences between at-home and in-clinic data is due to observer effect. Specifically, my results show higher gait speed in-clinic compared to at-home, suggesting an over-compensation that is more pronounced in older adults (Figures 3.2,3). Importantly, the improved sensitivity to small differences between cohorts, as well as the lack of bias due to observer effects, suggest symptom measurement in free-living environments may improve our ability to measure small disease and treatment related changes compared to traditional in-clinic assessments. Additionally, in Chapter 3, I investigate the amount of data needed to reliably estimate gait speed in free-living environments. I find that approximately 3 days of continuous monitoring is required for accurate estimation of gait speed, providing a minimum target for designing clinical studies.

Next, in Chapter 4, I validate the lower back sensor-based algorithm for gait detection in a PD population and demonstrate strong accuracy and reliability for most gait features. Additionally, I find that the algorithm has minimal reduction in accuracy compared to using additional devices for predicting degree of gait impairment in PD patients. Furthermore, the algorithm has sufficient sensitivity to discriminate between medication states. These results suggest the ability to measure disease related impairment and treatment effect using a minimal sensor set-up, feasible for at-home use. Lastly, in Chapter 5, I find synaptic connection strengths between STN and GPe determine whether

the network produces beta intrinsically or requires external entrainment. This finding has important implications for the origin of beta oscillations and network reorganization in PD. Specifically, beta may originate from outside STN-GPe or it may be produced from STN-GPe only after plastic changes have occurred.

Evidence for Benefits of At-Home Measurement

Free-living monitoring has become technologically feasible due to novel improvements in engineering and data analytics (Del Din, Godfrey, Mazzà, et al., 2016; Polhemus et al., 2021). The potential benefits of free-living monitoring, as opposed to traditional in-clinic assessments and patient-reported outcomes, are intriguing. Indeed, continuous, at-home patient monitoring is free from limitations of traditional measures such as recall bias, observer effects, the requirement of traveling to a clinic, subjective measurements, and increased cost. To this end, benefits of free-living patient monitoring include reduced burden, additional insight into disease burden and therapeutic response, reduced cost, enhanced patient recruitment, and expanded access to treatments. Despite potential benefits, lack of thorough evaluation and understanding of in-clinic compared to at-home digital mobility outcomes has prohibited widespread use as research and clinical assessment tools.

My dissertation results demonstrate benefits of sensor-based digital mobility outcomes derived in the at-home environment compared to in-clinic assessment. Specifically, in Chapter 3, I demonstrate that the ability to distinguish younger and older cohorts requires gait speed to be derived in the at-home environment. In contrast, gait speed derived from in-clinic assessment does not show significant differences between

age groups. My results, consistent with other studies (Del Din, Godfrey, Galna, et al., 2016), suggest at-home measurements of gait may be more sensitive to subtle differences, in this case between younger and older cohorts. By extension, free-living measurements may be more sensitive to disease state and treatment effects.

One reason for heightened sensitivity in the at-home environment may be due to reduced bias from the Hawthorne effect (McCambridge et al., 2014), defined as alteration in behavior by subjects of a study due to their awareness of being observed. Potential evidence for the presence of a Hawthorne effect in-clinic is presented in Chapter 3, in which I find in-clinic gait speed is higher than at-home gait speed across both younger and older healthy participants (Figure 3.4). Participants overperforming while being observed, and thus increasing their gait speed in-clinic, is consistent with the expected outcome of a Hawthorne effect. Assuming patient gait speed is uniformly increased in-clinic due to a Hawthorne effect, it would be reasonable to assume a stronger correlation would exist between in-clinic gait speed and at-home 95th percentile gait speed, an estimation of maximum effort. However, interestingly, I find weak correlation exists between at-home 95th percentile gait speed and in-clinic gait speed (Figure 3.4). Therefore, despite patients likely exerting extra effort in-clinic due to awareness of being observed, the degree of extra effort may vary by patient. Variable extra effort given by patients may lead to increased variability of gait measures in-clinic and provides a potential explanation for enhanced sensitivity in the at-home environment, where long periods of passive monitoring reduce likelihood that participants will change their behavior.

However, differences between at-home and in-clinic gait is likely multifold. For example, factors including daily cognitive distractions, fatigue, mood may also be implicated (Giannouli et al., 2018). Additionally, technical limitations from lack of thorough at-home validation of the gait algorithm I developed and used in this dissertation may also be a source of discrepancy between at-home and in-clinic gait speed. Additional technical validation as well as measuring the effect of cognitive distraction, fatigue, and mood on free-living gait warrant further investigation.

Considerations for At-Home Measurement

Results of my dissertation demonstrate several considerations exist for deriving reliable and repeatable results from at-home digital outcome studies. For example, consistent with other studies (Cheng et al., 2017; Del Din, Godfrey, Galna, et al., 2016; Storm et al., 2018), I find bout length has a significant impact on at-home gait features (Supplementary Figure A.2b). Specifically, I find gait speed increases with increasing bout length. Thus, controlling for bout length of interest is an important statistical design consideration in order to generate consistent results across studies. This is especially the case considering recent evidence that gait performance depends on bout length (Del Din, Godfrey, Galna, et al., 2016). Specifically, Del Din et al. found that group differences between patients with PD and healthy controls disappear when looking solely at short at-home bouts of gait. This is in contrast with other reports suggesting that short bouts of gait indeed do provide reliable symptom related measures in MS patients (Motti Ader et al., 2020). However, by extension, the very definition of bout length must be taken into consideration, as changes to maximum resting period between consecutive ambulatory

bouts results in changes in gait volume, variability, and pattern (Barry et al., 2015). Future work, in specific patient populations, providing insight into the effect of bout length and measurement sensitivity are needed. Though, it is clear that bout length is an important consideration in the statistical analysis of free-living data.

Additionally, day of the week impacts gait speed significantly. In Chapter 3, I find that both young and older cohorts walked slower during weekends compared to weekdays, likely a reflection of weekly scheduled activities, such as employment or hobbies. Furthermore, significant differences in gait speed between younger and older cohorts is driven by weekdays, not weekends (Supplementary Figure A.2a). These results may indicate that differences in daily activities may influence the sensitivity of at-home measurements to disease or treatment related effects.

Another factor influencing the reliability and sensitivity of at-home gait measurements is amount of data collected. In Chapter 3, I demonstrate that approximately 3 days of data is required to reliably estimate gait speed (Figure 3.5). This result is comparable with other studies measuring gait and physical activity in the home environment (Hart et al., 2011; Mueller et al., 2019; Van Schooten et al., 2015). However, more data was necessary in the younger cohort for reliable estimation of gait speed compared to the older cohort, implying greater day-to-day variability in the younger cohort. Therefore, day-to-day variability of at-home gait measures may vary between patient population and require additional data accordingly. Furthermore, additional data may be needed to detect a particularly small change related to a specific disease or treatment effect. Another factor complicating the amount of data actually

acquired from continuous recording days is wear time. A device that is assigned but not worn throughout the day may result in minimal or no analyzable gait data. Regrettably, significant algorithmic limitations exist for determining device wear/non-wear periods using solely IMU data currently. Specifically, wear-time detection algorithms exist, though they are generally unreliable at high resolution time scales, especially positioned at the lower back (Knaier et al., 2019). Another factor that affects amount of gait data collected is low levels of patient activity. Patients that seldom walk or cannot walk for any reason, such as may be the case with certain late stage disease complications, will likely be challenging to analyze due to lack of data and are likely not ideal candidates for gait monitoring technologies, unless the intention of an intervention is to facilitate the ability to walk. Indeed, number of days wearing a device, gait variability, wear time, and patient activity levels are all factors that may influence reliability and sensitivity of at-home digital mobility outcomes.

In addition to data and statistical procedures, clinical studies with at-home digital outcomes must take into account specific disease patient phenotypes and needs. Hospitals and rehabilitation clinics have traditionally focused on assessing gait in the context of an in-clinic, facility setting, such as a hospital hallway. To this end, gait speed and endurance are typically considered strong indicators of functional ability (Middleton & Fritz, 2013). Indeed, sensor-based measurements of typical spatiotemporal features of gait can indeed provide an accurate estimation of gait impairment and treatment effect (Figures 4.2,3). However, considering the start-stop nature of free-living gait, predominantly consisting of small numbers of steps over short bout lengths during typical

activities, it may be that gait features related to initiation, modulation, and termination are better indicators of functional mobility (Orendurff et al., 2008). Therefore, it is worth considering the types and features of gait that pose the most challenge to the patient achieving functional mobility when evaluating the effects of interventions.

Barriers to Digitization of Clinical Trials

Traditional clinical trials have been the standard by which new medications and treatments are evaluated for safety and efficacy in the modern era. However, various inefficiencies related to patient identification, recruitment, data acquisition, and follow-up raise costs and increase burden for patients (Inan et al., 2020). In contrast, decentralized, digital trials facilitate the ability to conduct clinical trials remotely, electronically, and independent of participant proximity and the requirement to travel to a research site (Steinhubl et al., 2017). Thus, the concept of the digitized trial has emerged as a promising strategy to overcome limitations of traditional clinical trial approaches. Indeed, regulatory agencies have promoted the adoption of digital tools and encouraged investigators to minimize specialized study infrastructure, minimize in-clinic visits, and employ novel, low-cost methods to obtain informed consent and monitor study conduct (Lauer & Bonds, 2014). In fact, digital mobility outcomes are being qualified as endpoints in pivotal clinical trials. For example, 95th percentile gait speed was approved in 2019 as an acceptable secondary endpoint in clinical trials for Duchenne muscular dystrophy (Committee for Medicinal Products for Human Use (CHMP), 2019). The promotion of digitized trials is not surprising given the potential benefits to patient outcomes, including enhanced access to treatments for geographically or mobility

challenged participants and reduced clinical trial failure rate due to higher recruitment and retention rates.

Despite promise, significant hurdles remain for digitized trials becoming common practice. Thorough validation and regulatory qualification for technical feasibility, relevance to patients, clinical meaningfulness, and cost effectiveness is necessary, though fragmented in the literature and lacking overall (Polhemus et al., 2021). Thus, calls for collaborative approaches between regulators, industry, academics, and precompetitive consortia to speed up validation of digital outcomes have been made (Rochester et al., 2020; Stephenson et al., 2020).

Toward the goal of collaborative validation approaches, standardization of devices, algorithms, protocols, data requirements, and statistical methods is vital. However, significant methodological variability exists in the literature to date and often algorithms and data are not readily accessible to researchers, thus hindering progress. To this end, in Chapter 2, I develop and make publicly available a python-based computational package for deriving features of gait from a lower back accelerometer. Although accurate and reliable in my studies, feedback and use from the community in various datasets in diverse disease populations will, ideally, enable future iterations and improvement toward a more robust algorithm, and eventually a qualified digital outcome. In addition to the goal of qualification, it is my hope that, ultimately, publicly available methodologies will lower the bar to conduct digitized clinical trials to a point where they are not be limited to those with advanced analytical development capabilities. Lastly, the

importance of open, transparent algorithms for translation of clinical health information for use in evaluating treatment efficacy cannot be understated.

Though not widespread, other efforts exist toward the goal of open-access digital algorithms. For example, GGIR is an open-source package for processing raw accelerometer data for measures related to physical activity and sleep (van Hees et al., 2021). Hundreds of studies have been conducted in various disease populations using GGIR in the past few years, a feat that could not have been accomplished by a single organization (Gill, 2021). Additionally, my colleagues at Pfizer have developed and completed validation work for several computational open-source packages related to sleep, scratch, and sit-to-stand activities with additional packages in development (Adamowicz & Patel, 2020; Christakis et al., 2019; Mahadevan et al., 2021).

Further collaboration, not only with digital algorithms, but with methodologies and data requirements are still needed. As mentioned previously, methods by which at-home measurement of gait is summarized into single values has significant impact on analysis results. To maximize patient outcomes, safe and transparent multicomponent systems and analysis methods are vital for qualification and effective use of digital outcomes.

Concluding Remarks

In this dissertation, I develop a sensor-based method for measuring gait and demonstrate evidence that continuous measurement in the at-home environment increases sensitivity to small cohort differences compared to the in-clinic environment. Furthermore, I demonstrate inherent differences between gait measures acquired from

each environment and hypothesize several sources for these differences, including Hawthorne effect, cognitive distractions, mood, and fatigue. Additionally, I demonstrate feasibility for a single accelerometer to estimate degree of gait impairment and detect treatment effect in PD patients. Lastly, I demonstrate STN-GPe synaptic connection strengths determine oscillatory power in the beta range and the ability to entrain to a wide range of frequencies.

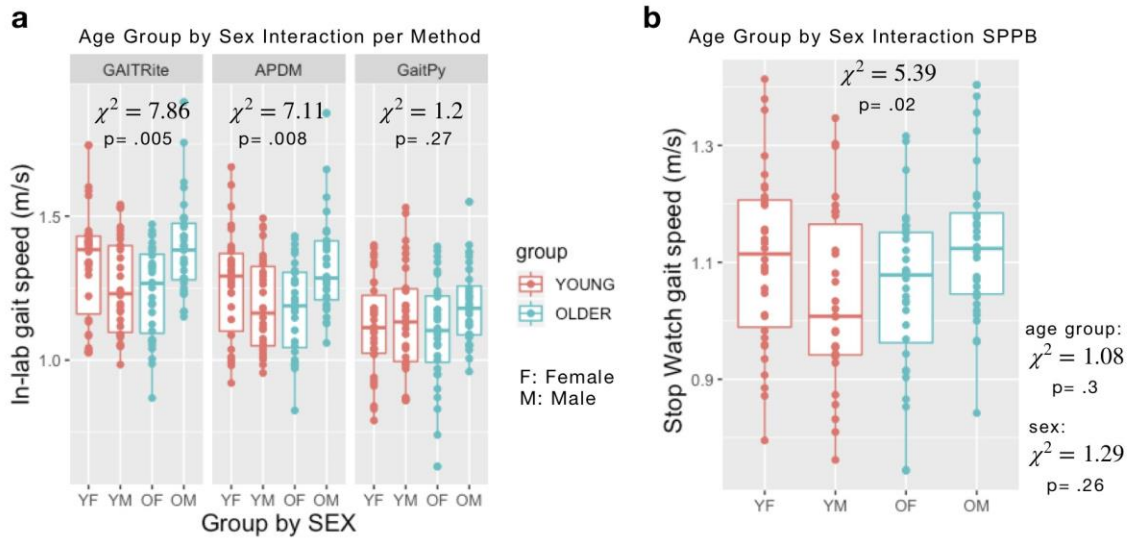
The results of this dissertation shed light on important facets and considerations regarding digital patient monitoring and invite new avenues for future work. Specifically, this work explores the sensitivity of sensor-based gait measurement to estimate gait impairment and treatment effect in PD. However, measures of gait are clinically relevant in various neurodegenerative and movement disorders. Indeed, adapting and evaluating digital algorithms in diverse patient populations will be critical toward qualification and use for treatment efficacy in those patients. Moreover, developing novel algorithms to measure aspects of mobility outside of gait will provide a more complete picture of disease symptoms and functional capacity.

The work presented in this dissertation also generates questions to be investigated regarding data requirements and protocol optimization. I find that approximately 3 days of remote monitoring enables reliable measurement of gait. However, data requirements for older participants is reduced compared to younger participants. Thus, degree of data variability and thus data requirements for various patient populations is unknown and may be necessary to evaluate on a case by case basis. Furthermore, the method by which data requirement was determined in this work is in the context of free-living conditions.

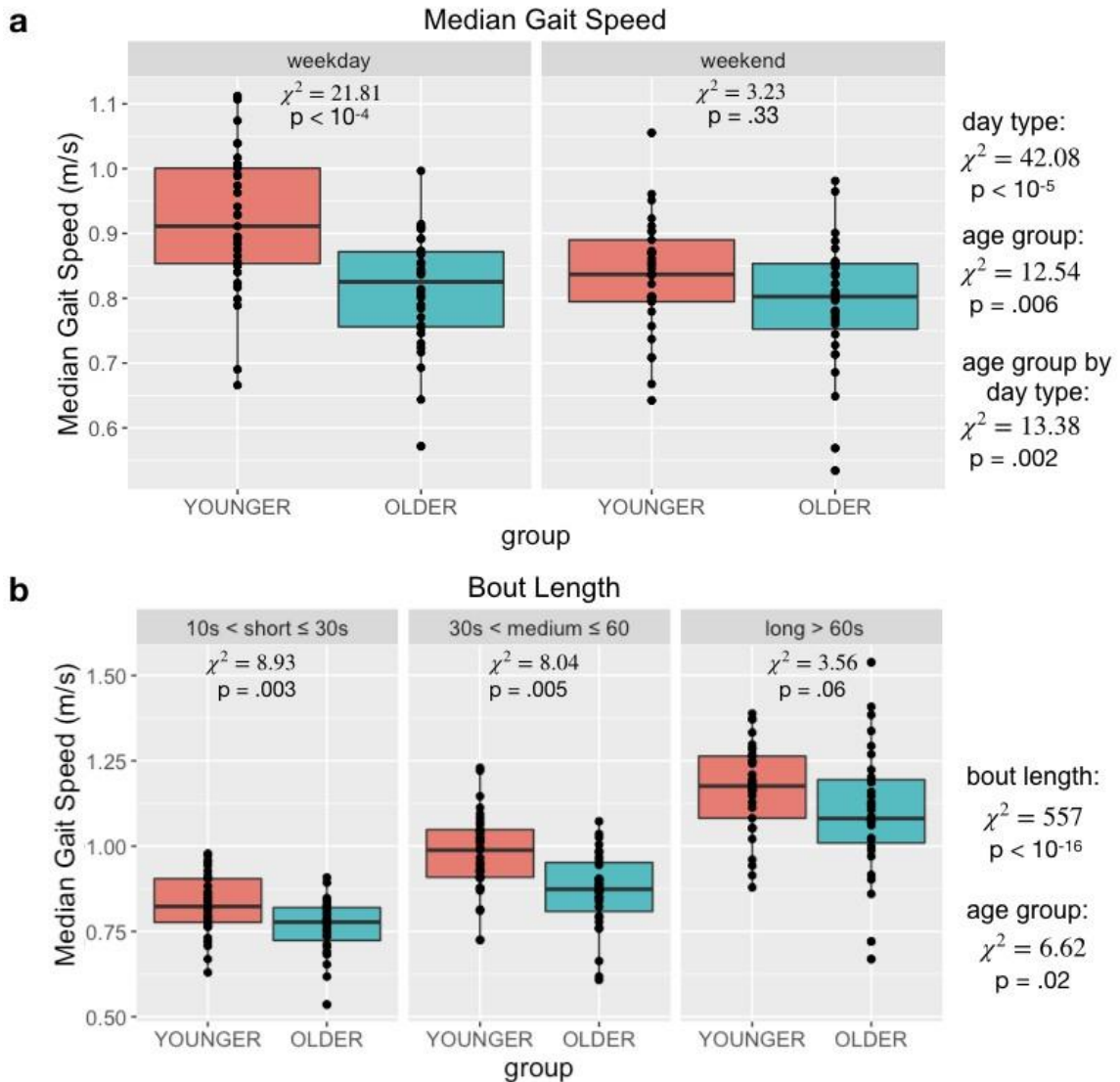
In contrast, remote digital assessments, akin to hospital tasks, though accomplished in an at-home environment, may consist of completely different data requirements. It is yet to be determined the amount of data needed, nor the tradeoffs between free-living versus periodic at-home digital assessments. Thus, questions regarding optimal at-home data collection and assessment procedures remain unanswered and may be an interesting target for future studies.

APPENDIX

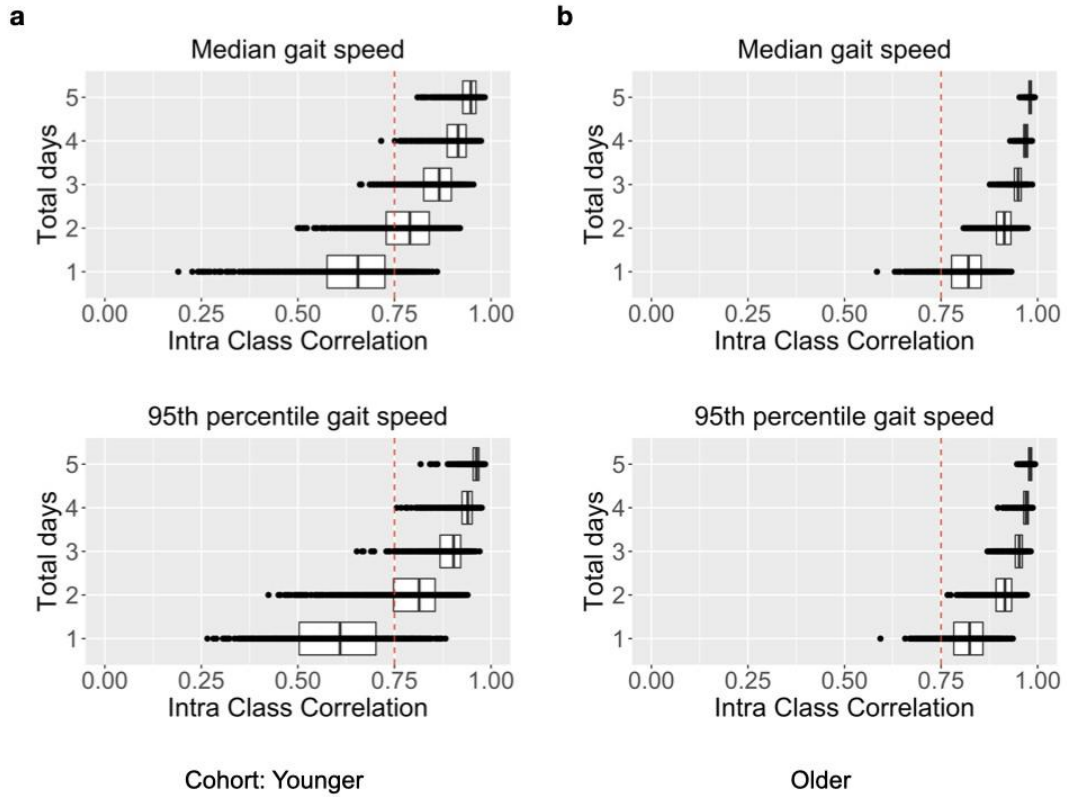
Chapter 3 Supplementary Information



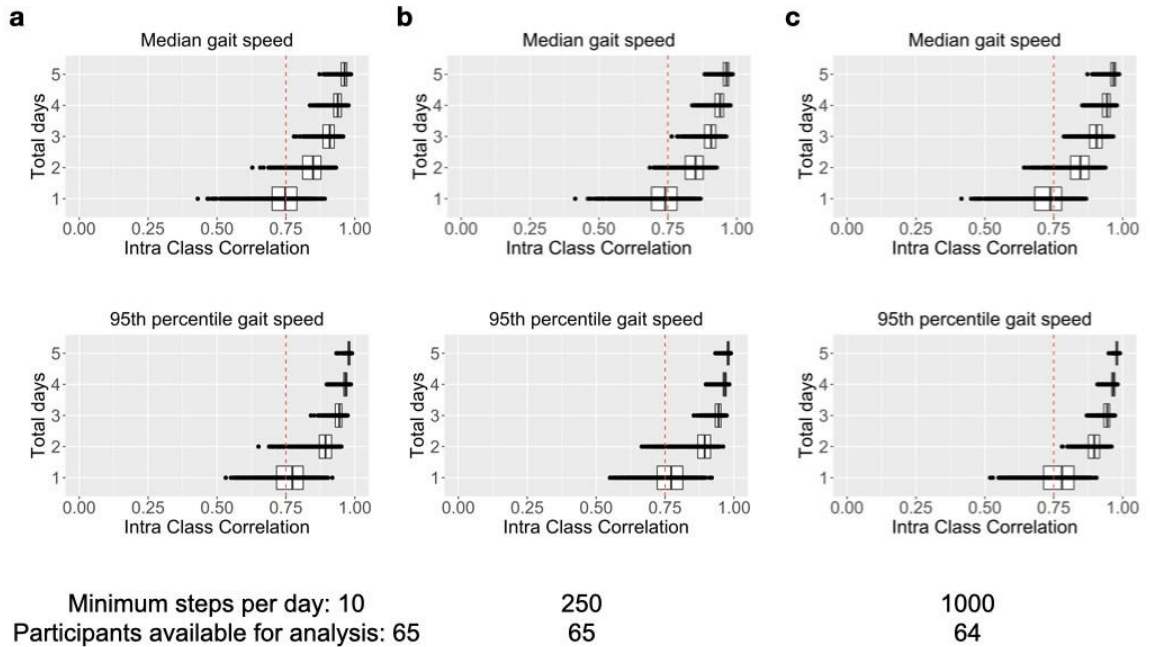
Supplementary Figure A.1: Effect of sex and age group interaction in in-lab measurements. (a) GAITRite and APDM showed a significant age group by sex interaction in in-lab measurements, in which younger males were slower than younger females whereas older males walked faster than older females. (b) Similar trend was observed with uninstrumented measurements as well. The uninstrumented gait speed was computed by dividing the walking distance; i.e., 4 meters, by the average time to walk 4 meters measured by stop watch as part of standard clinic assessment; i.e., SPPB.



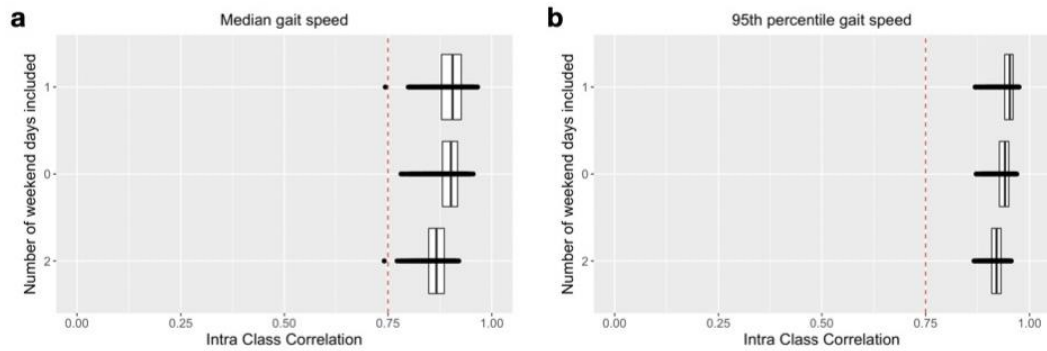
Supplementary Figure A.2: Effect of day type and bout length on median gait speed. (a) Both age groups walked slower during weekends compared to weekdays, however, the age group differences were driven by weekdays, not weekends. (b) Gait speed significantly differed and increased with increasing bout lengths (effect of bout length: $\chi^2 = 557$, $p < 10^{-16}$). Moreover, we observed significant or trending age group differences in all bout lengths (effect of age group: $\chi^2 = 6.62$, $p = .02$) with decreasing effect size; i.e., normalized χ^2 , with increasing bout length.



Supplementary Figure A.3: Quantity of data needed to estimate at-home gait speed reliably is different between younger and older cohorts. (a) Younger participants require at least two days of data to reliably estimate at-home gait speed, whereas (b) older participants require at least 1 day of data.



Supplementary Figure A.4: Number of monitoring days required for various criteria. Varying the minimum threshold for steps per day to be considered for analysis between (a) 10, (b) 250, and (c) 1,000 does not impact the quantity of data needed to estimate at-home gait speed reliably but does reduce the participants available for analysis.



Supplementary Figure A.5: Reliability of gait speed for weekends vs weekdays. Including one weekend day, but not two, out of three total days only slightly enhances reliability of estimated at-home (a) median and (b) 95th percentile gait speed. Random subsets of data that included three, two, and one weekdays out of three total days were compared to the full data set.

	GAITRite				APDM				GaitPy				Device			
	Visit 1 ^a		Visit 2 ^a		Visit 1 ^a		Visit 2 ^a		Visit 1 ^a		Visit 2 ^a		Age group		X ²	p
	Younger	Older	Younger	Older	Younger	Older	Younger	Older	Younger	Older	Younger	Older	X ²	p		
gait speed (m/s)	1.29 ± 0.18	1.3 ± 0.19	1.31 ± 0.19	1.33 ± 0.17	0.33 0.57	1.22 ± 0.17	1.24 ± 0.19	1.24 ± 0.18	1.27 ± 0.17	0.57 0.45	1.13 ± 0.16	1.13 ± 0.18	1.13 ± 0.19	1.15 ± 0.16	0.03 0.87	199.1 < 10 ⁻¹⁶
swing time (s)	0.4 ± 0.03	0.39 ± 0.03	0.4 ± 0.03	0.39 ± 0.03	3.18 0.07	0.44 ± 0.03	0.43 ± 0.03	0.44 ± 0.03	0.42 ± 0.03	3.88 0.05	0.42 ± 0.03	0.41 ± 0.03	0.42 ± 0.03	0.41 ± 0.03	0.88 0.35	514.4 < 10 ⁻¹⁶
stance time (s)	0.68 ± 0.07	0.66 ± 0.05	0.67 ± 0.07	0.65 ± 0.04	1.97 0.16	0.64 ± 0.06	0.63 ± 0.04	0.64 ± 0.06	0.62 ± 0.04	0.90 0.34	0.69 ± 0.06	0.68 ± 0.05	0.69 ± 0.05	0.67 ± 0.04	1.52 0.22	549.92 < 10 ⁻¹⁶
double support (s)	0.27 ± 0.05	0.26 ± 0.04	0.27 ± 0.05	0.26 ± 0.04	0.47 0.49	0.2 ± 0.04	0.2 ± 0.03	0.2 ± 0.05	0.2 ± 0.03	0.17 0.69	0.28 ± 0.03	0.27 ± 0.02	0.27 ± 0.02	0.26 ± 0.02	2.16 0.14	490.45 < 10 ⁻¹⁶
single limb support (s)	0.4 ± 0.03	0.39 ± 0.03	0.4 ± 0.03	0.39 ± 0.03	1.92 0.17	0.44 ± 0.03	0.43 ± 0.03	0.44 ± 0.03	0.42 ± 0.03	0.83 0.36	0.42 ± 0.03	0.41 ± 0.03	0.42 ± 0.03	0.41 ± 0.03	0.001 0.98	113.1 < 10 ⁻¹⁶
step time (s)	0.54 ± 0.05	0.53 ± 0.03	0.54 ± 0.05	0.52 ± 0.03	2.31 0.13	0.54 ± 0.04	0.53 ± 0.03	0.54 ± 0.04	0.52 ± 0.03	1.78 0.18	0.56 ± 0.05	0.54 ± 0.04	0.55 ± 0.04	0.54 ± 0.04	1.39 0.24	287.82 < 10 ⁻¹⁶
stride length (m)	1.41 ± 0.14	1.39 ± 0.19	1.42 ± 0.15	1.41 ± 0.2	0.01 0.93	1.31 ± 0.14	1.31 ± 0.19	1.32 ± 0.15	1.32 ± 0.19	0.16 0.69	1.25 ± 0.17	1.24 ± 0.18	1.24 ± 0.2	1.25 ± 0.18	0.03 0.86	183.98 < 10 ⁻¹⁶
stride time (s)	1.08 ± 0.09	1.05 ± 0.07	1.08 ± 0.09	1.04 ± 0.07	2.56 0.11	1.08 ± 0.09	1.06 ± 0.07	1.07 ± 0.09	1.04 ± 0.07	2.04 0.15	1.11 ± 0.09	1.09 ± 0.07	1.1 ± 0.08	1.07 ± 0.07	1.43 0.23	386.87 < 10 ⁻¹⁶

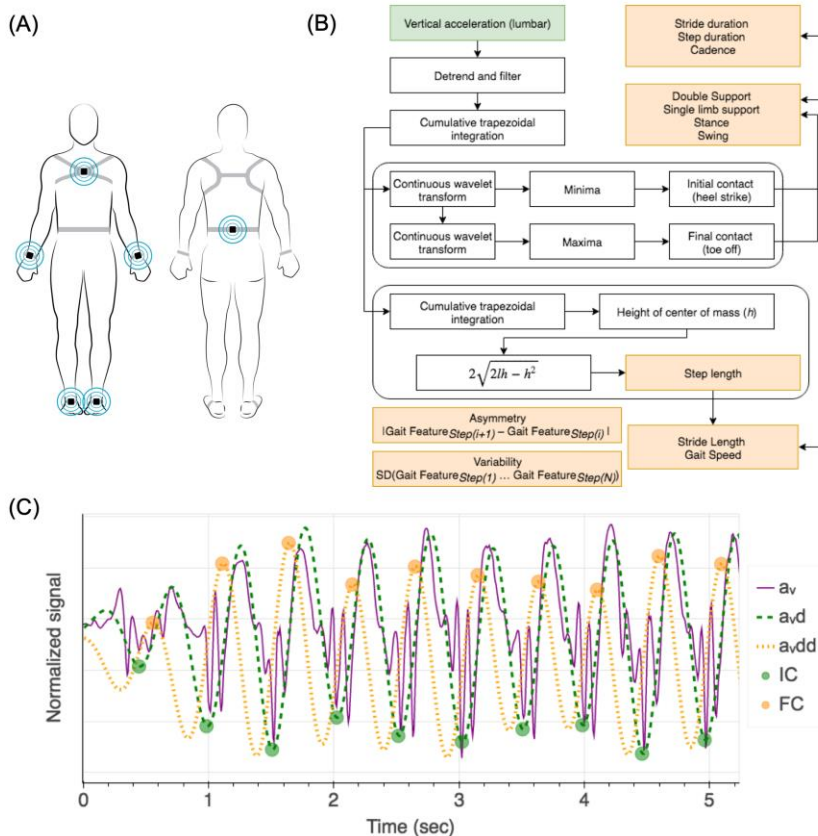
Supplementary Table A.1: In-Clinic Gait Metrics Derived From Instrumented Mat (GAITRite), APDM 6-Sensor Set, and GaitPy Algorithm Using One Lumbar Mounted Sensor. The common gait metrics were summarized for each visit and age group. The repeated mixed model regression showed that there is a significant effect of device on all gait metrics (Device: $p < 10^{-16}$). Posthoc analyses showed no age group differences in any of the gait metrics for any device (the p-values were not corrected for multiple comparisons for this analysis).

a Mean ± sd

	Age Group				Day Type				Age Group x Day Type				Sex		M.Mass		Height			
	Younger ^a	Older ^a	X ²	p	Weekday ^a	Weekend ^a	X ²	p	Younger WD ^a	Older WD ^a	Younger WE ^a	Older WE ^a	X ²	p	X ²	p	X ²	p		
95th gait speed	1.37 ± 0.13	1.19 ± 0.17	22.59	10 ⁻⁵										1.47	0.23	3.67	0.06	2.5	0.19	
gait speed	0.9 ± 0.1	0.81 ± 0.09	12.54	0.006	0.87 ± 0.1	0.81 ± 0.1	42.08	<10 ⁻⁵	0.92 ± 0.11	0.81 ± 0.09	0.83 ± 0.09	0.79 ± 0.1	13.38	0.002	0.74	1	3.102	0.4	2.76	0.24
steps	67.1 ± 20.37	55.67 ± 22.82	3.99	0.049	65.84 ± 26.46	52.3 ± 27.67	24.64	<10 ⁻⁵	70.99 ± 21.8	59.97 ± 26.3	57.31 ± 26.11	47.49 ± 22.82	0.24	0.672	0.73	1	2.426	0.4	2.04	0.24
gait cycle duration	1.24 ± 0.08	1.27 ± 0.07	5.16	0.030	1.25 ± 0.08	1.28 ± 0.07	39.50	<10 ⁻⁵	1.23 ± 0.08	1.27 ± 0.07	1.28 ± 0.07	1.29 ± 0.07	5.20	0.043	0.00	1	0.094	0.9	1.70	0.24
step duration	0.61 ± 0.04	0.63 ± 0.03	6.29	0.024	0.62 ± 0.04	0.64 ± 0.04	40.27	<10 ⁻⁵	0.61 ± 0.04	0.63 ± 0.03	0.63 ± 0.03	0.64 ± 0.04	5.07	0.043	0.01	1	0.196	0.9	1.60	0.24
cadence	100.47 ± 6.01	97.09 ± 5.27	8.54	0.012	99.54 ± 6.17	96.65 ± 5.24	42.49	<10 ⁻⁵	101.45 ± 6.36	97.55 ± 5.28	97.28 ± 4.86	96.05 ± 5.47	6.48	0.034	0.11	1	0.258	0.9	1.74	0.24
initial double support	0.15 ± 0.01	0.15 ± 0.01	10.51	0.008	0.15 ± 0.01	0.15 ± 0.01	31.47	<10 ⁻⁵	0.14 ± 0.01	0.15 ± 0.01	0.15 ± 0.01	0.15 ± 0.01	4.37	0.051	0.03	1	0	1	1.83	0.24
terminal double support	0.14 ± 0.01	0.15 ± 0.01	9.42	0.010	0.15 ± 0.01	0.15 ± 0.01	24.98	<10 ⁻⁵	0.14 ± 0.01	0.15 ± 0.01	0.15 ± 0.01	0.15 ± 0.01	4.70	0.047	0.02	1	0.069	0.9	2.86	0.24
double support	0.29 ± 0.01	0.3 ± 0.02	7.87	0.014	0.29 ± 0.02	0.3 ± 0.01	26.94	<10 ⁻⁵	0.29 ± 0.02	0.3 ± 0.01	0.3 ± 0.01	0.3 ± 0.02	5.16	0.043	0.00	1	0.051	0.9	2.22	0.24
single limb support	0.49 ± 0.04	0.5 ± 0.03	2.44	0.119	0.49 ± 0.04	0.51 ± 0.03	32.37	<10 ⁻⁵	0.48 ± 0.04	0.5 ± 0.03	0.51 ± 0.03	0.51 ± 0.03	4.14	0.053	0.00	1	0.296	0.9	0.90	0.34
stance	0.76 ± 0.04	0.78 ± 0.04	6.48	0.024	0.76 ± 0.04	0.78 ± 0.04	43.03	<10 ⁻⁵	0.75 ± 0.04	0.77 ± 0.04	0.78 ± 0.04	0.79 ± 0.04	6.31	0.034	0.01	1	0.036	0.9	2.18	0.24
swing	0.47 ± 0.03	0.48 ± 0.03	5.32	0.030	0.47 ± 0.03	0.48 ± 0.03	35.80	<10 ⁻⁵	0.46 ± 0.03	0.48 ± 0.03	0.48 ± 0.03	0.49 ± 0.03	3.99	0.053	0.00	1	0.29	0.9	1.37	0.26
step length	0.53 ± 0.05	0.5 ± 0.05	5.10	0.030	0.52 ± 0.06	0.5 ± 0.06	25.88	<10 ⁻⁵	0.54 ± 0.06	0.5 ± 0.06	0.51 ± 0.06	0.5 ± 0.05	13.06	0.002	0.62	1	2.938	0.4	6.84	0.06
stride length	1.07 ± 0.11	1 ± 0.1	5.32	0.030	1.04 ± 0.11	1.01 ± 0.11	25.59	<10 ⁻⁵	1.08 ± 0.11	1 ± 0.09	1.03 ± 0.11	0.99 ± 0.11	12.66	0.002	0.60	1	3.001	0.4	6.89	0.06
bout length	43.88 ± 11.67	37.4 ± 11.78	4.13	0.049	42.76 ± 14.03	36.31 ± 15.29	21.10	<10 ⁻⁵	45.68 ± 12.26	39.5 ± 13.33	39.41 ± 14.46	33.4 ± 12.35	0.09	0.764	0.57	1	1.816	0.5	2.11	0.24

Supplementary Table A.2: The Regression Analysis of All Gait Metrics Derived From the At-Home Monitoring Data. There were age group differences for almost all gait metrics except single support time. There was also a difference between the gait observed in the weekdays compared to the weekend. There was no effect of sex or muscle mass or height (except step length). There were no interaction effects between any of the variables. All the p-values were corrected for multiple comparisons using FDR. a Mean ± sd WD: Weekdays, WE: Weekend, M.Mass: Muscle Mass

Chapter 4 Supplementary Information

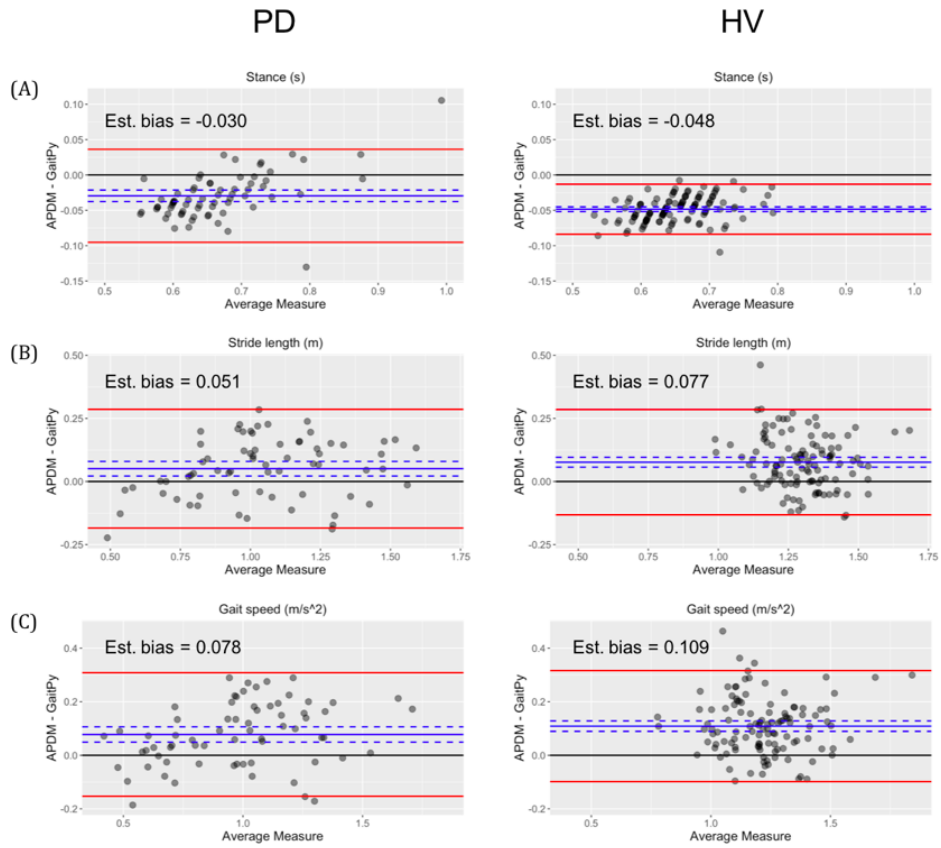


Supplementary Figure A.6. Participants instrumented with six wearable devices (Opal, APDM, Inc) located bilaterally on the wrist and foot, and at the lumbar (approximately at the L5 vertebra) and sternum. *(A) Adapted with permission from APDM Wearable Technologies.

Gait features	1 Device (lumbar)	3 Devices (lumbar and both feet)	6 Devices (lumbar, both feet, both wrists, and sternum)
Lower Limb Features			
Stride Time (s)	✓	✓	✓
Cadence (steps/min)	✓	✓	✓
Step Time (s)	✓	✓	✓
Stance Time (s)	✓	✓	✓
Swing Time (s)	✓	✓	✓
Initial Double Support (s)	✓	✓	✓
Terminal Double Support (s)	✓	✓	✓
Double Support (s)	✓	✓	✓
Single Limb Support (s)	✓	✓	✓
Step Length (m)	✓	*	*
Stride Length (m)	✓	✓	✓
Gait Speed (m/s)	✓	✓	✓
Elevation at Mid Swing (cm)		✓	✓
Lateral Step Deviation (cm)		✓	✓
Lateral Swing Max (cm)		✓	✓
Initial + Mid Swing Time (s)		✓	✓
Maximum Pitch (degrees)		✓	✓
Pitch at Initial Contact (degrees)		✓	✓
Pitch at Mid Swing (degrees)		✓	✓
Pitch at Tow Off (degrees)		✓	✓
Terminal Swing Time (s)		✓	✓
Toe Out Angle (degrees)		✓	✓
Toe Out Angle Max (degrees)		✓	✓
Toe Out Angle Min (degrees)		✓	✓
Lumbar Range of Motion			
Coronal Range of Motion (degrees)		✓	✓
Sagittal Range of Motion (degrees)		✓	✓
Transverse Range of Motion (degrees)		✓	✓
Trunk Range of Motion			

Coronal Range of Motion (degrees)			✓
Sagittal Range of Motion (degrees)			✓
Transverse Range of Motion (degrees)			✓
Upper Limb Features			
Foot Phase Difference (degrees)			✓
Maximum velocity (degrees/s)			✓
Range of motion (degrees)			✓

Supplementary Table A.3. Gait Features Derived Using GaitPy With a Single Lumbar-Mounted Device, APDM Mobility Lab With 3 Devices, and APDM Mobility Lab With 6 Devices. *Step length is not calculated by APDM Mobility Lab.

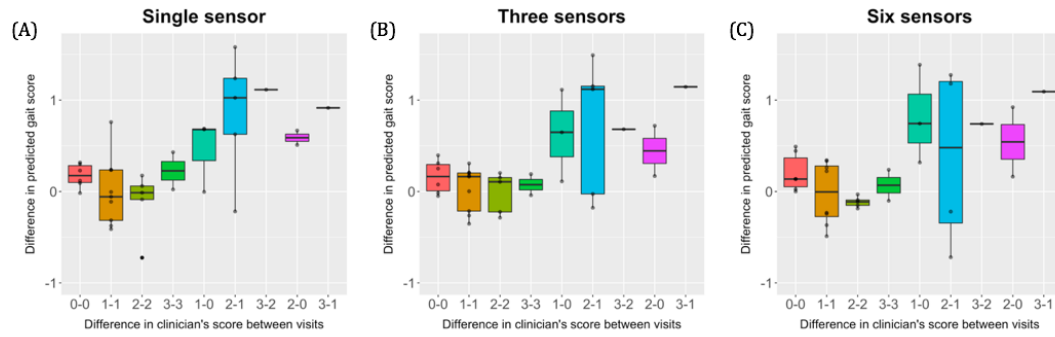


Supplementary Figure A.7. Bland-Altman analysis comparing (A) stance time, (B) stride length, and (C) gait speed agreement between GaitPy and APDM Mobility Lab in healthy volunteers (HV) and patients with Parkinson disease (PD).

Gait feature	PD	
	Kruskal-Wallis rank sum statistic	p-value
GaitPy (single device)		
Gait speed	41.66	< 0.001
Stride length	34.94	< 0.001
Step length	34.75	< 0.001
Swing time	25.79	< 0.001
Stride time	25.27	< 0.001
Gait speed var	24.76	< 0.001
Double support	24.32	< 0.001
Step time	24.12	< 0.001
Stance time	23.68	< 0.001
Stance asymmetry	18.90	< 0.001
Swing asymmetry	17.60	< 0.001
Step time asymmetry	15.72	0.001
Stance time var	14.46	0.002
APDM Mobility Lab (3 or 6 devices)		
Gait speed	34.98	< 0.001
Stride length	33.22	< 0.001
Step time var	32.77	< 0.001
Stride time var	32.55	< 0.001
Pitch at initial contact	26.84	< 0.001
Pitch at toe off	25.76	< 0.001
Maximum pitch	25.17	< 0.001
Double support var	25.13	< 0.001
Initial mid swing var	25.08	< 0.001
Trunk relative transverse range of motion	24.51	< 0.001
Stance time var	23.91	< 0.001
Swing time var	23.91	< 0.001
Terminal swing var	22.53	< 0.001
Single limb support var	21.58	< 0.001
Step time	21.02	< 0.001
Step time asymmetry	20.71	< 0.001
Stride time	20.38	< 0.001
Cadence	20.38	< 0.001
Maximum velocity	19.85	< 0.001
Terminal swing asymmetry	18.55	< 0.001
Lumbar coronal range of motion	17.07	0.001
Initial double support var	16.51	0.001
Upper limb range of motion	16.50	0.001
Stance asymmetry	15.70	0.001
Swing asymmetry	15.70	0.001
Single limb support asymmetry	15.70	0.001

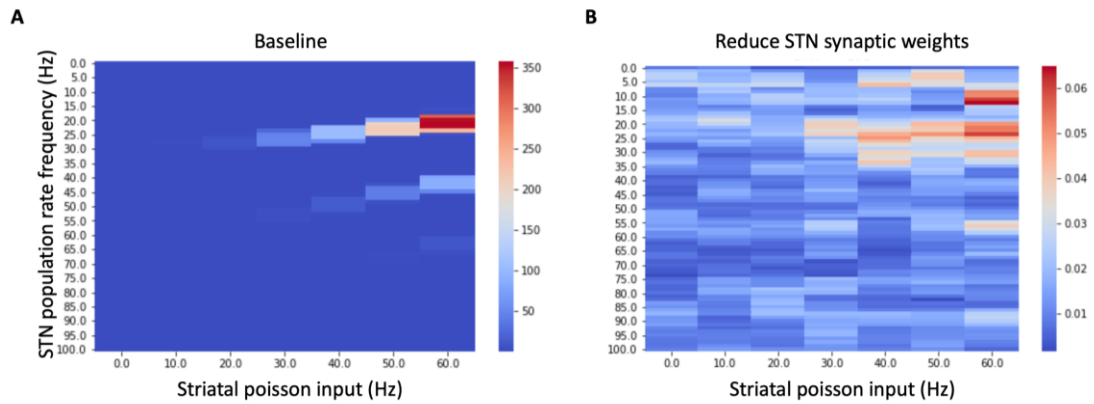
Initial mid swing asymmetry	15.25	0.002
Lumbar sagittal range of motion	13.85	0.003
Initial mid swing time	13.77	0.003
Trunk sagittal maximum angle	13.76	0.003
Foot phase difference var	13.61	0.004
Trunk sagittal average angle	13.56	0.0036
Terminal double support	13.48	0.0037
Trunk sagittal minimum angle	13.19	0.0042

Supplementary Table A.4. Kruskal-Wallis Rank Sum Statistics and P Values for Sensor-Derived Features of Gait in Participants With Parkinson disease That Varied Significantly ($P \leq 0.01$) With MDS-UPDRS Gait Score in Order of Significance.



Supplementary Figure A.8. A comparison between MDS-UPDRS gait scores and predicted score changes between (Off - ON) visits in patients with Parkinson disease.

Chapter 5 Supplementary Information



Supplementary Figure A.9. STN-GPe network model validation. (A) As expected, based on previous work, population rate in the beta frequency range increases with increasing striatal input. **(B)** By extension, as previously shown, beta synchrony is quenched by reducing excitability of STN neurons, even in the presence of strong striatal input.

BIBLIOGRAPHY

- Adamowicz, L., & Patel, S. (2020). Sit2StandPy: An Open-Source Python Package for Detecting and Quantifying Sit-to-Stand Transitions Using an Accelerometer on the Lower Back. *Journal of Open Source Software*, 5(52), 2449.
<https://doi.org/10.21105/joss.02449>
- APDM. (2019). *APDM Mobility Lab User Guide. Version 2.*
- Armstrong, D. M. (1986). Supraspinal contributions to the initiation and control of locomotion in the cat. *Progress in Neurobiology*, 26(4), 273–361.
[https://doi.org/10.1016/0301-0082\(86\)90021-3](https://doi.org/10.1016/0301-0082(86)90021-3)
- Ashizawa, T., & Xia, G. (2016). Ataxia. *Continuum : Lifelong Learning in Neurology*, 22(4 Movement Disorders), 1208–1226.
<https://doi.org/10.1212/CON.0000000000000362>
- Bahuguna, J., Sahasranamam, A., & Kumar, A. (2020). Uncoupling the roles of firing rates and spike bursts in shaping the STN-GPe beta band oscillations. *PLOS Computational Biology*, 16(3), e1007748.
<https://doi.org/10.1371/journal.pcbi.1007748>
- Barry, G., Galna, B., Lord, S., Rochester, L., & Godfrey, A. (2015). Defining ambulatory bouts in free-living activity: Impact of brief stationary periods on bout metrics. *Gait and Posture*, 42(4), 594–597.
<https://doi.org/10.1016/j.gaitpost.2015.07.062>

- Beach, T. G., & Adler, C. H. (2018). Importance of Low Diagnostic Accuracy for Early Parkinson's Disease. *Movement Disorders : Official Journal of the Movement Disorder Society*, 33(10), 1551–1554. <https://doi.org/10.1002/mds.27485>
- Beauchet, O., Annweiler, C., Callisaya, M. L., De Cock, A.-M., Helbostad, J. L., Kressig, R. W., Srikanth, V., Steinmetz, J.-P., Blumen, H. M., Verghese, J., MBBS, & Allali, G. (2016). Poor Gait Performance and Prediction of Dementia: Results From a Meta-Analysis. *Journal of the American Medical Directors Association*, 17(6), 482–490. <https://doi.org/10.1016/j.jamda.2015.12.092>. Poor
- Bevan, M. D., Magill, P. J., Terman, D., Bolam, J. P., & Wilson, C. J. (2002). Move to the rhythm: Oscillations in the subthalamic nucleus-external globus pallidus network. *Trends in Neurosciences*, 25(10), 525–531. [https://doi.org/10.1016/S0166-2236\(02\)02235-X](https://doi.org/10.1016/S0166-2236(02)02235-X)
- Bloem, B. R., Okun, M. S., & Klein, C. (2021). Parkinson's disease. *The Lancet*, 397(10291), 2284–2303. [https://doi.org/10.1016/S0140-6736\(21\)00218-X](https://doi.org/10.1016/S0140-6736(21)00218-X)
- Bouca-Machado, R., Maetzler, W., & Ferreira, J. J. (2018). What is functional mobility applied to Parkinson's disease? *Journal of Parkinson's Disease*, 8(1), 121–130. <https://doi.org/10.3233/JPD-171233>
- Braak, H., Ghebremedhin, E., Rüb, U., Bratzke, H., & Del Tredici, K. (2004). Stages in the development of Parkinson's disease-related pathology. *Cell and Tissue Research*, 318(1), 121–134. <https://doi.org/10.1007/s00441-004-0956-9>
- Breiman, L. (2001). Random Forests. *Machine Learning*, 45, 5–32.

- Brittain, J.-S., & Brown, P. (2014). Oscillations and the basal ganglia: Motor control and beyond. *NeuroImage*, *85*, 637–647.
<https://doi.org/10.1016/j.neuroimage.2013.05.084>
- Brodie, M. A. D., Coppens, M. J. M., Lord, S. R., Lovell, N. H., Gschwind, Y. J., Redmond, S. J., Del Rosario, M. B., Wang, K., Sturnieks, D. L., Persiani, M., & Delbaere, K. (2016). Wearable pendant device monitoring using new wavelet-based methods shows daily life and laboratory gaits are different. *Medical and Biological Engineering and Computing*, *54*(4), 663–674.
<https://doi.org/10.1007/s11517-015-1357-9>
- Brognara, L., Palumbo, P., Grimm, B., & Palmerini, L. (2019). Assessing Gait in Parkinson's Disease Using Wearable Motion Sensors: A Systematic Review. *Diseases*, *7*(1), 18. <https://doi.org/10.3390/diseases7010018>
- Brown, P. (2003). Oscillatory nature of human basal ganglia activity: Relationship to the pathophysiology of Parkinson's disease. *Movement Disorders*, *18*(4), 357–363. <https://doi.org/10.1002/mds.10358>
- Brown, P., Oliviero, A., Mazzone, P., Insola, A., Tonali, P., & Lazzaro, V. D. (2001). Dopamine Dependency of Oscillations between Subthalamic Nucleus and Pallidum in Parkinson's Disease. *Journal of Neuroscience*, *21*(3), 1033–1038.
<https://doi.org/10.1523/JNEUROSCI.21-03-01033.2001>
- Cassidy, M., Mazzone, P., Oliviero, A., Insola, A., Tonali, P., Lazzaro, V. D., & Brown, P. (2002). Movement-related changes in synchronization in the human basal ganglia. *Brain*, *125*(6), 1235–1246. <https://doi.org/10.1093/brain/awf135>

- Cheng, W.-Y., Lipsmeier, F., Scotland, A., Creagh, A., Kilchenmann, T., Jin, L., Schjodt-Eriksen, J., Wolf, D., Zhang-Schaerer, Y.-P., Garcia, I. F., Siebourg-Polster, J., Soto, J., Verselis, L., Facklam, M. M., Boess, F., Koller, M., Grundman, M., Monsch, A. U., Postuma, R., ... Lindemann, M. (2017). Smartphone-based continuous mobility monitoring of Parkinsons disease patients reveals impacts of ambulatory bout length on gait features. *2017 IEEE Life Sciences Conference (LSC)*, 166–169. <https://doi.org/10.1109/LSC.2017.8268169>
- Christakis, Y., Mahadevan, N., & Patel, S. (2019). SleepPy: A python package for sleep analysis from accelerometer data. *Journal of Open Source Software*, 4(44), 1663. <https://doi.org/10.21105/joss.01663>
- Committee for Medicinal Products for Human Use (CHMP). (2019). *Qualification opinion on stride velocity 95th centile as a secondary endpoint in Duchenne Muscular Dystrophy measured by a valid and suitable wearable device. April.*
- Cook, A., & Giunti, P. (2017). Friedreich’s ataxia: Clinical features, pathogenesis and management. *British Medical Bulletin*, 124(1), 19–30. <https://doi.org/10.1093/bmb/ldx034>
- Corbit, V. L., Whalen, T. C., Zitelli, K. T., Crilly, S. Y., Rubin, J. E., & Gittis, A. H. (2016). Pallidostriatal projections promote β oscillations in a dopamine-depleted biophysical network model. *Journal of Neuroscience*, 36(20), 5556–5571. <https://doi.org/10.1523/JNEUROSCI.0339-16.2016>
- Courtemanche, R., Fujii, N., & Graybiel, A. M. (2003). Synchronous, Focally Modulated β -Band Oscillations Characterize Local Field Potential Activity in

- the Striatum of Awake Behaving Monkeys. *Journal of Neuroscience*, 23(37), 11741–11752. <https://doi.org/10.1523/JNEUROSCI.23-37-11741.2003>
- Cruz, A. V., Mallet, N., Magill, P. J., Brown, P., & Averbeck, B. B. (2011). Effects of dopamine depletion on information flow between the subthalamic nucleus and external globus pallidus. *Journal of Neurophysiology*, 106(4), 2012–2023. <https://doi.org/10.1152/jn.00094.2011>
- Czech, M. D., & Patel, S. (2019). GaitPy: An Open-Source Python Package for Gait Analysis Using an Accelerometer on the Lower Back. *Journal of Open Source Software*, 4(43), 1778. <https://doi.org/10.21105/joss.01778>
- Czech, M., Demanuele, C., Erb, M. K., Ramos, V., Zhang, H., Ho, B., & Patel, S. (2020). The Impact of Reducing the Number of Wearable Devices on Measuring Gait in Parkinson Disease: Noninterventional Exploratory Study. *JMIR Rehabilitation and Assistive Technologies*, 7(2), e17986. <https://doi.org/10.2196/17986>
- de Bruin, E. D., Najafi, B., Murer, K., Uebelhart, D., & Aminian, K. (2007). Quantification of everyday motor function in a geriatric population. *Journal of Rehabilitation Research and Development*, 44(3), 417–428. <https://doi.org/10.1682/jrrd.2006.01.0003>
- Del Din, S., Godfrey, A., Galna, B., Lord, S., & Rochester, L. (2016). Free-living gait characteristics in ageing and Parkinson's disease: Impact of environment and ambulatory bout length. *Journal of Neuroengineering and Rehabilitation*, 13(1), 46. <https://doi.org/10.1186/s12984-016-0154-5>

- Del Din, S., Godfrey, A., Mazzà, C., Lord, S., & Rochester, L. (2016). Free-living monitoring of Parkinson's disease: Lessons from the field. *Movement Disorders, 31*(9), 1293–1313. <https://doi.org/10.1002/mds.26718>
- Del Din, S., Godfrey, A., & Rochester, L. (2016a). Validation of an Accelerometer to Quantify a Comprehensive Battery of Gait Characteristics in Healthy Older Adults and Parkinson's Disease: Toward Clinical and at Home Use. *IEEE Journal of Biomedical and Health Informatics, 20*(3), 838–847. <https://doi.org/10.1109/JBHI.2015.2419317>
- Del Din, S., Godfrey, A., & Rochester, L. (2016b). Validation of an Accelerometer to Quantify a Comprehensive Battery of Gait Characteristics in Healthy Older Adults and Parkinson's Disease: Toward Clinical and at Home Use. *IEEE Journal of Biomedical and Health Informatics, 20*(3), 838–847. <https://doi.org/10.1109/JBHI.2015.2419317>
- Dickson, D. W. (2018). Neuropathology of Parkinson disease. *Parkinsonism and Related Disorders, 46*, S30–S33. <https://doi.org/10.1016/j.parkreldis.2017.07.033>
- Digital Health Software Precertification (Pre-Cert) Program. (2021, June 22). FDA; FDA. <https://www.fda.gov/medical-devices/digital-health-center-excellence/digital-health-software-precertification-pre-cert-program>
- Domenic V, C. (1994). Guidelines, Criteria, and Rules of Thumb for Evaluating Normed and Standardized Assessment Instruments in Psychology.

Psychological Assessment, 6(4), 284–290. <https://doi.org/10.1037/1040-3590.6.4.284>

- Ebersbach, G., Moreau, C., Gandor, F., Defebvre, L., & Devos, D. (2013). Clinical syndromes: Parkinsonian gait. *Movement Disorders*, 28(11), 1552–1559. <https://doi.org/10.1002/mds.25675>
- Efron, B. (1979). Bootstrap Methods: Another Look at the Jackknife. *Annals of Statistics*, 7(1), 1–26.
- Erb, M. K., Karlin, D. R., Ho, B. K., Thomas, K. C., Parisi, F., Vergara-Diaz, G. P., Daneault, J.-F., Wacnik, P. W., Zhang, H., Kangarloo, T., Demanuele, C., Brooks, C. R., Detheridge, C. N., Shaafi Kabiri, N., Bhangu, J. S., & Bonato, P. (2020). MHealth and wearable technology should replace motor diaries to track motor fluctuations in Parkinson's disease. *Npj Digital Medicine*, 3(1), 1–10. <https://doi.org/10.1038/s41746-019-0214-x>
- Espay, A. J., Hausdorff, J. M., Sanchez-Ferro, Á., Klucken, J., Merola, A., Bonato, P., Paul, S. S., Horak, F. B., Vizcarra, J. A., Mestre, T. A., Reilmann, R., Nieuwboer, A., Dorsey, E. R., Rochester, L., Bloem, B. R., & Maetzler, W. (2019). A Roadmap for Implementation of Patient-Centered Digital Outcome Measures in Parkinson's disease Obtained Using Mobile Health Technologies. *Movement Disorders : Official Journal of the Movement Disorder Society*, 34(5), 657–663. <https://doi.org/10.1002/mds.27671>
- Esser, P., Dawes, H., Collett, J., Feltham, M. G., & Howells, K. (2011). Assessment of spatio-temporal gait parameters using inertial measurement units in

neurological populations. *Gait and Posture*, 34(4), 558–560.

<https://doi.org/10.1016/j.gaitpost.2011.06.018>

Esser, P., Dawes, H., Collett, J., Feltham, M. G., & Howells, K. (2012). Validity and inter-rater reliability of inertial gait measurements in Parkinson's disease: A pilot study. *Journal of Neuroscience Methods*, 205(1), 177–181.

<https://doi.org/10.1016/j.jneumeth.2012.01.005>

Fan, K. Y., Baufreton, J., Surmeier, D. J., Chan, C. S., & Bevan, M. D. (2012).

Proliferation of External Globus Pallidus-Subthalamic Nucleus Synapses following Degeneration of Midbrain Dopamine Neurons. *Journal of Neuroscience*, 32(40), 13718–13728.

<https://doi.org/10.1523/JNEUROSCI.5750-11.2012>

Favre, J., & Jolles, B. M. (2016). Gait analysis of patients with knee osteoarthritis highlights a pathological mechanical pathway and provides a basis for therapeutic interventions. *EFORT Open Reviews*, 1(10), 368–374.

<https://doi.org/10.1302/2058-5241.1.000051>

Frank, M. J. (2006). Hold your horses: A dynamic computational role for the subthalamic nucleus in decision making. *Neural Networks*, 19(8), 1120–1136.

<https://doi.org/10.1016/j.neunet.2006.03.006>

Frank, S. R. (2000). Digital health care—The convergence of health care and the Internet. *The Journal of Ambulatory Care Management*, 23(2), 8–17.

<https://doi.org/10.1097/00004479-200004000-00003>

- Fries, P. (2005). A mechanism for cognitive dynamics: Neuronal communication through neuronal coherence. *Trends in Cognitive Sciences*, 9(10), 474–480.
<https://doi.org/10.1016/j.tics.2005.08.011>
- Fritz, S., & Lusardi, M. (2009). White paper: “walking speed: the sixth vital sign.” *Journal of Geriatric Physical Therapy* (2001), 32(2), 46–49.
- Gaenslen, A., Swid, I., Liepelt-Scarfone, I., Godau, J., & Berg, D. (2011). The Patients’ Perception of Prodromal Symptoms Before the Initial Diagnosis of Parkinson’s Disease. *Movement Disorders*, 26(4), 653–658.
<https://doi.org/10.1002/mds.23499>
- Galperin, I., Hillel, I., Del Din, S., Bekkers, E. M. J., Nieuwboer, A., Abbruzzese, G., Avanzino, L., Nieuwhof, F., Bloem, B. R., Rochester, L., Della Croce, U., Cereatti, A., Giladi, N., Mirelman, A., & Hausdorff, J. M. (2019). Associations between daily-living physical activity and laboratory-based assessments of motor severity in patients with falls and Parkinson’s disease. *Parkinsonism and Related Disorders*, 62(October 2018), 85–90.
<https://doi.org/10.1016/j.parkreldis.2019.01.022>
- GBD 2016 Parkinson’s Disease Collaborators. (2018). Global, regional, and national burden of Parkinson’s disease, 1990–2016: A systematic analysis for the Global Burden of Disease Study 2016. *The Lancet. Neurology*, 17(11), 939–953. [https://doi.org/10.1016/S1474-4422\(18\)30295-3](https://doi.org/10.1016/S1474-4422(18)30295-3)
- Giannouli, E., Bock, O., & Zijlstra, W. (2018). Cognitive functioning is more closely related to real-life mobility than to laboratory-based mobility parameters.

European Journal of Ageing, 15(1), 57–65. <https://doi.org/10.1007/s10433-017-0434-3>

Gill, G. (2021, September 21). Streamlining Adoption of Digital Technology in Clinical Trials Through Use of Open-Source Algorithms. *ACRP*.

<https://acrpnnet.org/2021/09/21/streamlining-adoption-of-digital-technology-in-clinical-trials-through-use-of-open-source-algorithms/>

Godfrey, A., Del Din, S., Barry, G., Mathers, J. C., & Rochester, L. (2015). Instrumenting gait with an accelerometer: A system and algorithm examination. *Medical Engineering and Physics*, 37(4), 400–407.

<https://doi.org/10.1016/j.medengphy.2015.02.003>

Godfrey, A., Lord, S., Mathers, J. C., Burn, D. J., & Rochester, L. (2014). The association between retirement and age on physical activity in older adults. *Age and Ageing*, 43(3), 386–393. <https://doi.org/10.1093/ageing/aft168>

Godinho, C., Domingos, J., Cunha, G., Santos, A. T., Fernandes, R. M., Abreu, D., Gonçalves, N., Matthews, H., Isaacs, T., Duffen, J., Al-Jawad, A., Larsen, F., Serrano, A., Weber, P., Thoms, A., Sollinger, S., Graessner, H., Maetzler, W., & Ferreira, J. J. (2016). A systematic review of the characteristics and validity of monitoring technologies to assess Parkinson's disease. *Journal of NeuroEngineering and Rehabilitation*, 13(1), 1–10.

<https://doi.org/10.1186/s12984-016-0136-7>

Goetz, C. G., Fahn, S., Martinez-Martin, P., Poewe, W., Sampaio, C., Stebbins, G. T., Stern, M. B., Tilley, B. C., Dodel, R., Dubois, B., Holloway, R., Jankovic, J.,

- Kulisevsky, J., Lang, A. E., Lees, A., Leurgans, S., LeWitt, P. A., Nyenhuis, D., Olanow, W., ... LaPelle, N. (2019). *The MDS-sponsored Revision of the Unified Parkinson's Disease Rating Scale*. 33.
- Goetz, C. G., Tilley, B. C., Shaftman, S. R., Stebbins, G. T., Fahn, S., Martinez-Martin, P., Poewe, W., Sampaio, C., Stern, M. B., Dodel, R., Dubois, B., Holloway, R., Jankovic, J., Kulisevsky, J., Lang, A. E., Lees, A., Leurgans, S., LeWitt, P. A., Nyenhuis, D., ... Zweig, R. M. (2008). Movement Disorder Society-Sponsored Revision of the Unified Parkinson's Disease Rating Scale (MDS-UPDRS): Scale presentation and clinimetric testing results. *Movement Disorders*, 23(15), 2129–2170. <https://doi.org/10.1002/mds.22340>
- Gretebeck, R. J., & Montoye, H. J. (1992). Variability of some objective measures of physical activity. *Medicine and Science in Sports and Exercise*, 24(10), 1167–1172.
- Guo, C., Ashrafian, H., Ghafur, S., Fontana, G., Gardner, C., & Prime, M. (2020). Challenges for the evaluation of digital health solutions—A call for innovative evidence generation approaches. *NPJ Digital Medicine*, 3, 110. <https://doi.org/10.1038/s41746-020-00314-2>
- Halje, P., Brys, I., Mariman, J. J., da Cunha, C., Fuentes, R., & Petersson, P. (2019). Oscillations in cortico-basal ganglia circuits: Implications for Parkinson's disease and other neurologic and psychiatric conditions. *Journal of Neurophysiology*, 122(1), 203–231. <https://doi.org/10.1152/jn.00590.2018>

- Hammond, C., Bergman, H., & Brown, P. (2007). Pathological synchronization in Parkinson's disease: Networks, models and treatments. *Trends in Neurosciences*, 30(7), 357–364. <https://doi.org/10.1016/j.tins.2007.05.004>
- Hanson, J. E., & Jaeger, D. (2002). Short-term plasticity shapes the response to simulated normal and parkinsonian input patterns in the globus pallidus. *The Journal of Neuroscience: The Official Journal of the Society for Neuroscience*, 22(12), 5164–5172.
- Hardy, S. E., Perera, S., Roumani, Y. F., Chandler, J. M., & Studenski, S. A. (2007). Improvement in usual gait speed predicts better survival in older adults. *Journal of the American Geriatrics Society*, 55(11), 1727–1734. <https://doi.org/10.1111/j.1532-5415.2007.01413.x>
- Hart, T. L., Swartz, A. M., & Strath, S. J. (2011). How many days of monitoring are needed to accurately estimate physical activity in older adults. *International Journal on Behavioral Nutrition and Physical Activity*, 8, 62–69.
- Hartmann, C. J., Fliegen, S., Groiss, S. J., Wojtecki, L., & Schnitzler, A. (2019). An update on best practice of deep brain stimulation in Parkinson's disease. *Therapeutic Advances in Neurological Disorders*, 12, 1756286419838096. <https://doi.org/10.1177/1756286419838096>
- Hausdorff, J. M. (2009). Gait dynamics in Parkinson's disease: Common and distinct behavior among stride length, gait variability, and fractal-like scaling. *Chaos*, 19(2), 1–14. <https://doi.org/10.1063/1.3147408>

- Hauser, R. A., Friedlander, J., Zesiewicz, T. A., Adler, C. H., Seeberger, L. C., O'Brien, C. F., Molho, E. S., & Factor, S. A. (2000). A home diary to assess functional status in patients with Parkinson's disease with motor fluctuations and dyskinesia. *Clinical Neuropharmacology*, *23*(2), 75–81.
<https://doi.org/10.1097/00002826-200003000-00003>
- Hillel, I., Gazit, E., Nieuwboer, A., Avanzino, L., Rochester, L., Cereatti, A., Della Croce, U., Rikkert, M. O., Bloem, B. R., Pelosin, E., Del Din, S., Ginis, P., Giladi, N., Mirelman, A., & Hausdorff, J. M. (2019). Is every-day walking in older adults more analogous to dual-task walking or to usual walking? Elucidating the gaps between gait performance in the lab and during 24/7 monitoring. *European Review of Aging and Physical Activity*, *5*, 1–12.
- Hinsey, J. C., Ranson, S. W., & McNattin, R. F. (1930). The role of the Hypothalamus and Mesencephalon in Locomotion. *Archives of Neurology & Psychiatry*, *23*(1), 1–43. <https://doi.org/10.1001/archneurpsyc.1930.02220070004001>
- Hirschmann, J., Özkurt, T. E., Butz, M., Homburger, M., Elben, S., Hartmann, C. J., Vesper, J., Wojtecki, L., & Schnitzler, A. (2011). Distinct oscillatory STN-cortical loops revealed by simultaneous MEG and local field potential recordings in patients with Parkinson's disease. *NeuroImage*, *55*(3), 1159–1168. <https://doi.org/10.1016/j.neuroimage.2010.11.063>
- Holden, S. K., Finseth, T., Sillau, S. H., & Berman, B. D. (2018). Progression of MDS-UPDRS Scores Over Five Years in De Novo Parkinson Disease from the

- Parkinson's Progression Markers Initiative Cohort. *Movement Disorders Clinical Practice*, 5(1), 47–53. <https://doi.org/10.1002/mdc3.12553>
- Hollman, J., McDade, E., & Peterson, R. (2011). Normative Spatiotemporal Gait Parameters in Older Adults. *Gait & Posture*, 34(1), 111–118. <https://doi.org/10.1016/j.gait.2010.01.003>
- Holt, A. B., & Netoff, T. I. (2016). Computational modeling to advance deep brain stimulation for the treatment of Parkinson's disease. *Drug Discovery Today: Disease Models*, 19, 31–36. <https://doi.org/10.1016/j.ddmod.2017.02.006>
- Hornyak, V., Vanswearingen, J. M., & Brach, J. S. (2012). Measurement of gait speed. *Topics in Geriatric Rehabilitation*, 28(1), 27–32. <https://doi.org/10.1097/TGR.0b013e318233e75b>
- Hubble, R. P., Naughton, G. A., Silburn, P. A., & Cole, M. H. (2015). Wearable sensor use for assessing standing balance and walking stability in people with Parkinson's disease: A systematic review. *PLoS ONE*, 10(4), 1–22. <https://doi.org/10.1371/journal.pone.0123705>
- Humphries, M. D., Obeso, J., & Dreyer, J. K. (2018). Insights into Parkinson's disease from computational models of the basal ganglia. *Journal of Neurology, Neurosurgery, and Psychiatry*, 89(11), 1181–1188. <https://doi.org/10.1136/jnnp-2017-315922>
- Inan, O. T., Tenaerts, P., Prindiville, S. A., Reynolds, H. R., Dizon, D. S., Cooper-Arnold, K., Turakhia, M., Pletcher, M. J., Preston, K. L., Krumholz, H. M., Marlin, B. M., Mandl, K. D., Klasnja, P., Spring, B., Iturriaga, E., Campo, R., Desvigne-Nickens,

- P., Rosenberg, Y., Steinhubl, S. R., & Califf, R. M. (2020). Digitizing clinical trials. *Npj Digital Medicine*, 3(1), 1–7. <https://doi.org/10.1038/s41746-020-0302-y>
- Jankovic, J. (2008). Parkinson's disease: Clinical features and diagnosis. *Journal of Neurology, Neurosurgery & Psychiatry*, 79(4), 368–376. <https://doi.org/10.1136/jnnp.2007.131045>
- Kang, M., Bjornson, K., Barreira, T. V., Ragan, B. G., & Song, K. (2014). The minimum number of days required to establish reliable physical activity estimates in children aged 2-15 years. *Physiological Measurement*, 35(11), 2229–2237. <https://doi.org/10.1088/0967-3334/35/11/2229>
- King, C., Henze, D. A., Leinekugel, X., & Buzsáki, G. (1999). Hebbian modification of a hippocampal population pattern in the rat. *The Journal of Physiology*, 521(Pt 1), 159–167. <https://doi.org/10.1111/j.1469-7793.1999.00159.x>
- Kingsley, C., & Patel, S. (2017). Patient-reported outcome measures and patient-reported experience measures. *BJA Education*, 17(4), 137–144. <https://doi.org/10.1093/bjaed/mkw060>
- Knaier, R., Höchsmann, C., Infanger, D., Hinrichs, T., & Schmidt-Trucksäss, A. (2019). Validation of automatic wear-time detection algorithms in a free-living setting of wrist-worn and hip-worn ActiGraph GT3X+. *BMC Public Health*, 19(1), 244. <https://doi.org/10.1186/s12889-019-6568-9>
- Kumar, A., Cardanobile, S., Rotter, S., & Aertsen, A. (2011). The role of inhibition in generating and controlling Parkinson's disease oscillations in the basal

ganglia. *Frontiers in Systems Neuroscience*, 5(October), 1–14.

<https://doi.org/10.3389/fnsys.2011.00086>

Lauer, M. S., & Bonds, D. (2014). Eliminating the “expensive” adjective for clinical trials. *American Heart Journal*, 167(4), 419–420.

<https://doi.org/10.1016/j.ahj.2013.12.003>

Levin, S., Jacobs, D. R., Ainsworth, B. E., Richardson, M. T., & Leon, A. S. (1999). Intra-individual variation and estimates of usual physical activity. *Annals of Epidemiology*, 9(8), 481–488. [https://doi.org/10.1016/S1047-](https://doi.org/10.1016/S1047-2797(99)00022-8)

[2797\(99\)00022-8](https://doi.org/10.1016/S1047-2797(99)00022-8)

Liddell, E. G. T., & Phillips, C. G. (1944). Pyramidal Section in the Cat. *Brain*, 67(1), 1–9. <https://doi.org/10.1093/brain/67.1.1>

Little, S., & Brown, P. (2014). The functional role of beta oscillations in Parkinson’s disease. *Parkinsonism & Related Disorders*, 20, S44–S48.

[https://doi.org/10.1016/S1353-8020\(13\)70013-0](https://doi.org/10.1016/S1353-8020(13)70013-0)

Litvak, V., Jha, A., Eusebio, A., Oostenveld, R., Foltynie, T., Limousin, P., Zrinzo, L.,

Hariz, M. I., Friston, K., & Brown, P. (2011). Resting oscillatory cortico-subthalamic connectivity in patients with Parkinson’s disease. *Brain*, 134(2),

[359–374. https://doi.org/10.1093/brain/awq332](https://doi.org/10.1093/brain/awq332)

Lozano, A. M., Lipsman, N., Bergman, H., Brown, P., Chabardes, S., Chang, J. W.,

Matthews, K., McIntyre, C. C., Schlaepfer, T. E., Schulder, M., Temel, Y.,

Volkman, J., & Krauss, J. K. (2019). Deep brain stimulation: Current

challenges and future directions. *Nature Reviews. Neurology*, 15(3), 148–160.

<https://doi.org/10.1038/s41582-018-0128-2>

Maetzler, W., Domingos, J., Srujijes, K., Ferreira, J. J., & Bloem, B. R. (2013).

Quantitative wearable sensors for objective assessment of Parkinson's disease. *Movement Disorders*, 28(12), 1628–1637.

<https://doi.org/10.1002/mds.25628>

Maetzler, W., & Rochester, L. (2015). Body-worn sensors—The brave new world of

clinical measurement? *Movement Disorders : Official Journal of the Movement Disorder Society*, 30(9), 1203–1205. <https://doi.org/10.1002/mds.26317>

Mahadevan, N., Christakis, Y., Di, J., Bruno, J., Zhang, Y., Dorsey, E. R., Pigeon, W. R.,

Beck, L. A., Thomas, K., Liu, Y., Wicker, M., Brooks, C., Kabiri, N. S., Bhangu, J., Northcott, C., & Patel, S. (2021). Development of digital measures for

nighttime scratch and sleep using wrist-worn wearable devices. *Npj Digital Medicine*, 4(1), 1–10. <https://doi.org/10.1038/s41746-021-00402-x>

Majumder, S., & Deen, M. J. (2019). Smartphone Sensors for Health Monitoring and

Diagnosis. *Sensors (Basel, Switzerland)*, 19(9), 2164.

<https://doi.org/10.3390/s19092164>

Mancini, M., & Horak, F. B. (2016). Potential of APDM Mobility Lab for the

monitoring of the progression of Parkinson's disease. *Expert Review of Medical Devices*, 13(5), 455–462.

<https://doi.org/10.1097/SLA.0000000000001177>.Complications

- Marceglia, S., Foffani, G., Bianchi, A. M., Baselli, G., Tamma, F., Egidi, M., & Priori, A. (2006). Dopamine-dependent non-linear correlation between subthalamic rhythms in Parkinson's disease. *The Journal of Physiology*, *571*(Pt 3), 579–591. <https://doi.org/10.1113/jphysiol.2005.100271>
- Marras, C., Beck, J. C., Bower, J. H., Roberts, E., Ritz, B., Ross, G. W., Abbott, R. D., Savica, R., Van Den Eeden, S. K., Willis, A. W., & Tanner, C. (2018). Prevalence of Parkinson's disease across North America. *Npj Parkinson's Disease*, *4*(1), 21. <https://doi.org/10.1038/s41531-018-0058-0>
- Masquelier, T., Hugues, E., Deco, G., & Thorpe, S. J. (2009). Oscillations, Phase-of-Firing Coding, and Spike Timing-Dependent Plasticity: An Efficient Learning Scheme. *Journal of Neuroscience*, *29*(43), 13484–13493. <https://doi.org/10.1523/JNEUROSCI.2207-09.2009>
- Mathews, S. C., McShea, M. J., Hanley, C. L., Ravitz, A., Labrique, A. B., & Cohen, A. B. (2019). Digital health: A path to validation. *Npj Digital Medicine*, *2*(1), 1–9. <https://doi.org/10.1038/s41746-019-0111-3>
- Matthews, C. E., Ainsworth, B. E., Thompson, R. W., & Bassett, D. R. (2002). Sources of variance in daily physical activity levels as measured by an accelerometer. *Medicine and Science in Sports and Exercise*, *34*(8), 1376–1381.
- Mayo, E. (1934). The Human Problems of an Industrial Civilization. *Nature*, *134*(3380), 201–201. <https://doi.org/10.1038/134201b0>
- McCambridge, J., Witton, J., & Elbourne, D. R. (2014). Systematic review of the Hawthorne effect: New concepts are needed to study research participation

effects. *Journal of Clinical Epidemiology*, 67(3), 267–277.

<https://doi.org/10.1016/j.jclinepi.2013.08.015>

McCamley, J., Donati, M., Grimpampi, E., & Mazzà, C. (2012). An enhanced estimate of initial contact and final contact instants of time using lower trunk inertial sensor data. *Gait and Posture*, 36(2), 316–318.

<https://doi.org/10.1016/j.gaitpost.2012.02.019>

McCarthy, M. M., Gu, X., Boyden, E. S., Han, X., Moore-Kochlacs, C., & Kopell, N. (2011). Striatal origin of the pathologic beta oscillations in Parkinson's disease. *Proceedings of the National Academy of Sciences*, 108(28), 11620–11625. <https://doi.org/10.1073/pnas.1107748108>

McGregor, M. M., & Nelson, A. B. (2019). Circuit Mechanisms of Parkinson's Disease. *Neuron*, 101(6), 1042–1056. <https://doi.org/10.1016/j.neuron.2019.03.004>

Meissner, W., Leblois, A., Hansel, D., Bioulac, B., Gross, C. E., Benazzouz, A., & Boraud, T. (2005). Subthalamic high frequency stimulation resets subthalamic firing and reduces abnormal oscillations. *Brain: A Journal of Neurology*, 128(Pt 10), 2372–2382. <https://doi.org/10.1093/brain/awh616>

Middleton, A., & Fritz, S. L. (2013). Assessment of Gait, Balance, and Mobility in Older Adults: Considerations for Clinicians. *Current Translational Geriatrics and Experimental Gerontology Reports*, 2(4), 205–214.

<https://doi.org/10.1007/s13670-013-0057-2>

Middleton, A., Fritz, S. L., & Lusardi, M. (2015). Walking Speed: The Functional Vital

Sign. *Journal of Aging and Physical Activity*, 23(2), 314–322.

<https://doi.org/10.1123/japa.2013-0236.Walking>

Mielke, M. M., Roberts, R. O., Savica, R., Cha, R., Drubach, D. I., Christianson, T.,

Pankratz, V. S., Geda, Y. E., Machulda, M. M., Ivnik, R. J., Knopman, D. S., Boeve,

B. F., Rocca, W. A., & Petersen, R. C. (2013). Assessing the temporal

relationship between cognition and gait: Slow gait predicts cognitive decline

in the mayo clinic study of aging. *Journals of Gerontology - Series A Biological*

Sciences and Medical Sciences, 68(8), 929–937.

<https://doi.org/10.1093/gerona/gls256>

Mirelman, A., Bonato, P., Camicioli, R., Ellis, T. D., Giladi, N., Hamilton, J. L., Hass, C. J.,

Hausdorff, J. M., Pelosin, E., & Almeida, Q. J. (2019). Gait impairments in

Parkinson's disease. *The Lancet Neurology*, 4422(19), 1–12.

[https://doi.org/10.1016/S1474-4422\(19\)30044-4](https://doi.org/10.1016/S1474-4422(19)30044-4)

Mirzaei, A., Kumar, A., Leventhal, D., Mallet, N., Aertsen, A., Berke, J., & Schmidt, R.

(2017). Sensorimotor Processing in the Basal Ganglia Leads to Transient Beta

Oscillations during Behavior. *Journal of Neuroscience*, 37(46), 11220–11232.

<https://doi.org/10.1523/JNEUROSCI.1289-17.2017>

Morgan, C., Rolinski, M., McNaney, R., Jones, B., Rochester, L., Maetzler, W., Craddock,

I., & Whone, A. L. (2020). Systematic Review Looking at the Use of

Technology to Measure Free-Living Symptom and Activity Outcomes in

- Parkinson's Disease in the Home or a Home-like Environment. *Journal of Parkinson's Disease*, 10(2), 429–454. <https://doi.org/10.3233/JPD-191781>
- Motti Ader, L. G., Greene, B. R., McManus, K., Tubridy, N., & Caulfield, B. (2020). Short Bouts of Gait Data and Body-Worn Inertial Sensors Can Provide Reliable Measures of Spatiotemporal Gait Parameters from Bilateral Gait Data for Persons with Multiple Sclerosis. *Biosensors*, 10(9), 128. <https://doi.org/10.3390/bios10090128>
- Mueller, A., Hoefling, H. A., Muaremi, A., Praestgaard, J., Walsh, L. C., Bunte, O., Huber, R. M., Fürmetz, J., Keppler, A. M., Schieker, M., Böcker, W., Roubenoff, R., Brachat, S., Rooks, D. S., & Clay, I. (2019). Continuous digital monitoring of walking speed in frail elderly patients: Noninterventional validation study and longitudinal clinical trial. *Journal of Medical Internet Research*, 21(11), 1–12. <https://doi.org/10.2196/15191>
- Muro-de-la-Herran, A., García-Zapirain, B., & Méndez-Zorrilla, A. (2014). Gait analysis methods: An overview of wearable and non-wearable systems, highlighting clinical applications. *Sensors (Switzerland)*, 14(2), 3362–3394. <https://doi.org/10.3390/s140203362>
- Najafi, B., Aminian, K., Paraschiv-Ionescu, A., Loew, F., Büla, C. J., & Robert, P. (2003). Ambulatory system for human motion analysis using a kinematic sensor: Monitoring of daily physical activity in the elderly. *IEEE Transactions on Biomedical Engineering*, 50(6), 711–723. <https://doi.org/10.1109/TBME.2003.812189>

- Orendurff, M. S., Schoen, J. A., Bernatz, G. C., Segal, A. D., & Klute, G. K. (2008). How humans walk: Bout duration, steps per bout, and rest duration. *Journal of Rehabilitation Research and Development*, *45*(7), 1077–1090.
<https://doi.org/10.1682/JRRD.2007.11.0197>
- Papapetropoulos, S. (Spyros). (2011). Patient Diaries As a Clinical Endpoint in Parkinson's Disease Clinical Trials. *CNS Neuroscience & Therapeutics*, *18*(5), 380–387. <https://doi.org/10.1111/j.1755-5949.2011.00253.x>
- Parkinson, J. (2002). An Essay on the Shaking Palsy. *The Journal of Neuropsychiatry and Clinical Neurosciences*, *14*(2), 223–236.
<https://doi.org/10.1176/jnp.14.2.223>
- Peel, N. M., Kuys, S. S., & Klein, K. (2012). Gait speed as a measure in geriatric assessment in clinical settings: A systematic review. *Journals of Gerontology - Series A Biological Sciences and Medical Sciences*, *68*(1), 39–46.
<https://doi.org/10.1093/gerona/gls174>
- Pickering, T. G., Gerin, W., & Schwartz, A. R. (2002). What is the white-coat effect and how should it be measured? *Blood Pressure Monitoring*, *7*(6), 293–300.
<https://doi.org/10.1097/00126097-200212000-00001>
- Pieruccini-Faria, F., Sarquis-Adamson, Y., Anton-Rodrigo, I., Noguerón-García, A., Bray, N. W., Camicioli, R., Muir-Hunter, S. W., Speechley, M., McIlroy, B., & Montero-Odasso, M. (2020). Mapping Associations Between Gait Decline and Fall Risk in Mild Cognitive Impairment. *Journal of the American Geriatrics Society*, *68*(3), 576–584. <https://doi.org/10.1111/jgs.16265>

- Pirker, W., & Katzenschlager, R. (2017). Gait disorders in adults and the elderly: A clinical guide. *Wiener Klinische Wochenschrift*, *129*(3–4), 81–95.
<https://doi.org/10.1007/s00508-016-1096-4>
- Plenz, D., & Kital, S. T. (1999). A basal ganglia pacemaker formed by the subthalamic nucleus and external globus pallidus. *Nature*, *400*(6745), 677–682.
<https://doi.org/10.1038/23281>
- Podsiadlo, D., & Richardson, S. (1991). The Timed “Up & Go”: A Test of Basic Functional Mobility for Frail Elderly Persons. *Journal of the American Geriatrics Society*, *39*(2), 142–148. <https://doi.org/10.1111/j.1532-5415.1991.tb01616.x>
- Poewe, W., Seppi, K., Tanner, C. M., Halliday, G. M., Brundin, P., Volkmann, J., Schrag, A.-E., & Lang, A. E. (2017). Parkinson disease. *Nature Reviews Disease Primers*, *3*(1), 1–21. <https://doi.org/10.1038/nrdp.2017.13>
- Polhemus, A., Ortiz, L. D., Brittain, G., Chynkiamis, N., Salis, F., Gaßner, H., Gross, M., Kirk, C., Rossanigo, R., Taraldsen, K., Balta, D., Breuls, S., BATTERY, S., Cardenas, G., Endress, C., Gugenhan, J., Keogh, A., Kluge, F., Koch, S., ... Puhan, M. (2021). Walking on common ground: A cross-disciplinary scoping review on the clinical utility of digital mobility outcomes. *Npj Digital Medicine*, *4*(1), 1–14.
<https://doi.org/10.1038/s41746-021-00513-5>
- Postuma, R. B., Berg, D., Stern, M., Poewe, W., Olanow, C. W., Oertel, W., Obeso, J., Marek, K., Litvan, I., Lang, A. E., Halliday, G., Goetz, C. G., Gasser, T., Dubois, B., Chan, P., Bloem, B. R., Adler, C. H., & Deuschl, G. (2015). MDS clinical

diagnostic criteria for Parkinson's disease. *Movement Disorders: Official Journal of the Movement Disorder Society*, 30(12), 1591–1601.

<https://doi.org/10.1002/mds.26424>

Psaltos, D., Chappie, K., Karahanoglu, F. I., Chasse, R., Demanuele, C., Kelekar, A., Zhang, H., Marquez, V., Kangarloo, T., Patel, S., Czech, M., Caouette, D., & Cai, X. (2019). Multimodal Wearable Sensors to Measure Gait and Voice. *Digital Biomarkers*, 3, 133–144. <https://doi.org/10.1159/000503282>

R Core Team. (2017). *R: A Language and Environment for Statistical Computing*. R Foundation for Statistical Computing. <https://www.r-project.org/>

Rascol, O., Payoux, P., Ory, F., Ferreira, J. J., Brefel-Courbon, C., & Montastruc, J.-L. (2003). Limitations of current Parkinson's disease therapy. *Annals of Neurology*, 53(S3), S3–S15. <https://doi.org/10.1002/ana.10513>

Regnault, A., Boroojerdi, B., Meunier, J., Bani, M., Morel, T., & Cano, S. (2019). Does the MDS-UPDRS provide the precision to assess progression in early Parkinson's disease? Learnings from the Parkinson's progression marker initiative cohort. *Journal of Neurology*, 266(8), 1927–1936. <https://doi.org/10.1007/s00415-019-09348-3>

Rochester, L., Mazzà, C., Mueller, A., Caulfield, B., McCarthy, M., Becker, C., Miller, R., Piraino, P., Viceconti, M., Dartee, W. P., Garcia-Aymerich, J., Aydemir, A. A., Vereijken, B., Arnera, V., Ammour, N., Jackson, M., Hache, T., Roubenoff, R., & behalf of the Mobilise-D Consortium, O. (2020). A Roadmap to Inform Development, Validation and Approval of Digital Mobility Outcomes: The

Mobilise-D Approach. *Digital Biomarkers*, 4(1), 13–27.

<https://doi.org/10.1159/000512513>

Rodríguez-Molinero, A., Samà, A., Pérez-López, C., Rodríguez-Martín, D., Alcaine, S., Mestre, B., Quispe, P., Giuliani, B., Vainstein, G., Browne, P., Sweeney, D., Arostegui, J. M. M., Bayes, àngels, Lewy, H., Costa, A., Annicchiarico, R., Counihan, T., Laighin, G. O., & Cabestany, J. (2017). Analysis of correlation between an accelerometer-Based algorithm for Detecting Parkinsonian gait and UPDRS subscales. *Frontiers in Neurology*, 8(SEP), 1–6.

<https://doi.org/10.3389/fneur.2017.00431>

Salvi, D., Poffley, E., Orchard, E., & Tarassenko, L. (2020). The mobile-based 6-minute walk test: Usability study and algorithm development and validation. *Journal of Medical Internet Research*, 22(1), 1–15. <https://doi.org/10.2196/13756>

Schimpl, M., Moore, C., Lederer, C., Neuhaus, A., Sambrook, J., Danesh, J., Ouwehand, W., & Daumer, M. (2011). Association between walking speed and age in healthy, free-living individuals using mobile accelerometry—a cross-sectional study. *PLoS ONE*, 6(8). <https://doi.org/10.1371/journal.pone.0023299>

Shah, V. V., McNames, J., Mancini, M., Carlson-Kuhta, P., Spain, R. I., Nutt, J. G., El-Gohary, M., Curtze, C., & Horak, F. B. (2020). Quantity and Quality of Mobility in People with Multiple Sclerosis, Parkinson’s Disease and Matched Controls During Daily Living. *Journal of Neurology*, 267(4), 1188–1196.

<https://doi.org/10.1007/s00415-020-09696-5>

- Soderbom, G. (2020). Chapter Six—Status and future directions of clinical trials in Parkinson’s disease. In G. Soderbom, R. Esterline, J. Oscarsson, & M. P. Mattson (Eds.), *International Review of Neurobiology* (Vol. 154, pp. 153–188). Academic Press. <https://doi.org/10.1016/bs.irn.2020.02.009>
- Stacy, M., Bowron, A., Guttman, M., Hauser, R., Hughes, K., Larsen, J. P., LeWitt, P., Oertel, W., Quinn, N., Sethi, K., & Stocchi, F. (2005). Identification of motor and nonmotor wearing-off in Parkinson’s disease: Comparison of a patient questionnaire versus a clinician assessment. *Movement Disorders*, *20*(6), 726–733. <https://doi.org/10.1002/mds.20383>
- Steinhubl, S. R., McGovern, P., Dylan, J., & Topol, E. J. (2017). The digitised clinical trial. *The Lancet*, *390*(10108), 2135. [https://doi.org/10.1016/S0140-6736\(17\)32741-1](https://doi.org/10.1016/S0140-6736(17)32741-1)
- Steins, D., Dawes, H., Esser, P., & Collett, J. (2014). Wearable accelerometry-based technology capable of assessing functional activities in neurological populations in community settings: A systematic review. *Journal of NeuroEngineering and Rehabilitation*, *11*(1), 1–13. <https://doi.org/10.1186/1743-0003-11-36>
- Stephenson, D., Alexander, R., Aggarwal, V., Badawy, R., Bain, L., Bhatnagar, R., Bloem, B. R., Boroojerdi, B., Burton, J., Cedarbaum, J. M., Cosman, J., Dexter, D. T., Dockendorf, M., Dorsey, E. R., Dowling, A. V., Evers, L. J. W., Fisher, K., Frasier, M., Garcia-Gancedo, L., ... behalf of the Critical Path for Parkinson’s Consortium, O. (2020).

Precompetitive Consensus Building to Facilitate the Use of Digital Health Technologies to Support Parkinson Disease Drug Development through Regulatory Science. *Digital Biomarkers*, 4(1), 28–49.

<https://doi.org/10.1159/000512500>

Storm, F. A., Buckley, C. J., & Mazzà, C. (2016). Gait event detection in laboratory and real life settings: Accuracy of ankle and waist sensor based methods. *Gait and Posture*, 50, 42–46. <https://doi.org/10.1016/j.gaitpost.2016.08.012>

Storm, F. A., Nair, K. P. S., Clarke, A. J., Meulen, J. M. V. D., & Mazz, C. (2018). *Free-living and laboratory gait characteristics in patients with multiple sclerosis*. 1–15.

Takakusaki, K. (2017). Functional Neuroanatomy for Posture and Gait Control. *Journal of Movement Disorders*, 10(1), 1–17.

<https://doi.org/10.14802/jmd.16062>

Takayanagi, N., Sudo, M., Yamashiro, Y., Lee, S., Kobayashi, Y., Niki, Y., & Shimada, H. (2019). Relationship between Daily and In-laboratory Gait Speed among Healthy Community-dwelling Older Adults. *Scientific Reports*, 9(1), 2–3.

<https://doi.org/10.1038/s41598-019-39695-0>

Tao, W., & Feng, H. (2012). Gait analysis using wearable sensors. *Sensors*, 12(2), 2255–2283. <https://doi.org/10.1109/ICESA.2015.7503353>

Trojaniello, D., Cereatti, A., & Della Croce, U. (2014). Accuracy, sensitivity and robustness of five different methods for the estimation of gait temporal

- parameters using a single inertial sensor mounted on the lower trunk. *Gait and Posture*, 40(4), 487–492. <https://doi.org/10.1016/j.gaitpost.2014.07.007>
- Trojaniello, D., Ravaschio, A., Hausdorff, J. M., & Cereatti, A. (2015). Comparative assessment of different methods for the estimation of gait temporal parameters using a single inertial sensor: Application to elderly, post-stroke, Parkinson's disease and Huntington's disease subjects. *Gait and Posture*, 42(3), 310–316. <https://doi.org/10.1016/j.gaitpost.2015.06.008>
- Udupa, K., & Chen, R. (2013). Motor Cortical Plasticity in Parkinson's Disease. *Frontiers in Neurology*, 4, 128. <https://doi.org/10.3389/fneur.2013.00128>
- van Hees, V., Fang, Z., Mirkes, E., Heywood, J., Zhao, J. H., Joan, C. P., Sabia, S., Migueles, J. H., Patterson, M., Jackson, D., Chen, M., & Manasa, Y. (2021). GGIR (2.4-3) [R]. <https://doi.org/10.5281/zenodo.1051064>
- Van Schooten, K. S., Rispens, S. M., Elders, P. J. M., Lips, P., Van Dieën, J. H., & Pijnappels, M. (2015). Assessing physical activity in older adults: Required days of trunk accelerometer measurements for reliable estimation. *Journal of Aging and Physical Activity*, 23(1), 9–17. <https://doi.org/10.1123/JAPA.2013-0103>
- Verghese, J., Wang, C., Lipton, R. B., Holtzer, R., & Xue, X. (2007). Quantitative gait dysfunction and risk of cognitive decline and dementia. *Journal of Neurology, Neurosurgery and Psychiatry*, 78(9), 929–935. <https://doi.org/10.1136/jnnp.2006.106914>

- Villablanca, J., & Marcus, R. (1972). Sleep-wakefulness, EEG and behavioral studies of chronic cats without neocortex and striatum: The “diencephalic” cat. *Archives Italiennes De Biologie*, *110*(3), 348–382.
- Villablanca, J. R. (2010). Why do we have a caudate nucleus? *Acta Neurobiologiae Experimentalis*, *70*(1), 95–105.
- Walton, M. K., Cappelleri, J. C., Byrom, B., Goldsack, J. C., Eremenco, S., Harris, D., Potero, E., Patel, N., Flood, E., & Daumer, M. (2020). Considerations for development of an evidence dossier to support the use of mobile sensor technology for clinical outcome assessments in clinical trials. *Contemporary Clinical Trials*, *91*, 105962. <https://doi.org/10.1016/j.cct.2020.105962>
- Washabaugh, E. P., Kalyanaraman, T., Adamczyk, P. G., Claflin, E. S., & Krishnan, C. (2017). Validity and repeatability of inertial measurement units for measuring gait parameters. *Gait & Posture*, *55*, 87–93. <https://doi.org/10.1016/j.gaitpost.2017.04.013>. Validity
- Weiss, A., Sharifi, S., Plotnik, M., Van Vugt, J. P. P., Giladi, N., & Hausdorff, J. M. (2011). Toward automated, at-home assessment of mobility among patients with Parkinson disease, using a body-worn accelerometer. *Neurorehabilitation and Neural Repair*, *25*(9), 810–818. <https://doi.org/10.1177/1545968311424869>
- Wespatat, V., Tennigkeit, F., & Singer, W. (2004). Phase Sensitivity of Synaptic Modifications in Oscillating Cells of Rat Visual Cortex. *Journal of Neuroscience*, *24*(41), 9067–9075. <https://doi.org/10.1523/JNEUROSCI.2221-04.2004>

- Wiest, C., Tinkhauser, G., Pogosyan, A., He, S., Baig, F., Morgante, F., Mostofi, A., Pereira, E. A., Tan, H., Brown, P., & Torrecillos, F. (2021). Subthalamic deep brain stimulation induces finely-tuned gamma oscillations in the absence of levodopa. *Neurobiology of Disease*, *152*, 105287.
<https://doi.org/10.1016/j.nbd.2021.105287>
- Wishart, S., & Macphee, G. J. A. (2011). Evaluation and Management of the Non-Motor Features of Parkinson's Disease. *Therapeutic Advances in Chronic Disease*, *2*(2), 69–85. <https://doi.org/10.1177/2040622310387847>
- Womelsdorf, T., & Fries, P. (2007). The role of neuronal synchronization in selective attention. *Current Opinion in Neurobiology*, *17*(2), 154–160.
<https://doi.org/10.1016/j.conb.2007.02.002>
- Xia, R., & Mao, Z.-H. (2012). Progression of motor symptoms in Parkinson's disease. *Neuroscience Bulletin*, *28*(1), 39–48. <https://doi.org/10.1007/s12264-012-1050-z>
- Zanos, S., Rembado, I., Chen, D., & Fetz, E. E. (2018). Phase-Locked Stimulation during Cortical Beta Oscillations Produces Bidirectional Synaptic Plasticity in Awake Monkeys. *Current Biology*, *28*(16), 2515-2526.e4.
<https://doi.org/10.1016/j.cub.2018.07.009>
- Zhong, R., & Rau, P. L. P. (2020). A Mobile Phone-Based Gait Assessment App for the Elderly: Development and Evaluation. *JMIR MHealth and UHealth*, *8*(2), e14453. <https://doi.org/10.2196/14453>

Zijlstra, W., & Hof, A. L. (2003). Assessment of spatio-temporal gait parameters from trunk accelerations during human walking. *Gait and Posture*, *18*(2), 1–10.
[https://doi.org/10.1016/S0966-6362\(02\)00190-X](https://doi.org/10.1016/S0966-6362(02)00190-X)

CURRICULUM VITAE

